GLOBAL PERFORMANCE ANALYSIS OF A FLOATING HARBOR AND A CONTAINER SHIP FOR LOADING AND OFFLOADING OPERATIONS

A Thesis

by

SUNG HO LIM

Submitted to the Office of Graduate Studies of
Texas A&M University
in partial fulfillment of the requirements for the degree of

MASTER OF SCIENCE

December 2007

Major Subject: Ocean Engineering

GLOBAL PERFORMANCE ANALYSIS OF A FLOATING HARBOR AND A CONTAINER SHIP FOR LOADING AND OFFLOADING OPERATIONS

A Thesis

by

SUNG HO LIM

Submitted to the Office of Graduate Studies of
Texas A&M University
in partial fulfillment of the requirements for the degree of

MASTER OF SCIENCE

Approved by:

Chair of Committee,	Moo Hyun Kim
Committee Members,	Richard S. Mercier
	Achim Stössel
Head of Department,	David V. Rosowsky

December 2007

Major Subject: Ocean Engineering

ABSTRACT

Global Performance Analysis of a Floating Harbor and a Container Ship

for Loading and Offloading Operations. (December 2007)

Sung Ho Lim, B.E., Pusan National University, Korea

Chair of Advisory Committee: Dr. Moo Hyun Kim

The feasibility and general performance of a floating harbor system is studied with regard to the relative motion of a floating quay and a container ship. A 350[m]$\times$160[m] box-type barge is selected as the floating harbor and it is positioned by a dolphin mooring system. The container ship is tied to the land wall by hawsers. The hydrodynamic interactions between floating bodies and a fixed quay wall in close proximity with a side-by-side arrangement are investigated. A three dimensional wave-body diffraction/radiation panel program WAMIT is used for the calculation of hydrodynamic information and response amplitude operators (RAO) of the three bodies in frequency domain. Subsequently, the vessel-mooring coupled dynamic analysis program WINPOST is employed to produce motion time histories in time domain. The frequency-domain RAO is successfully compared with time-domain RAO in case viscous forces are neglected. Compared to Brajesh Kumar's (2005) study, 12×12 full hydrodynamic interactions between the two floating bodies are included and dynamic wind loading is considered in addition to wave and current loadings. All the relative motion statistics are calculated from the respective motion time histories for a typical operational condition and a typical survival condition. The relative motion between the interacting bodies is small in the operational condition to ensure the efficacy of container loading and offloading operation from both sides of the ship while the loading and offloading operation is not available in the survival condition.

Dedicated

to

my father Jae Woo Lim, mother Jung Boon Kim, my sister So Young Lim,

and my friends who I love and love me.

ACKNOWLEDGMENTS

I would like to extend my sincere gratitude to my committee chair Dr. Moo-Hyun Kim for his excellent guidance, encouragement, and incredible patience during my course of study. I would like to thank Dr. Richard S. Mercier and Dr. Achim Stössel for serving as advisory committee members and for their guidance and support throughout the course of this research. I would like to thank my laboratory group members, Dr. Dong Hwan Lee, Chan Kyu Yang, Seung Jae Lee, Brajesh Kumar, Sang Yun Sim, Zhi Zhang, and Yun Hyuk Bae for helping my study and the Korean Ocean Research and Development Institute (KORDI) for special observations and financial support for this project. I would also like to thank Nung Soo Kim, James Slaughter, Jena Slaughter, Lori Jones, Jolly James, Chang Hyun Park, Young Min Jung and Jake Herrera for being good friends and my great English teachers. Finally, I am indebted to my parents, Jae Woo Lim and Jung Boon Kim, for their support and encouragement throughout this research and being there for me always.

NOMENCLATURE

FQ	Floating Quay Wall
FixedQ	Fixed Quay Wall
SHIP	Container Ship
FQ + FixedQ	Floating Quay in the presence of Fixed Quay
SHIP + FixedQ	Container Ship in the presence of Fixed Quay
FQ + SHIP	Floating Quay and Container Ship
FQ + SHIP + FixedQ	Floating Quay and Container Ship in the presence of Fixed Quay
deg	Degrees
rad	Radians
U	Fluid velocity
t	Time
m	Meter
g	Acceleration due to gravity
ω	Cyclic frequency
sec	Second
p	Pressure
ρ	Density
∞	Infinity
S	Surface
A	Area
e	Exponential function

TABLE OF CONTENTS

LIST OF FIGURES

Page

Page

LIST OF TABLES

CHAPTER I

INTRODUCTION

1.1 Floating Quay Wall System

A floating quay type container terminal is assessed for loading and unloading among a floating quay, a container ship and a fixed harbor. However, advantages and disadvantages must be taken into account. There are advantages and disadvantages of the floating harbor compared to the ground based harbor as explained below.

Advantages of Floating Mobile Quay System (Kumar 2005)

- Capability of loading and unloading is easily expanded or changeable.
- Floating Quay System is least effected by the change of water-level by tide and storm surge.
- The container freights, cargos and floating quay structure can be protected from direct seismic shocks on earth, because it is positioned on the water surface.
- It is less effected by sea-bottom condition such as scour, liquefaction, sinkage, and deposition.
- It requires less expensive construction cost and no foundation work. Each unit can be built at different places before final assembly step at the purported harbor.
- Easy relocation.

This thesis follows the style of Ocean Engineering.

Disadvantages of Floating Mobile Quay System (Kumar 2005)

- Potential non-operability in relatively extreme wave condition.
- Due to the materials of the floating harbor, floating structures must be offered with anti-corrosion system.
- Potential degradation due to corrosion or crack growth (fatigue) needs proper ways for inspection and monitoring.

Total weight of the container freights, crew, and mechanical devices (payloads) and the static self weight are balanced by buoyant force in a floating body. In case a floating body is moored by a compliant mooring system, for example, composed of catenary chain mooring systems, the horizontal wave forces are carried by inertia forces. And when the horizontal length of the structure is bigger than the wave length, the resultant horizontal forces are going to be decreased, because wave force on each structural member has different phase, direction, location and size. The forces in the mooring system can not be larger than the total wave forces. The purpose of the mooring is not to move and to prevent drift-off due to wind forces and water currents as well as potential steady and slow-drift wave forces.

The shape, size, and the strength of the floating body and the shape of its mooring system depend on its environmental conditions including wave, current and wind conditions along with design purpose. The design of floating structures is restricted by peak loading according to survival environmental conditions such as design significant wave height, water current, wind force and tide.

1.2 Environmental Data and Layout of the Interacting Bodies

The equation of linear and angular momentum conservation is given by

$$(M + a)x^{"} + Bx^{'} + Cx = F_{exciting}$$

where a_{ij} is added mass coefficient, equivalent mass caused from additional force which occurs when the floating body moves and accelerates the fluid around and B_{ij} is radiation damping coefficient and C_{ij} is stiffness coefficient including hydrostatic stiffness factor and external stiffness factor and $\{F\} = \{F_X^{(1)}, F_Y^{(1)}, F_Z^{(1)}, \mathrm{T}_X^{(1)}, \mathrm{T}_Y^{(1)}, \mathrm{T}_Z^{(1)}\}^T$ are the exciting forces and moments acting on the body.

Mass Matrix

$$[M] = \begin{bmatrix} m & 0 & 0 & 0 & mz_{B,g} & -my_{B,g} \\ 0 & m & 0 & -mz_{B,g} & 0 & mx_{B,g} \\ 0 & 0 & m & my_{B,g} & -mx_{B,g} & 0 \\ 0 & -mz_{B,g} & my_{B,g} & (\mathrm{I}_{XX}^B) & -\mathrm{I}_{YX}^B & -\mathrm{I}_{Zx}^B \\ mz_{B,g} & 0 & -mx_{B,g} & -\mathrm{I}_{XY}^B & (\mathrm{I}_{YY}^B) & -\mathrm{I}_{ZY}^B \\ -my_{B,g} & mx_{B,g} & 0 & -\mathrm{I}_{XZ}^B & -\mathrm{I}_{YZ}^B & (\mathrm{I}_{ZZ}^B) \end{bmatrix}$$

where $\mathrm{I}_{XY}^B = \mathrm{I}_{YX}^B, \mathrm{I}_{XZ}^B = \mathrm{I}_{ZX}^B, \mathrm{I}_{YZ}^B = \mathrm{I}_{ZY}^B$: Mass moments of inertia defined with respect to the origin of the body fixed coordinate system.

$x_{b,g}$: the distance between the point of center of gravity and the origin point of body fixed coordinate system in x direction.

$y_{b,g}$: the distance between the point of center of gravity and the origin point of body fixed coordinate system in y direction.

$z_{b,g}$: the distance between the point of center of gravity and the origin point of body fixed coordinate system in z direction.

Hydrostatic Stiffness Matrix (Dr. Mercier's lecture note 2005)

$$[K]=\begin{bmatrix} 0 & 0 & 0 & 0 & 0 & 0 \\ 0 & 0 & 0 & 0 & 0 & 0 \\ 0 & 0 & \rho g A^{(0)} & \rho g \mathrm{I}_Y^A & -\rho g A_X^A & 0 \\ 0 & 0 & \rho g \mathrm{I}_Y^A & \rho g\left[\mathrm{I}_{YY}^A + V^{(0)} z_{B,b}\right] - mgz_{B,g} & -\rho g \mathrm{I}_{XY}^A & -\rho g V^{(0)} x_{B,b} + mgx_{B,g} \\ 0 & 0 & \rho g \mathrm{I}_X^A & \rho g \mathrm{I}_{YX}^A & \rho g\left[\mathrm{I}_{XX}^A + V^{(0)} z_{B,b}\right] - mgz_{B,g} & -\rho g V^{(0)} y_{B,b} + mgy_{B,g} \\ 0 & 0 & 0 & 0 & 0 & 0 \end{bmatrix}$$

where I_X^A, I_Y^A, I_{XX}^A, I_{YY}^A, $\mathrm{I}_{XY}^A = \mathrm{I}_{YX}^A$: the moments of area.

$(x_{B,b}, y_{B,b}, z_{B,b})$: coordinates of center of buoyancy

$A^{(0)}$: water plane area

$V^{(0)}$: submerged volume

The diagonal terms in the above [M] and [K] matrices represent pure motions such as Surge, Sway, Heave, Roll, Pitch and Yaw. In [K] off-diagonal terms are mixed or coupled terms. Figure 1-1 shows six degrees of freedom of motion and the coordinate system.

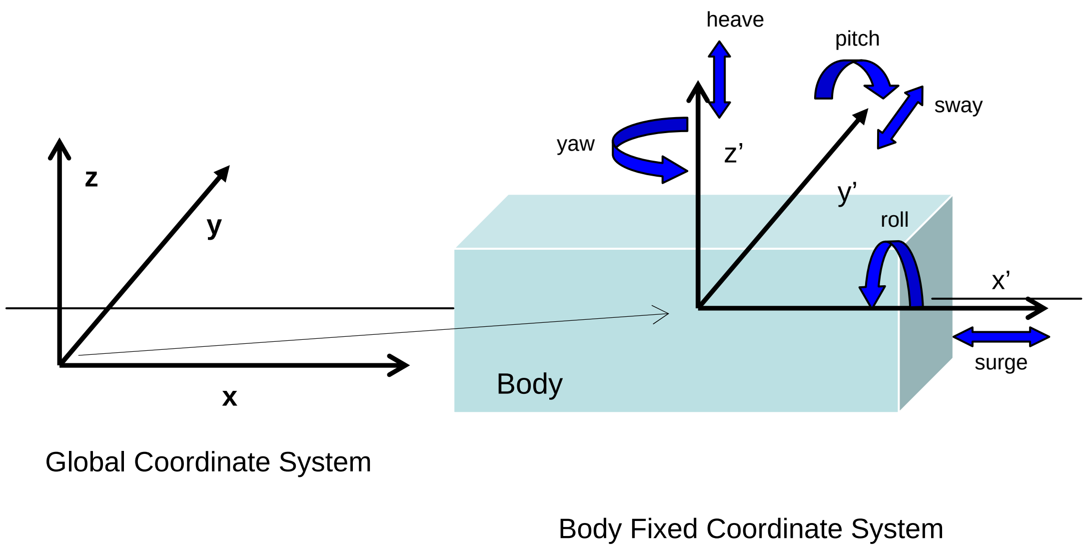

Fig. 1-1. Global Coordinate System and Body Fixed Coordinate System

1.2.1 Layout of the Interacting Bodies

Container Ship is positioned at the center of the gap between Fixed Quay and Floating Quay. The gap between Floating Quay and Fixed Quay is 40 [m].

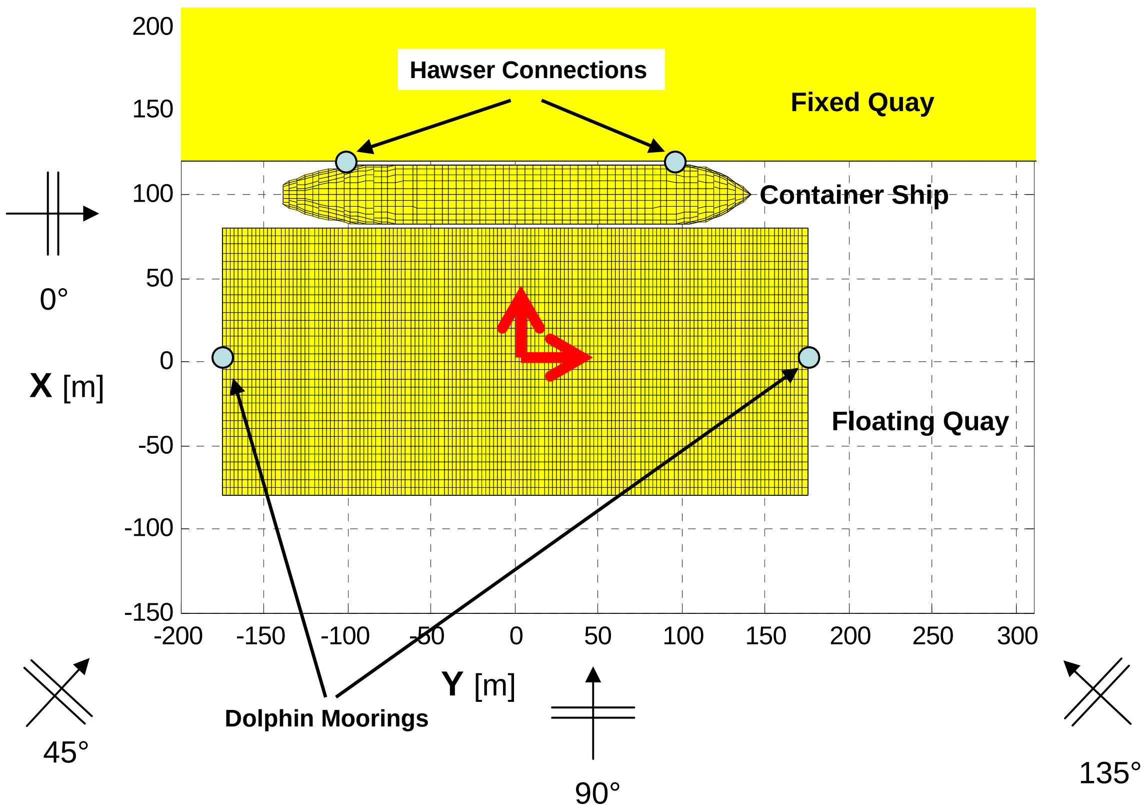

Fig. 1-2. Layout (x-y plane view) of Fixed Quay, Container Ship, and Floating Quay (with incident angles)

As shown in Fig.1-2, waves propagating in the positive x-axis direction has 0 degree incident angle while waves traveling in the positive y-axis has 90 degree incident angle. Figure 1-3 illustrates layout of the interacting bodies and three wave directions to be considered. Table 1-1 displays wave, wind, and current data for the operational and survival conditions.

Here, interest is in the response motions of Floating Harbor and Container Ship and relative motions of the container ship with respect to floating quay and fixed quay for proper loading and unloading operation. The hydrodynamic interaction among Floating Quay, Container Ship, and

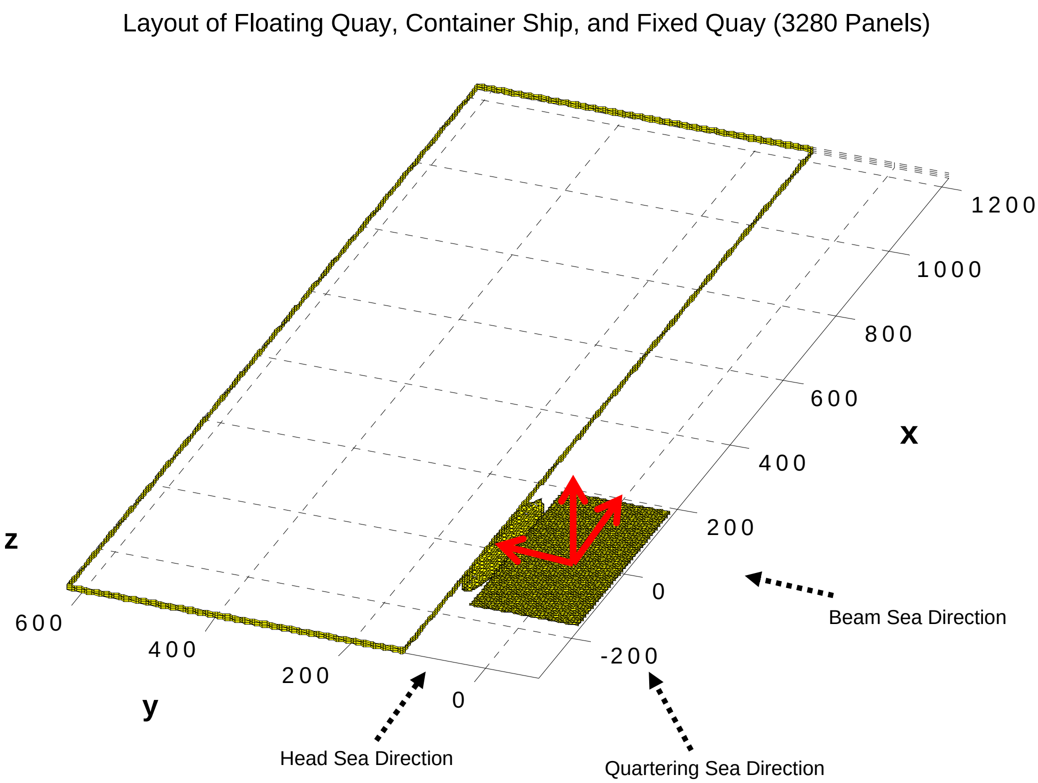

Fig.1-3. Global Coordinate System of Fixed Quay, Container Ship, and Floating Quay

Fixed Quay is simulated using WAMIT and WINPOST. Due to the entrapment of the water waves between two bodies (e.g. Container Ship and Fixed Quay or Container Ship and Floating Quay) there is a standing wave formation when the entrapped length of the water column is approximately equal to one quarter of the incident wave length. The effect of entrapment as well as the effect of the motion of one body on the motion of the other body will be analyzed in detail for determining the hydrodynamic motion of the bodies.

Table 1-1 Environmental Data for Operational and Survival Conditions

CASE		Head Sea	Quartering Sea	Beam Sea
Wave Heading Angle		0 [deg]	45[deg]	90[deg]
Gap between FQ & FixedQ		40[m]		
Cutoff Frequencies		0.1, 1.5 [rad/sec]		
Survival Condition	Water Depth	16 [m]		
	Hs	1.8 [m]		
	Tp	14 [sec]		
	Gamma	1.5		
	Water Current	0.23 [m/sec] at surface Current profile = $VC(1+z/Depth)^{1/7}$		
	Water Current Angle	45 [deg]		
	Wind Velocity at the height of 10[m]	75[m/sec]		
	Wind Heading Angle	45 [deg]		
Operational Condition	Water Depth	16 [m]		
	Hs	0.5 [m]		
	Tp	9 [sec]		
	Gamma	1.2		
	Water Current	0.115[m/sec] at surface Current profile = $VC(1+z/Depth)^{1/7}$		
	Water Current Angle	45 [deg]		
	Wind Velocity at the height of 10[m]	16 [m/sec]		
	Wind Heading Angle	45 [deg]		

Panel discretization and local coordinate origin of floating bodies are shown in Fig. 1-4 and Fig. 1-5. Specification of the interacting bodies is seen in Table 1-2 and Table 1-3.

Table. 1-2. Specification of Floating Quay Wall

Body Specification (Floating Quay Wall)					
Length :	350 [m]	Breadth :	160 [m]	Draft :	2.3 [m]
Average Height :	4.9 [m]	KG :	3.0 [m]	KB :	1.15 [m]
Projected Area of super-structure	Head Sea Wave Direction (0 [deg]) :			604[m^2]	
	Quadrant Sea Wave Direction (45[deg]) :			2689[m^2]	
	Beam Sea wave Direction (90[deg]) :			3198[m^2]	

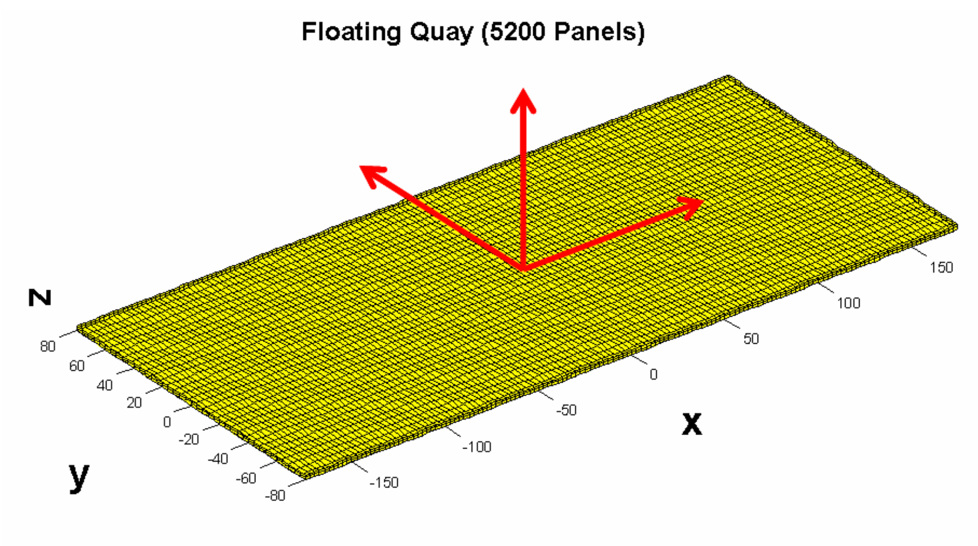

Mass Matrix [kg, kgm^2] of Floating Quay

$$\begin{bmatrix} 132020000 & 0 & 0 & 0 & 92414000 & 0 \\ 0 & 132020000 & 0 & -92414000 & 0 & 0 \\ 0 & 0 & 132020000 & 0 & 0 & 0 \\ 0 & -92414000 & 0 & 2.823262E+11 & 0 & 0 \\ 92414000 & 0 & 0 & 0 & 1.34838E+12 & 0 \\ 0 & 0 & 0 & 0 & 0 & 1.6293468E+12 \end{bmatrix}$$

Fig. 1-4. Panel Discretization and Body Fixed Coordinate System of Floating Quay

Table. 1-3. Specification of Container Ship

Body Specification (4000 TEU Container Ship)					
Length :	280 [m]	Breadth :	35.8 [m]	Draft :	13 [m]
Average Height :	28 [m]	KG :	9.162 [m]	KB :	6.78 [m]
Projected Area of super-structure	Head Sea Wave Direction (0 [deg]) :			862 [m^2]	
	Quadrant Sea Wave Direction (45[deg]) :			4869 [m^2]	
	Beam Sea wave Direction (90[deg]) :			6030 [m^2]	

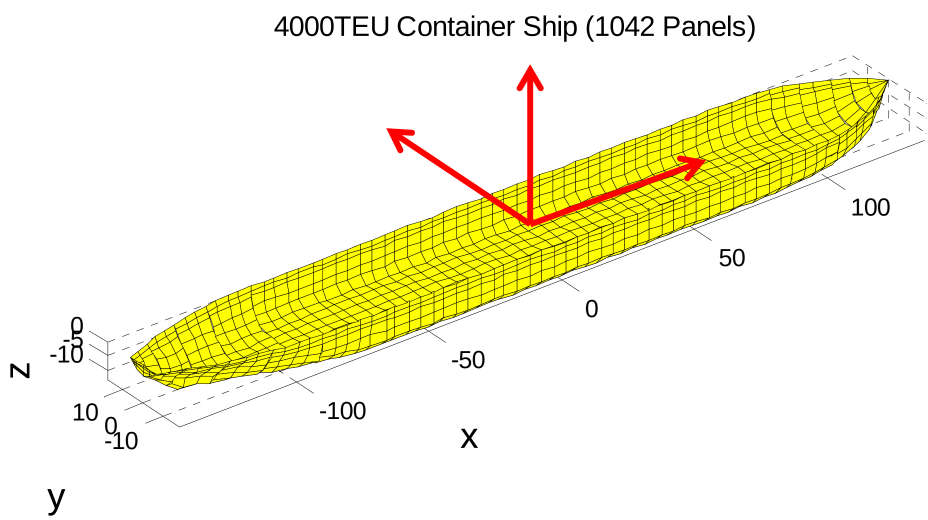

Mass Matrix [kg, kgm^2] of Container Ship

$$
\begin{bmatrix}
111028000 & 0 & 0 & 0 & -426141007.9 & 0 \\
0 & 111028000 & 0 & 426141007.9 & 0 & 0 \\
0 & 0 & 111028000 & 0 & 0 & 0 \\
0 & 426141007.9 & 0 & 1.389628E+10 & 0 & -2.7E+10 \\
-426141007.9 & 0 & 0 & 0 & 5.440372E+11 & 0 \\
0 & 0 & 0 & -2.7E+10 & 0 & 5.50837665E+11
\end{bmatrix}
$$

Fig.1-5. Panel Discretization and Body Fixed Coordinate System of Container Ship

1.2.2 External Stiffness Setting

Connections between the floating and fixed bodies and Dolphin mooring and hawser stiffness are shown in Fig. 1-6.

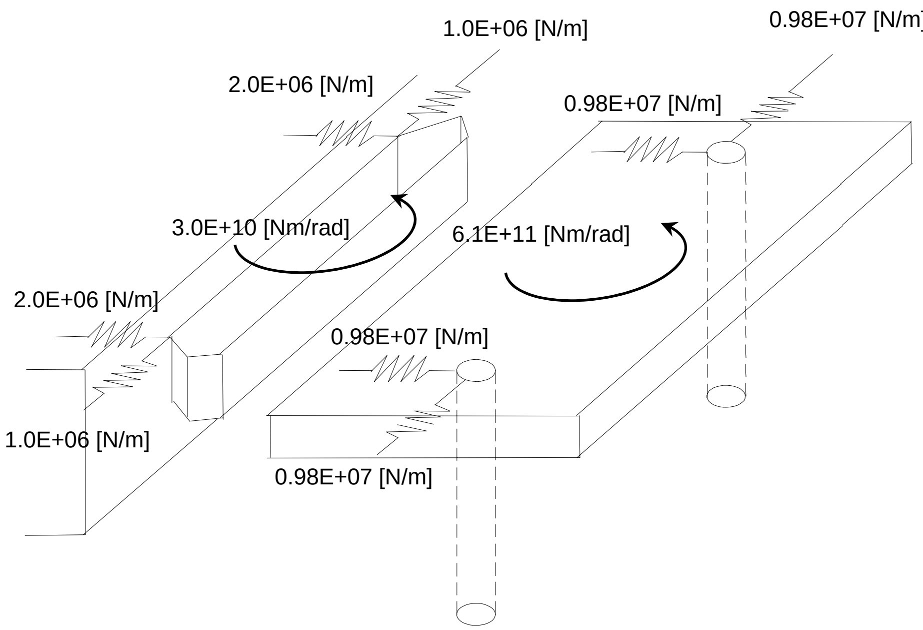

External Stiffness Matrix for Dolphin Moorings [N/m, N-m/rad]

$$\begin{bmatrix} 1.96E+07 & 0 & 0 & 0 & 0 & 0 \\ 0 & 1.96E+07 & 0 & 0 & 0 & 0 \\ 0 & 0 & 0 & 0 & 0 & 0 \\ 0 & 0 & 0 & 0 & 0 & 0 \\ 0 & 0 & 0 & 0 & 0 & 0 \\ 0 & 0 & 0 & 0 & 0 & 6.1E+11 \end{bmatrix}$$

External Stiffness Matrix for Hawser Connections [N/m, N-m/rad]

$$\begin{bmatrix} 2.0E+06 & 0 & 0 & 0 & 0 & 0 \\ 0 & 4.0E+06 & 0 & 0 & 0 & 0 \\ 0 & 0 & 0 & 0 & 0 & 0 \\ 0 & 0 & 0 & 0 & 0 & 0 \\ 0 & 0 & 0 & 0 & 0 & 0 \\ 0 & 0 & 0 & 0 & 0 & 3.0E+10 \end{bmatrix}$$

Fig.1-6. Dolphin Mooring Stiffness and Hawser Stiffness (External Stiffness)

1.2.3 Drag Plate Model

Fig. 1-7 and Fig. 1-8 show drag plate models in order to consider drag force under the water surface. 1.9 is used for drag coefficient Cd.

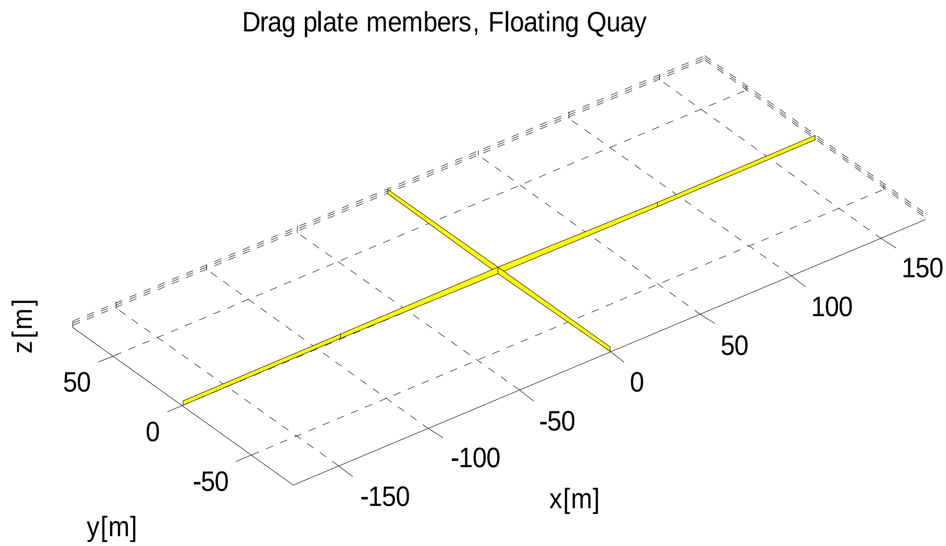

Fig.1-7. Drag Plate Model of Floating Quay

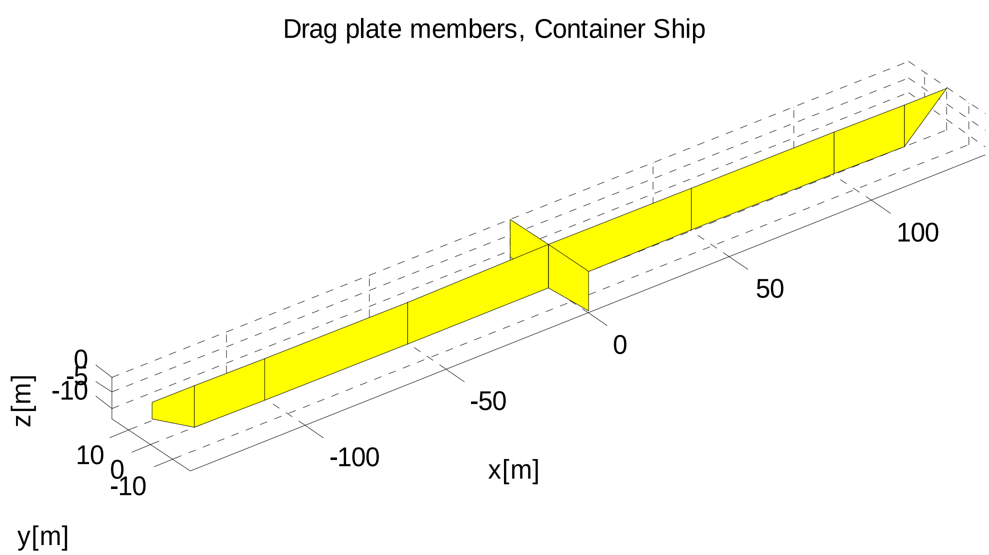

Fig.1-8. Drag Plate Model of Container Ship

1.3 Objectives

This research discusses operability of using a floating harbor container terminal for loading and unloading between a floating harbor container terminal and a container ship. In order to investigate feasibility of using a floating quay wall instead of a ground base harbor, hydrodynamic interaction effects must be analyzed among these interacting bodies. A container ship is positioned at the center of the gap between a fixed harbor and a floating harbor. Those two floating bodies and one fixed body are arranged side-by-side parallel to each other. In this multi-body system, the interacting phenomena between the fixed body and the floating bodies are inevitable. The individual motions influence other body's motion, because they are in close proximity. The interaction between the floating or fixed structures is named hydrodynamic coupling. In this multi-body system, viscous effects will be ignored. This three-body system of floating and fixed structures can be described using potential theory which leads to a boundary value problem. Frequency domain result will be obtained first by using WAMIT. Added mass, radiation damping and hydrostatic stiffness on the frequency domain will also be calculated. This frequency-domain data from WAMIT will be transformed into time-domain results in WINPOST by using retardation function. This takes memory effect into consideration. And wind effect will be also added, which is based on API (American Petroleum Institute) spectrum. The motion time history can be finally obtained. WAMIT (Wave Analysis Massachusetts Institute of Technology) is a radiation, diffraction program developed for the analysis of the interaction of surface waves with offshore structures. WAMIT is a three-dimensional panel method to evaluate frequency domain results including added mass coefficients, potential damping coefficients, diffraction force profiles, and Response Amplitude Operator (RAO). WINPOST is a finite element program for coupled dynamic analysis. The program is developed for coupled dynamic analysis both in time domain and frequency domain. WINPOST transforms frequency domain result and data into time domain result by using retardation function to consider memory effect and adding water current and wind force profile.

The resulting RAOs and time-domain results will be compared and analyzed for wave heading angle and the presence or absence of interacting bodies. Wave headings will be dealt at 0 [deg] (Head sea wave), 45 [deg] (Quadrant sea wave), and 90 [deg] (Beam sea wave) directions.

1 BODY CASE - Only Floating Quay Wall, Only Container Ship

2 BODY CASE - Fixed Quay Wall + Floating Quay Wall
Fixed Quay Wall + Container Ship
Floating Quay Wall + Container Ship

3 BODY CASE - Floating Quay + Container Ship + Fixed Quay Wall

The loads including hydrostatic pressure, hydrodynamic pressure, dead load, wind load, earth pressure on mooring systems such as dolphins, water current, storm effect, effects of tidal change and other effects must be taken into account.

1.4 Literature Review

Brajesh Kumar (2005) researched floating harbor case with non-coupled analysis. In contrast to Kumar, this research incorporates coupled analysis. Coupled analysis means off-diagonal terms in matrix calculations are considered. The gap between the fixed harbor and the floating quay wall was 60 [m] in Kumar's thesis while the gap of this research is 40[m] in this research. And 350[m] length container ship and 350[m]$\times$140[m] floating quay wall was used while 280[m] length container ship and 350[m]$\times$160[m] floating quay wall are used in this research. Wind force was not considered in Kumar's research (2005). The wind force profile obtained from API spectrum is now used. Hong et al. (2005) analyzed coupled motion behavior of side by side moored vessels. Hydrodynamic interactions in time domain was considered and characteristics of memory effects in two-body motion simulation was focused comparing a case considered hydrodynamic interaction with another case that was neglected hydrodynamic interaction effect. Dr. Zhihuang Ran (2000) studied coupled dynamic analysis of floating bodies in wave trains and water currents. Dr. Lee and Dr. Kim (2005) analyzed the two-body resonant interaction using fully coupled analysis method and partially coupled analysis method. Tahar, A. and Dr. Kim (2003) studied Hull/Mooring/Riser coupled dynamic analysis and sensitivity study of a tanker-based FPSO. Buchner et al. (2001) studied the interaction between a LNG Carrier and a LNG FPSO in side by side mooring. The conclusion of this research is that hydrodynamic cross coupling can not be neglected when interacting bodies are in close proximity.

CHAPTER II

THEORETICAL BACKGROUND

2.1 Wave Mechanics

In order to determine wave exciting forces and response motions of free-floating bodies in wave trains, diffraction theory will be applied here. The fluid field around the floating bodies is explained by using the concept of velocity potentials on the assumption that the fluid is ideal, which means the fluid is inviscid, incompressible, and irrotational. Laplace equation governs this boundary value problem.

$$\nabla^2\phi = \frac{\partial^2\phi}{\partial x^2} + \frac{\partial^2\phi}{\partial y^2} + \frac{\partial^2\phi}{\partial z^2} = 0 \qquad cf.\ \nabla = i\frac{\partial}{\partial x} + j\frac{\partial}{\partial y} + k\frac{\partial}{\partial z}$$

This velocity potential allows superposition of the incident wave potential, scattered wave potential, and radiation potential, because this research is based on linear wave theory. For obtaining response to incident regular waves of frequency ω, it is necessary to determine the pressure distribution on the free-floating body due to the wave motion and the body motion. The velocity potential should be solved. For a body undergoing small amplitude motions relative to the wave length i.e. $|\mathrm{X}_j| \ll \lambda$, the velocity potential is described as the sum of the incident, scattered and radiated waves:

$$\phi(x, y, z, t) = \phi_{Incident} + \phi_{Scattered} + \phi_{Radiation} = A\Phi_I + A\Phi_S + \sum_{j=1}^{6N} X_j \Phi_j$$

$$= A\Phi_I + A\sum_{i=6N+1}^{6N+N} \Phi_i + \sum_{j=1}^{6N} X_j \Phi_j = A\Phi_D + \sum_{j=1}^{6N} X_j \Phi_j$$

where $\phi_I = A\Phi_I$: incident wave potential without the body disturbing the flow.

$\phi_S = A\Phi_S$: scattered wave potential representing the disturbance of the incident waves due to the presence of the body which is fixed in space.

$\phi_D = A\Phi_D$: the wave diffraction which is the combined effects of incident and scattered waves.

$\phi_R = \sum_{j=1}^{6N} X_j \Phi_j$:the radiated wave potential generated by the body motion in all six modes of motion of the floating bodies.

N : the number of the floating bodies.

The boundary conditions of the fluid domain, including free surface, sea bottom, infinity, and body surface conditions must be satisfied. The boundary value problem is solved according to Green's second theorem. After the boundary conditions applied, the remaining integral equation is composed solely of the integral on the surface of the floating body, because the Green function satisfies the Laplace equation $\nabla^2\phi = \frac{\partial^2\phi}{\partial x^2} + \frac{\partial^2\phi}{\partial y^2} + \frac{\partial^2\phi}{\partial z^2} = 0$ and the surrounding boundary conditions except the condition on the surface of the body.

$$2\pi\phi + \iint_{Sb} \phi \frac{\partial G}{\partial n} dS = \iint_{Sb} G \frac{\partial \phi}{\partial n} dS$$ where G is the Green function.

This formula is applied in the diffraction code of WAMIT. In order to solve these integral equations numerically, the wetted surface area of the floating body should be discretized. The irregular frequency problem is averted by a large number of discretized panels sacrificing calculation time or by using the WAMIT input option, IRR, to remove the effect of irregular frequency.

2.2 Hydrodynamics

The fluid pressure is derived from the linearized Bernoulli equation. The exciting forces and moments exerted on the body are obtained by integrating the fluid pressure over the surface of the body.

$$p = -\rho g z - \rho \frac{\partial \phi}{\partial t} \qquad\qquad F = \iint_{Sb} pndS = F_{static} + F_{dynamic}$$

Governing equation

$$(M+a)x^{"} + Bx^{'} + Cx = F_{exciting} \quad \text{or} \quad \sum_{j=1}^{6N}\left[(M_{ij}+a_{ij})x^{"}_{j} + B_{ij}x^{'}_{j} + C_{ij}x_{j}\right] = \sum_{j=1}^{6N} F_i$$

Assuming that waves are harmonic type function

$\alpha(t) = \alpha_{amp} \cdot e^{-iwt}$: wave amplitude

$F_{exciting} = F_{amp} \cdot e^{-iwt+i\gamma}$: wave excitation force

$x(t) = X_{amp} \cdot e^{-iwt+i\varepsilon}$: body motion

$x^{'}(t) = -iw \cdot X_{amp} \cdot e^{-iwt+i\varepsilon} = -iw \cdot X(t)$: velocity

$x^{"}(t) = -w^2 \cdot X_{amp} \cdot e^{-iwt+i\varepsilon} = -w^2 \cdot X(t)$: acceleration

The governing equation becomes time-independent

$$\left[-w^2(M+a) - iwB + C\right] \cdot \frac{X_{amp}}{\alpha_{amp}} e^{i\varepsilon} = \frac{F_{amp}}{\alpha_{amp}} e^{i\gamma}$$

Added mass a_{ij} and radiation damping B_{ij} are derived from the radiation potentials:

$$a_{ij} - \frac{i}{w} B_{ij} = \rho \iint_{Sb} n_i \varphi_j dS$$

The response amplitude operators, solution of the governing equation means amplitude and phase of the motions of the structures in harmonic waves.

2.3 Transformation from Frequency to Time Domain

Velocity Potential: $\phi(t) = \mathrm{Re}[\phi(x, y, z) \cdot \exp(-iwt)]$

where $\phi(x, y, z) = \phi_{Incident} + \phi_{Scattering} + (-iw)X\phi_{radiation}$

$F_{exciting} = iw\rho \iint_{Sb} (\phi_{Incident} + \phi_{Scattering}) \cdot n \cdot ds$: wave excitation force

$a(w) = \rho\,\mathrm{Re}[\iint_{Sb} \phi_R n \cdot ds]$: added mass

$b(w) = -\rho w \cdot \mathrm{Im}[\iint_{Sb} \phi_R n \cdot ds]$: potential damping

Governing equation:

$$[M + a(\infty)]x''(t) + \int_0^\infty R(t-\tau) \cdot x'(\tau) \cdot d\tau + C \cdot x(t) = F_{exciting}(t)$$

where $R(t) = \frac{2}{\pi} \int_0^\infty B(w) \cdot \frac{\sin(wt)}{w} \cdot dw$: retardation function

$a(\infty) = a(w) - \int_0^\infty R(t) \cdot \cos(wt) \cdot dt$: added mass

$F_{exciting}(t) = \int_{-\infty}^{+\infty} h(\tau) \cdot \eta(t-\tau) \cdot d\tau$: wave excitation force

$h(\tau)$: linear impulse function, $\eta(t)$: wave elevation

Governing equation can be solved in the time domain by using the retardation function and impulse function.

2.4 API (American Petroleum Institute) **Wind Model** (Dr. Mercier's lecture note 2005)

In modeling the mean flow it is assumed that the wind speed is horizontally uniform but varies with height above the water surface according to a power law profile,

$$\overline{U}(z) = \overline{U}_{ref}\left(\frac{z}{z_{ref}}\right)^{a}$$

where z : the elevation above mean water level

z_{ref} : the reference elevation, $z_{ref} = 10[m]$

$\overline{U}_{ref}$: the mean speed at the reference elevation

The overbar typically denotes a time average over a period of one hour

a : conventionally adopted as 0.125.

The wind speed spectrum is also assumed to vary only in the vertical direction. The wind spectrum is modeled as $S_{uu}(f,z) = \dfrac{\sigma_u^2(z)\cdot f/f_r}{(1+1.5\cdot f/f_r)}$.

where $\sigma_u^2(z)$: the variance of the wind speed at elevation z

f_r : a reference frequency given by $f_r = b\cdot\overline{U}(z)/z$ with $0.01 \le b \le 0.10$

The standard deviation of wind speed is specified independently through a turbulence intensity model. One such model for the turbulence intensity in storms over water is

$$I(z) = \frac{\sigma_u(z)}{\overline{U}(z)} = 0.15\cdot(z/z_s)^{-0.125} \quad \text{for } z/z_s \le 1$$

$$0.15(z/z_s)^{-0.125} \quad \text{for } z/z_s > 1 \qquad \text{where } z_s = 20[m]$$

To complement the spectrum of the wind speed, when wind speed or gust speed of some averaging time is needed to know. This information is used in quasi-static design analysis of individual elements of the platform superstructure. A gust factor $g(T)$ is defined according to

$$\frac{\frac{1}{T}\int_{t}^{t+T} U(t^{'},z)dt^{'}}{\overline{U}(z)} = 1 + g(T)\cdot I(z)$$

When T is the averaging time period. A commonly used relation for the gust factor is

$g(T) = 3.0 + \ln[(3/T)^{0.6}]$ for $T \leq 60[\sec]$

Given the above model for the wind field, the instantaneous wind force on an element of the structure is given by

$$F^{w}(z,t) = \frac{1}{2}\rho_a C_d A_p \left(\overline{U}(z) + u^{'}(t) - X^{'}(t)\right)^2$$

where ρ_a : the air density, A_p : the projected area of the structure,

C_d is a drag coefficient, $u^{'}(t)$: the instantaneous velocity fluctuation

$X^{'}(t)$ is the instantaneous velocity of the structural element.

The mean wind force is therefore $\overline{F}^{w} = \frac{1}{2}\rho_a C_d A_p \left(\overline{U}(z_{cp})\right)^2$ and the fluctuating wind force is $F^{'w} = \rho_a C_d A_p \left(\overline{U}(z_{cp})\cdot u^{'}(t)\right)$, where z_{cp} is the elevation of the center of wind pressure. The effect of the squared velocity fluctuation is neglected in both of these expressions since it is relatively small.

In the frequency domain, the spectrum of the wind force is described as

$$S_{F^wF^w}(f) = \left(\rho_a C_d A_p \overline{U}^2(z_{cp})\right)^2 \cdot S_{uu}(f, z_{cp}) \cdot \left|\chi(f)\right|^2$$

where $\chi(f)$ is the aerodynamic admittance function which acts to filter out high frequency force fluctuation.

CHAPTER III

NUMERICAL SIMULATION

3.1 Frequency Domain Results

3.1.1 Added Mass and Damping Coefficient

Added masses and damping coefficients of Floating quay and Container ship for pure motions have been plotted with single, two and three body cases in Fig. 3-1, Fig. 3-2, Fig 3-3, and Fig 3-4. When it is single body case, added mass is usually high on the low frequency region, and low on the high frequency region. But when there exist other interacting bodies around, a combination of upward peak and downward peak occur somewhere on the frequency region at added mass graphs, and a sharp peak happens at damping graphs. The interaction effect with another body causes steep high added mass and negative added mass. There exist a sharp peak at about 0.8 [rad/sec] at Floating Quay added masses, and sharp peaks at about 0.45 [rad/sec], 0.6 [rad/sec], and 0.8 [rad/sec] at Container Ship added masses. And it is also observed that added masses of 2body (FQ + FixedQ) case and 3body (FQ + SHIP + FixedQ) case are going similar through the frequency region, and added masses of single body case and two floating body (FQ + SHIP) case are also getting similar. In this case, added masses are more effected by the presence of fixed quay than another floating body. But those are influenced by the presence of both fixed body and another floating body. The damping coefficients for the floating quay and container ship have sharp peaks at 0.6 [rad/sec], 0.8 [rad/sec], and so forth due to hydrodynamic interaction effect between bodies. The natural frequency points that are close to incident wave frequencies are well matched with high peaks in Response Amplitude Operators for each mode. The 12 mode natural frequencies from dolphin mooring, hawser stiffness, hydrostatic stiffness, mass of the floating body, and added mass for 12 modes is given in Table 3-1.

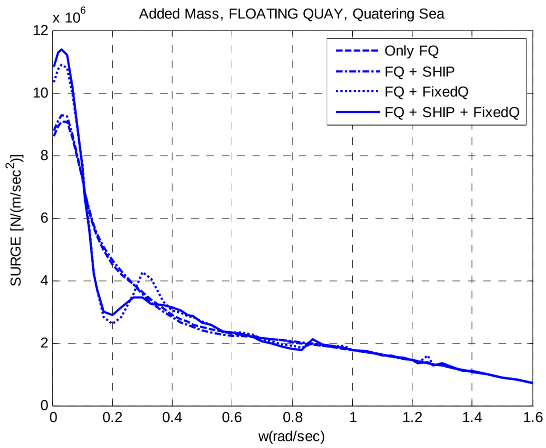

(i)

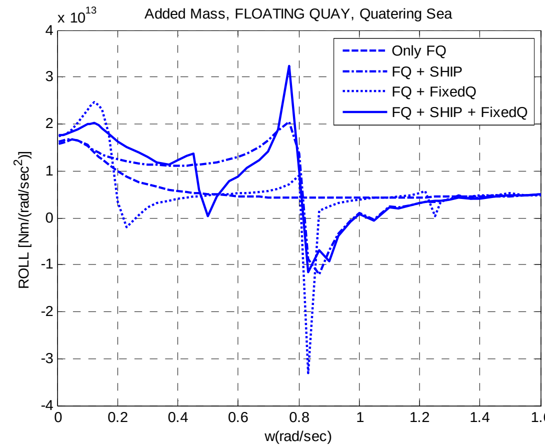

(iv)

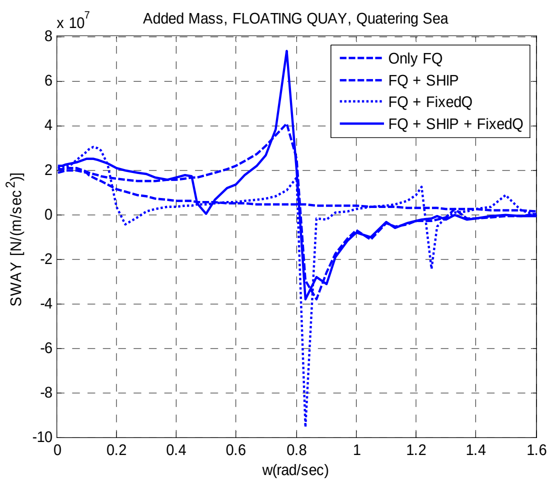

(ii)

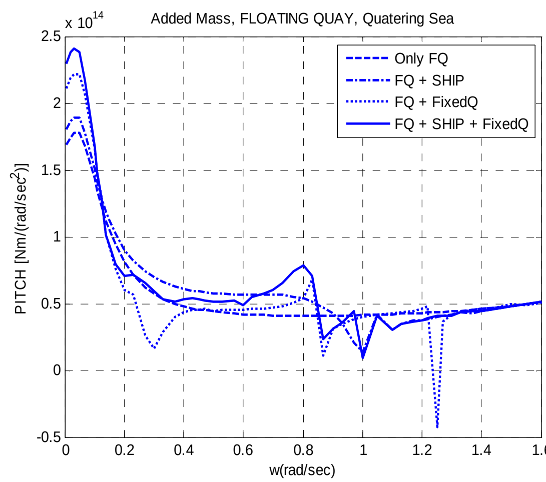

(v)

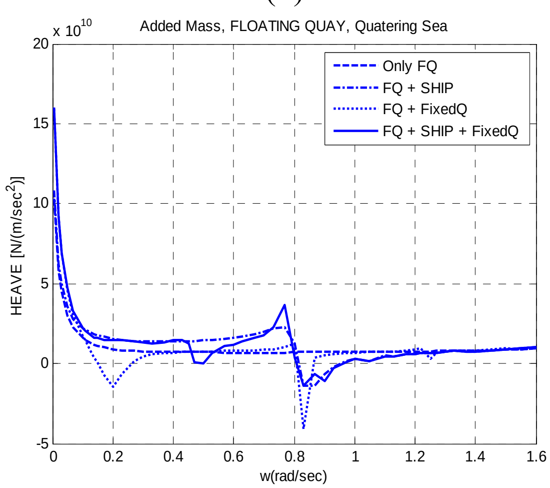

(iii)

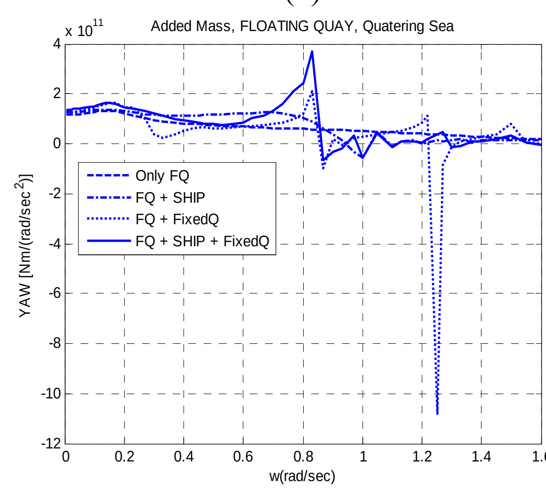

(vi)

Fig. 3-1. Added Mass Coefficients of Floating Quay

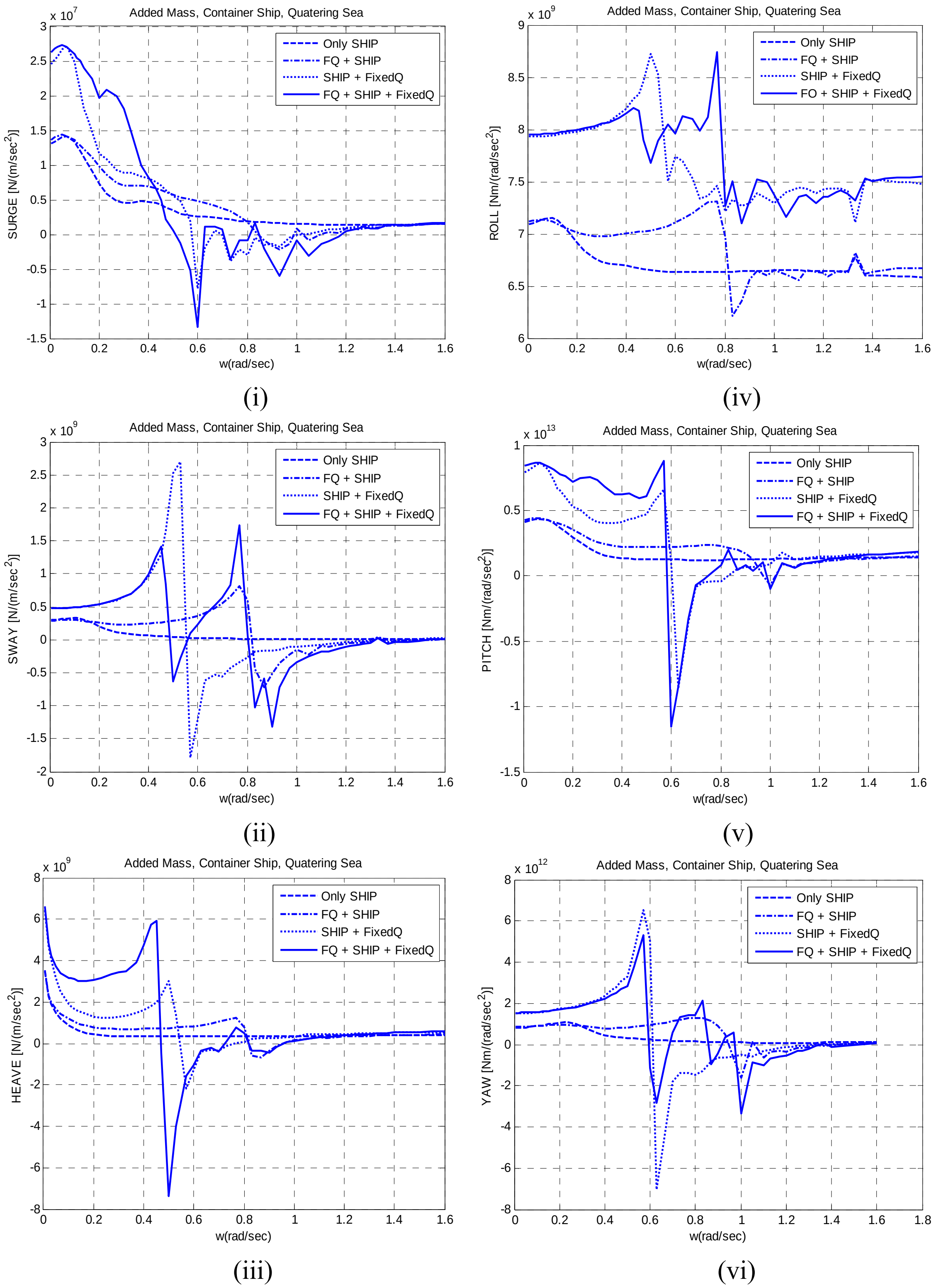

Fig. 3-2. Added Mass Coefficients of Container Ship

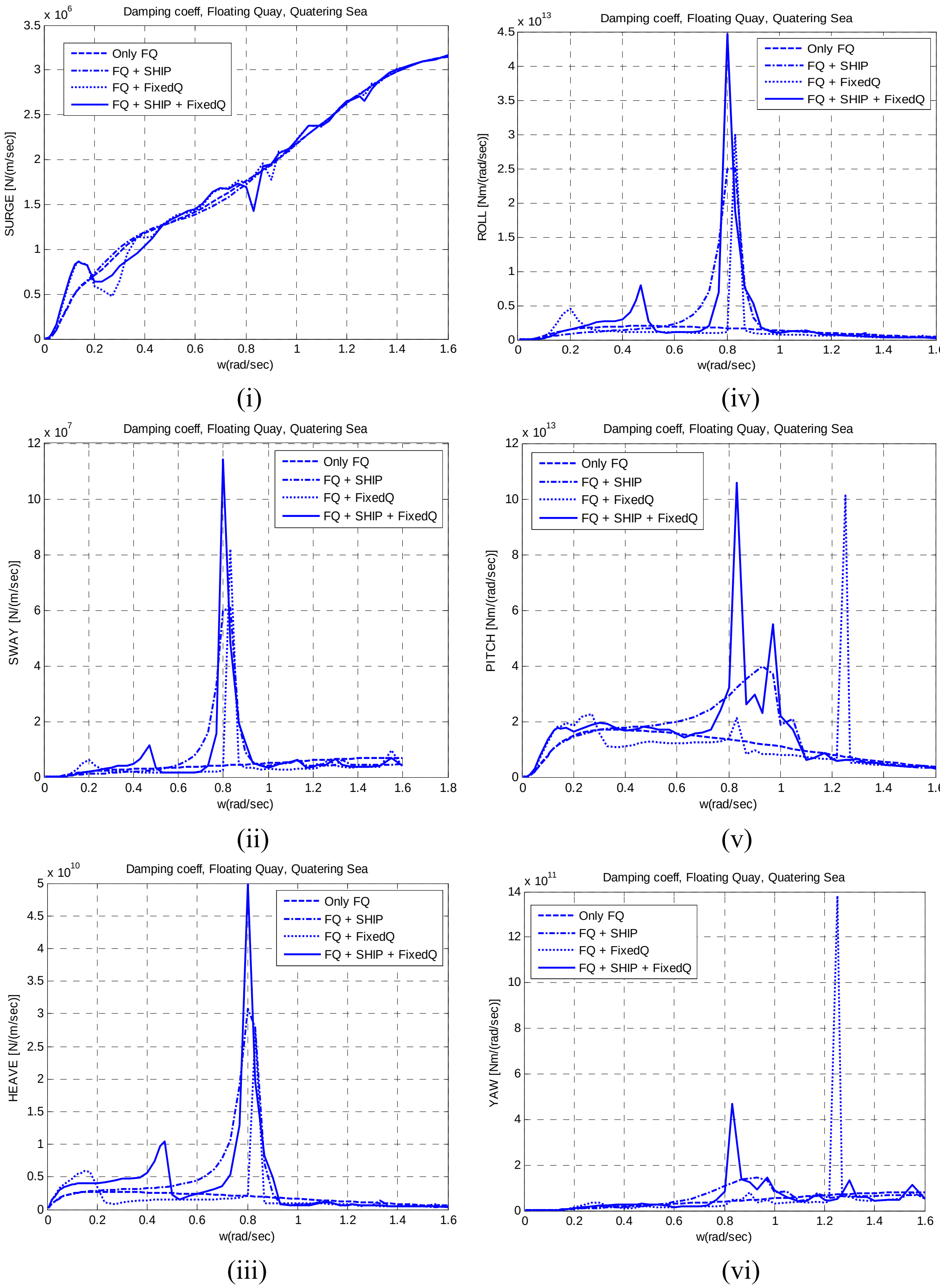

Fig. 3-3. Damping Coefficients of Floating Quay

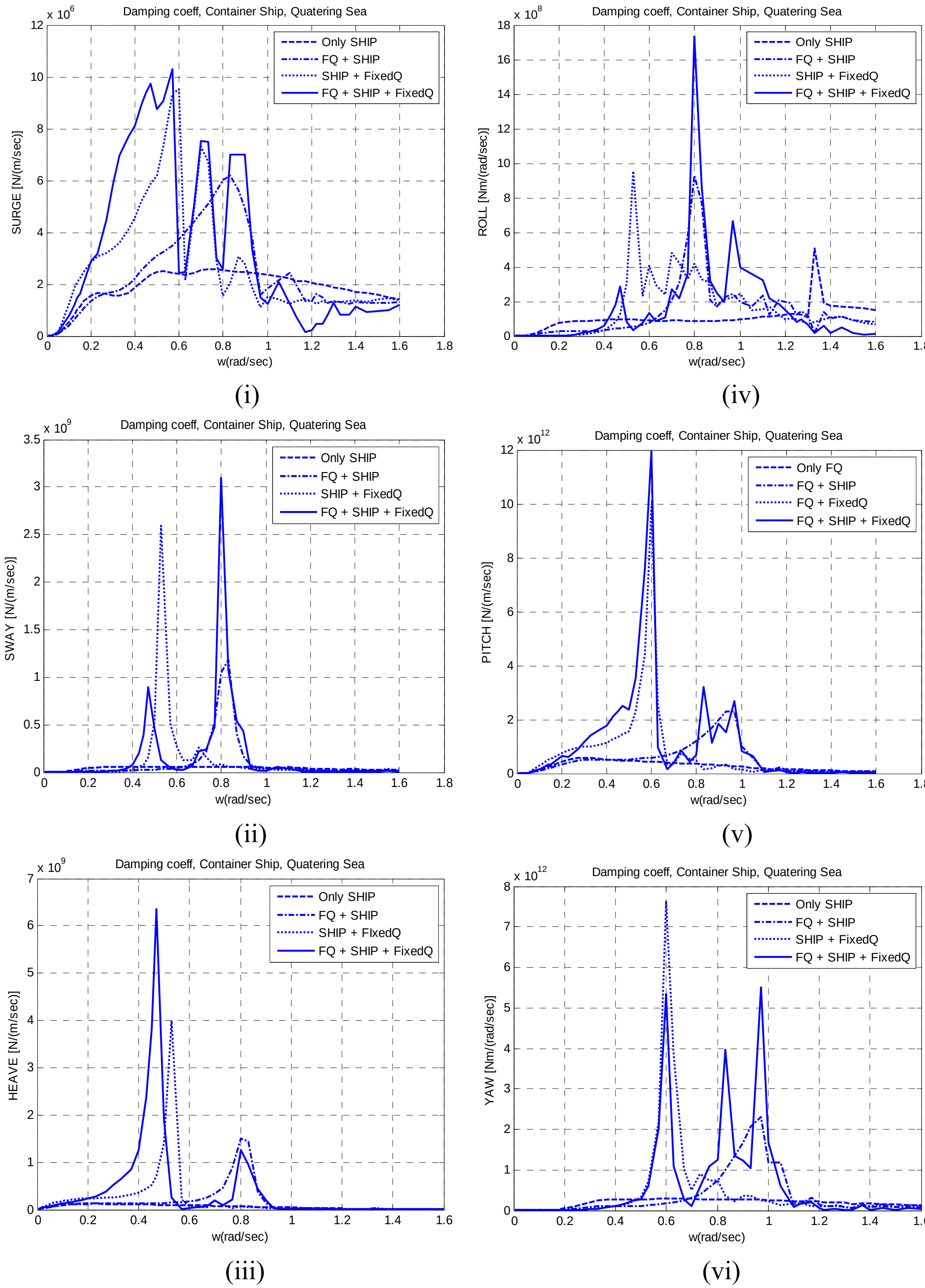

Fig. 3-4. Damping Coefficients of Container Ship

Table. 3-1. Natural Frequency for Each Mode

	Natural Frequency [rad/sec]			
Case	2body case [SHIP + FixedQ]	2body case [FQ + FixedQ]	3body case [FQ + SHIP + FixedQ]	
Mode	Container Ship	Floating Quay	Floating Quay	Container Ship
Surge	0.125	0.37	0.37	0.125
Sway	0.07	0.37	0.37	0.07
Heave	0.27	0.33	0.2	0.17
Roll	0.53	0.15	0.3	0.53
Pitch	0.33	0.37	0.33	0.27
Yaw	0.125	0.6	0.6	0.125

3.1.2 Wave Excitation Forces at 0 [deg] of Wave Heading

Frequency domain wave exciting forces are given in Fig.3-5 and Fig.3-6. Exciting forces of multi-body cases are pretty similar. The presence of Fixed Quay Wall makes little contribution to formation of exciting forces of 3 body case. The presence of another body also influences process of formation of exciting forces of 3 body case. There are resonant wave exciting forces at 0.6 [rad/sec] in Fig. 3-6 [(iii), (v), (vi)] and 0.8 [rad/sec] in Fig.3-5 [(ii), (iii), (iv), (v), (vi)] and Fig 3-6 [(ii), (iv)].

Figure 3-7 shows mean drift forces exerted on the floating quay and the container ship. As the shape of the floating quay is symmetrical about the Y-Z plane, the surge direction drift force for single body is relatively small. From Figure 3-7[(ii), (v)], it shows that the sway drift force from 0.9 [rad/sec] to 1.4 [rad/sec] is considerable to make the floating quay and container ship move away from each other. The floating quay tends to move in the opposite direction to the incident wave away from the container ship whereas the container ship tends to move in the direction of the incident wave towards the fixed quay wall.

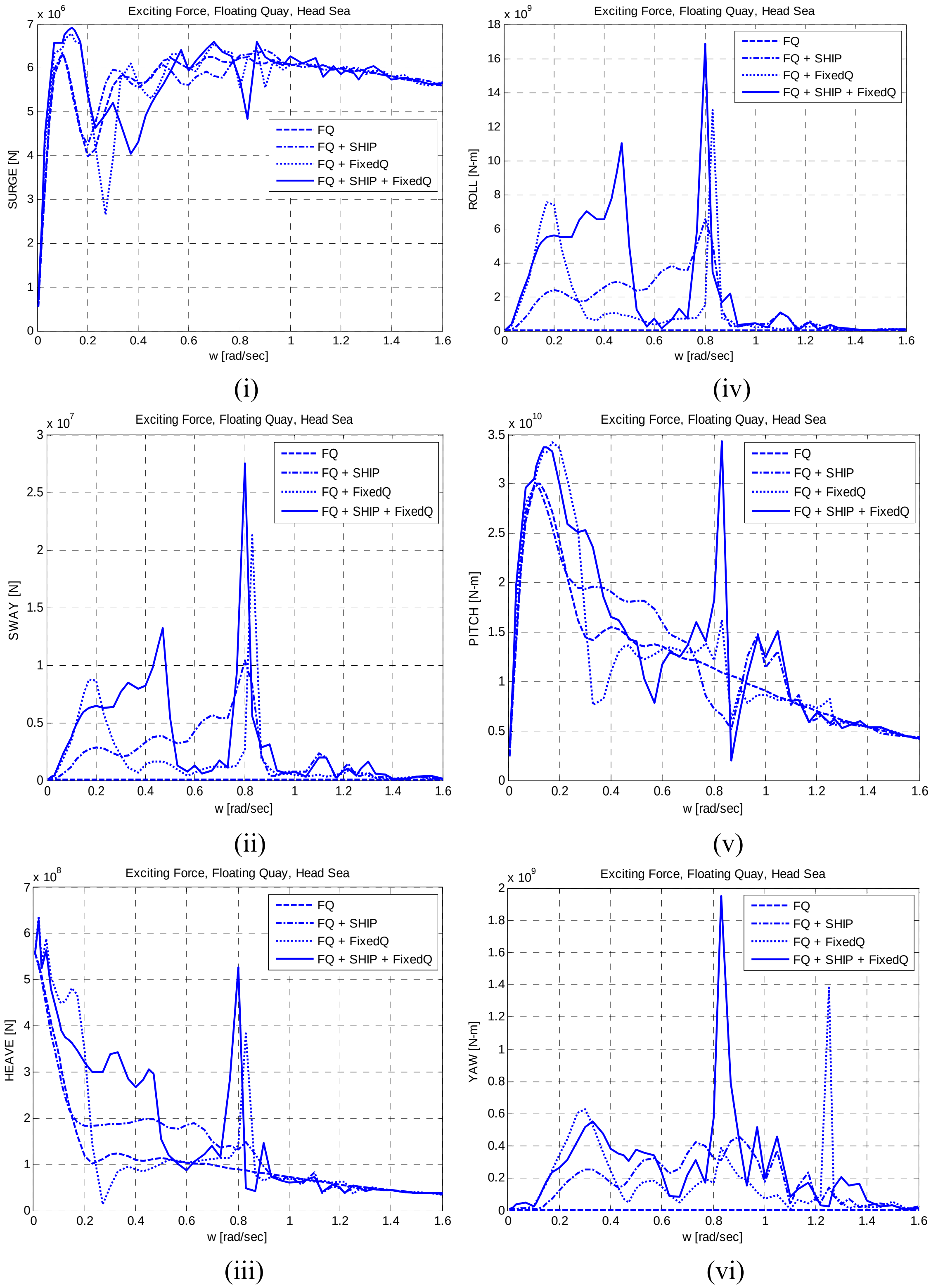

Fig. 3-5. Wave Excitation Forces for Floating Quay for 0 [deg] Wave Heading

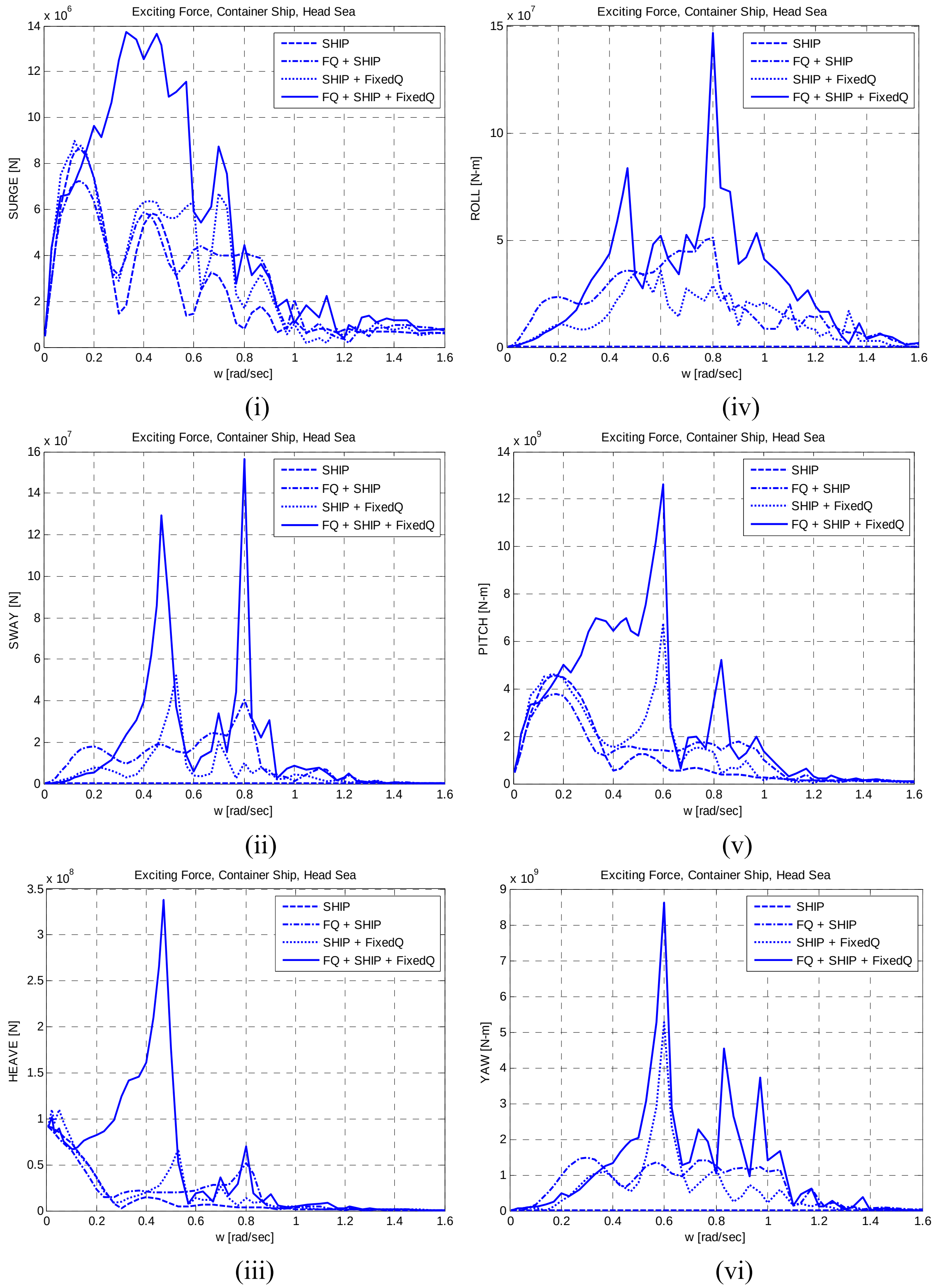

Fig. 3-6. Wave Excitation Forces for Container Ship for 0 [deg] Wave Heading

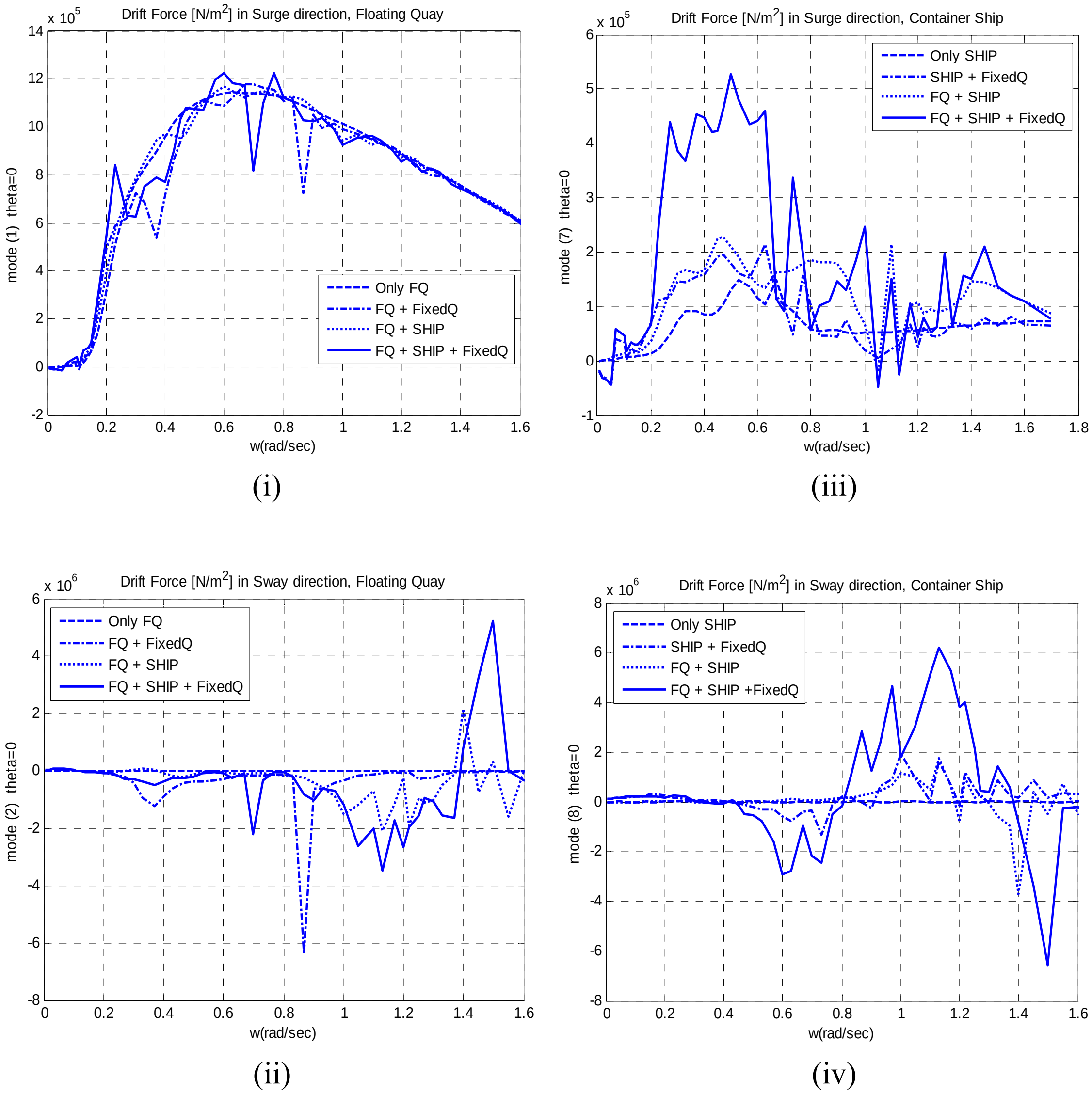

Fig. 3-7. Drift Forces for 0 [deg] Wave Heading

3.1.3 Response Amplitude Operators at 0 [deg] of Wave Heading

The incident wave train travels parallel to side by side arrangement of Floating Quay, Container Ship, and Fixed Quay Wall i.e. looking to the positive Y-direction in the layout. This is the condition in which two dolphins, one on the forward and the other on the aft portion of Floating Quay have been placed to curb horizontal motions (surge, sway and yaw), although small motion of surge, sway, and yaw is allowed. And hawser connections were put between Fixed Quay Wall and Container Ship for the same cause. Because the three body arrangement is unsymmetrical to the incident wave direction, the reflected waves are not equally spread around the floating body surfaces. And three bodies are placed side by side in close proximity, so interaction between bodies occurs.

Figure 3-8 and Figure 3-9 illustrate the response motions of Floating Quay and Container Ship respectively. Due to symmetric body shape of Floating Quay and Container Ship, no sideways motion of the single body exists. The sway motion of single body is negligibly small. The interaction effect in the multi-body case makes sway motion greater than that in single body case, which means sway motion in multi-body case is not negligible. There are spiky motions at frequencies mentioned in Table.3-1. Spiky motions do not always synchronize with natural frequency points. However, they are well matched. Those motions also happen because of interaction effect between interacting bodies. The resulting surge, heave, pitch response motions of single body case and multi-body case are pretty similar.

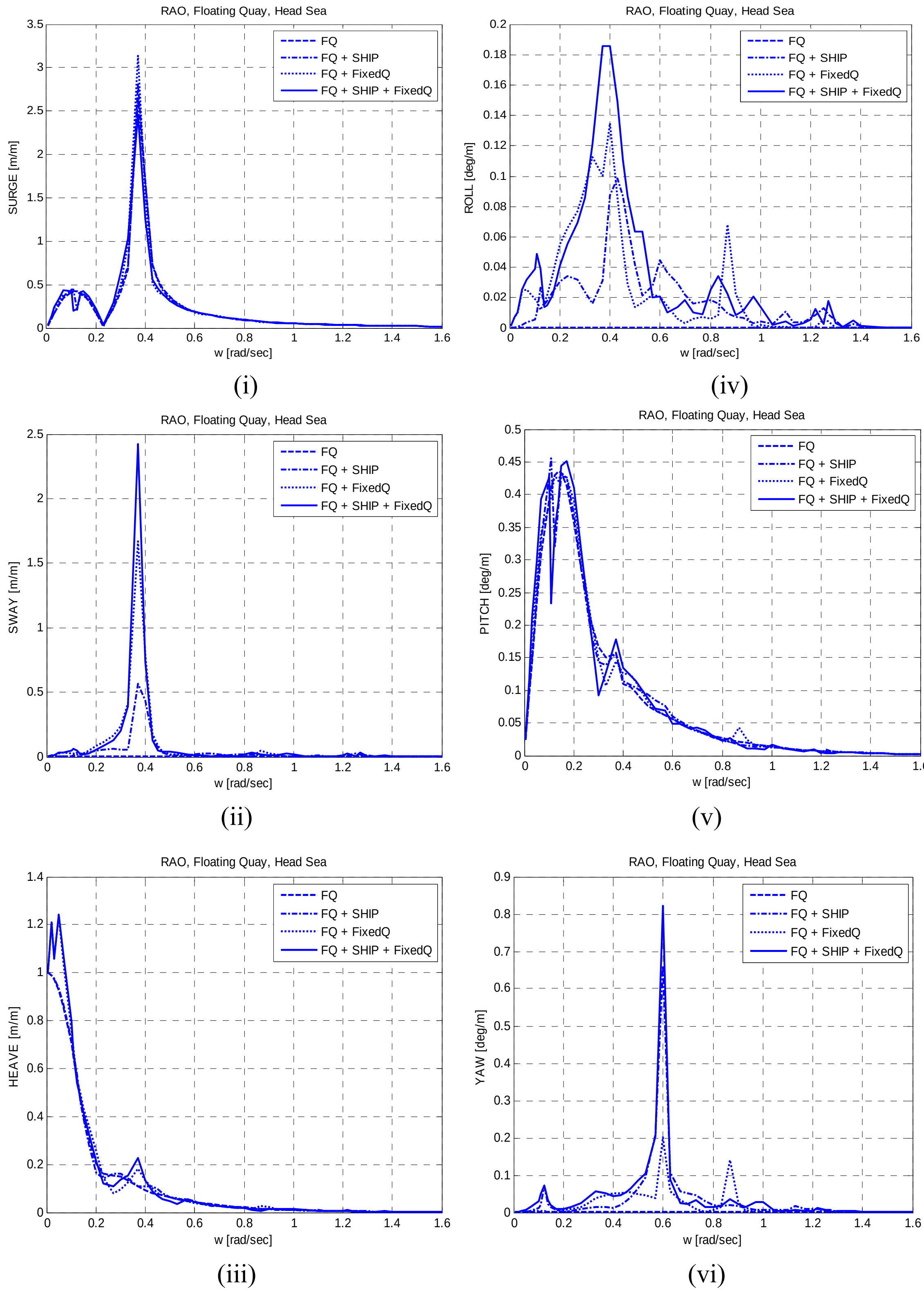

Fig. 3-8. Response Amplitude Operators of Floating Quay for 0 [deg] Wave Heading

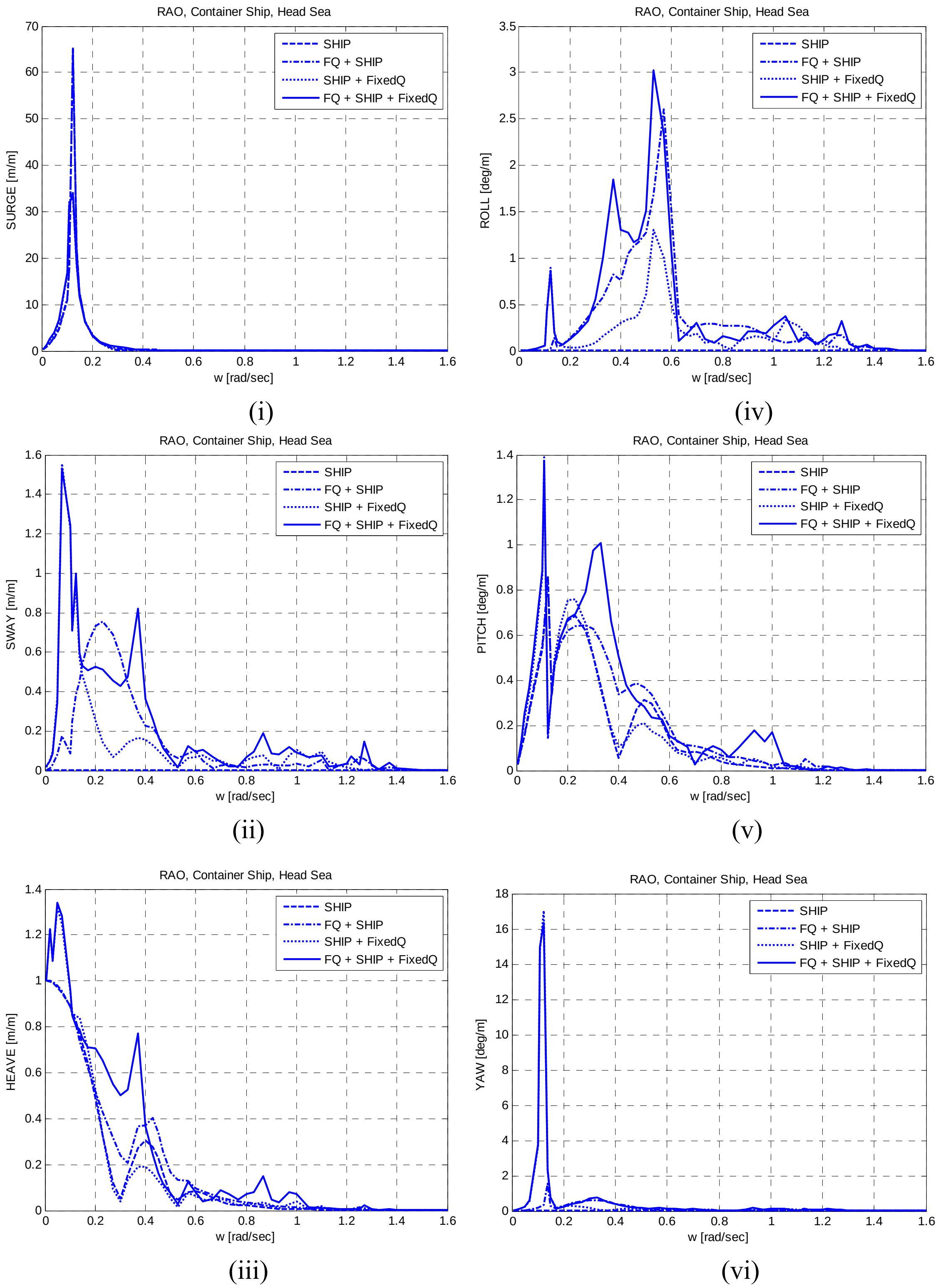

Fig. 3-9. Response Amplitude Operators of Container Ship for 0 [deg] Wave Heading

3.1.4 Wave Elevation in the Gap at 0[deg] of Wave Heading

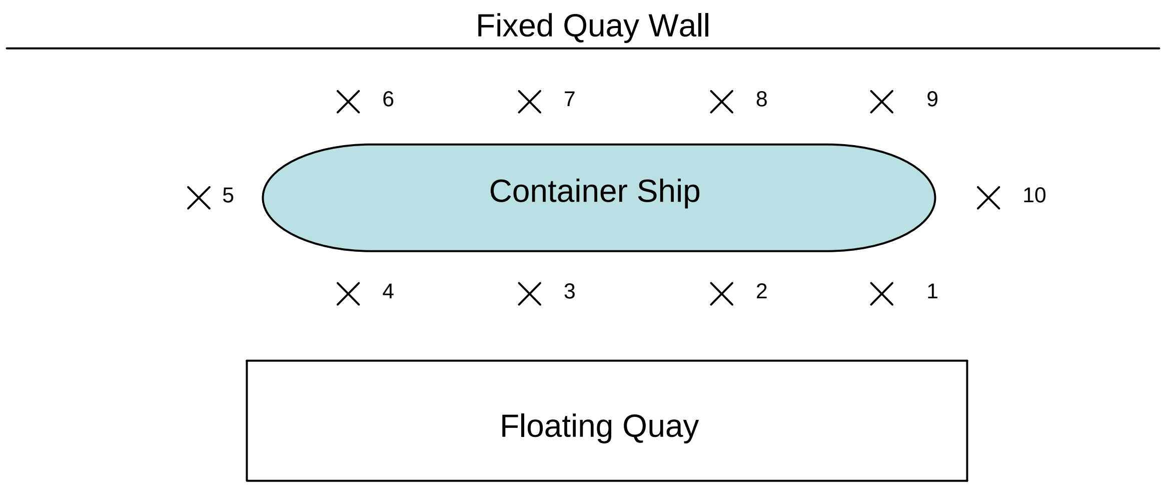

Fig. 3-10. Point Location for Wave Elevations

The 3 body case wave elevations are influenced by the presence of Fixed Quay Wall, Container Ship, and Floating Quay. The wave elevations at point 1, 2, 3, 9 are relatively small, because of closeness to open sea and gap 40 [m] between Floating Quay and Fixed Quay, and those points are less influenced by Container Ship due to wave direction. The wave elevations at point 4, 5, 6, 10 are bigger than the previous points due to the narrow channel 2.1[m] between Container Ship and Floating Quay, interaction between two floating bodies and reflection from Fixed Quay Wall. The wave elevations at point 7, 8 are biggest because of the narrow channel 2.1[m] and strong reflection effect from the presence of Fixed Quay and Container Ship. The wave energy can not penetrate Fixed Quay Wall. These events make those wave elevations biggest. Point location is seen in Fig. 3-10, and frequency domain wave elevation at each point is shown in Fig. 3-11.

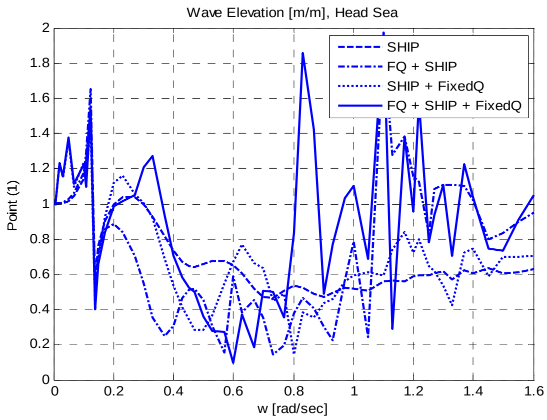

Wave Elevation at Point 1

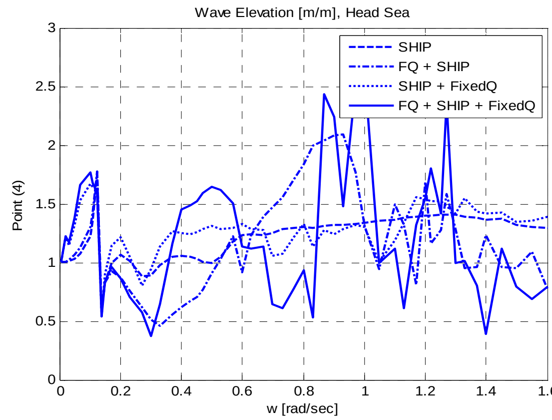

Wave Elevation at Point 4

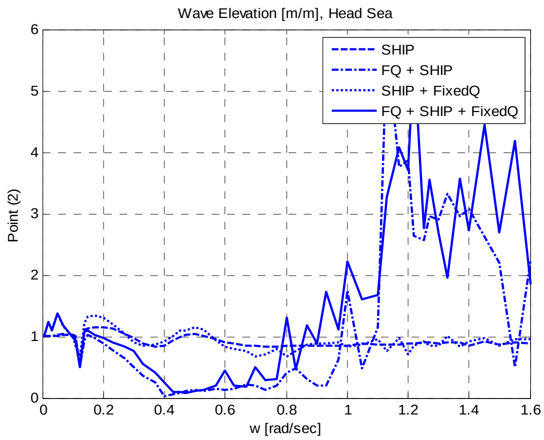

Wave Elevation at Point 2

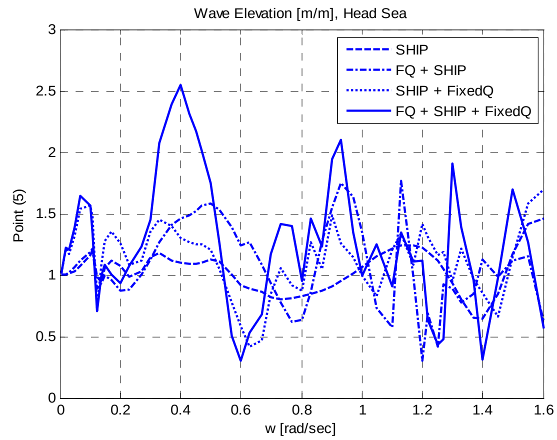

Wave Elevation at Point 5

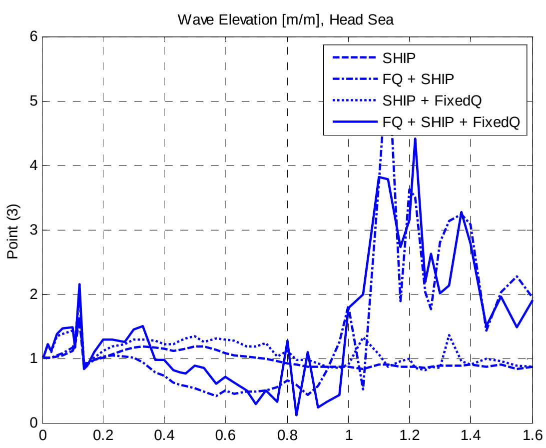

Wave Elevation at Point 3

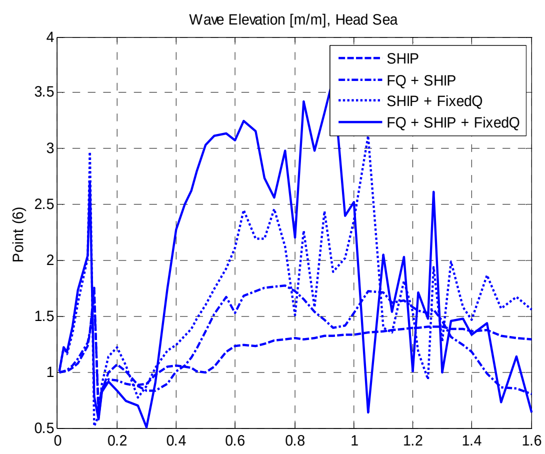

Wave Elevation at Point 6

Fig. 3-11. Wave Elevation at 0[deg] Wave Heading

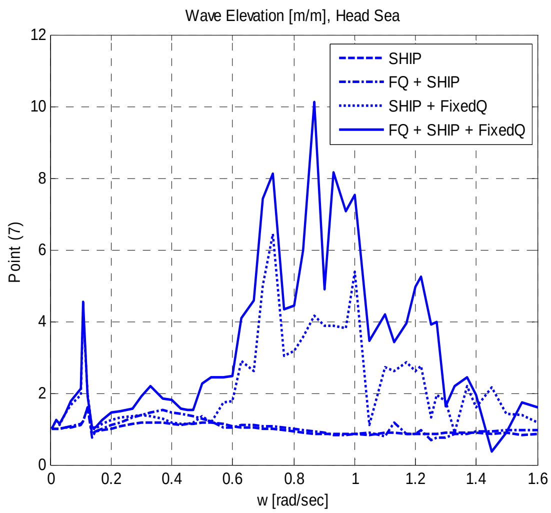

Wave Elevation at Point 7

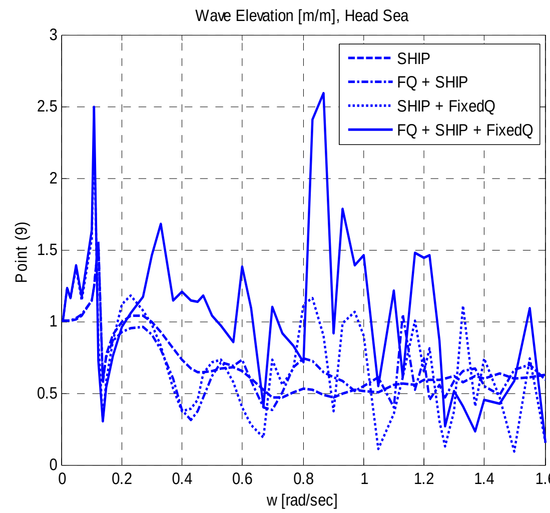

Wave Elevation at Point 9

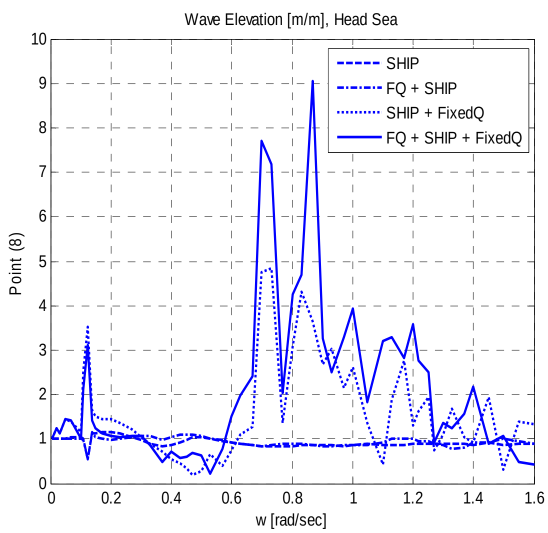

Wave Elevation at Point 8

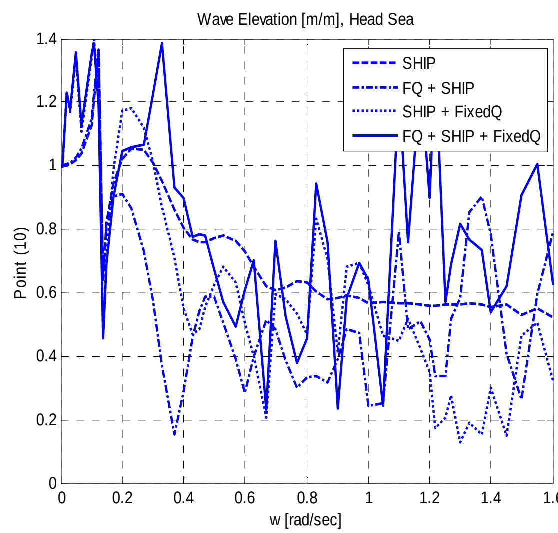

Wave Elevation at Point 10

Fig. 3-11. Continued

3.1.5 Wave Excitation Forces at 45[deg] of Wave Heading

Frequency domain wave exciting forces are given in Fig. 3-12 and Fig. 3-13. Exciting forces of single body case and FQ + SHIP case are similar, and Exciting forces of 2body (FQ + FixedQ, SHIP + FixedQ) case and 3body (FQ + SHIP + FixedQ) case are also pretty identical. The presence of a Fixed Quay Wall mainly contributes to formation of exciting forces of 3 body case. The presence of another body also effects process of formation of exciting forces of 3 body case.

In Figure 3-12(iii), the multi-body heave exciting force for the floating quay at low frequency (long wave) is bigger than the single body heave exciting force due to the additional effects of the reflected waves in the multi-body case. There are spiky exciting forces at 0.47 [rad/sec] in Fig. 3-12(iii) and Fig. 3-13[(ii), (iii)], at 0.6 [rad/sec] in Fig. 3-13[(v), (vi)], and 0.8 [rad/sec] in Fig. 3-12[(ii), (iii), (iv), (v), (vi)].

Fig. 3-14 show mean drift forces exerted on the floating quay and the container ship. And the surge drift force for multi-body is also relatively small compared to the sway and heave drift force for multi-body. From Fig. 3-14 [(ii), (v)], it shows that the sway drift force at 1.05 [rad/sec] is large to make the floating quay and container ship move away from each other. The floating quay will tend to move in the opposite direction to the incident wave away from the container ship while the container ship will tend to move in the direction of the incident wave towards the fixed quay wall.

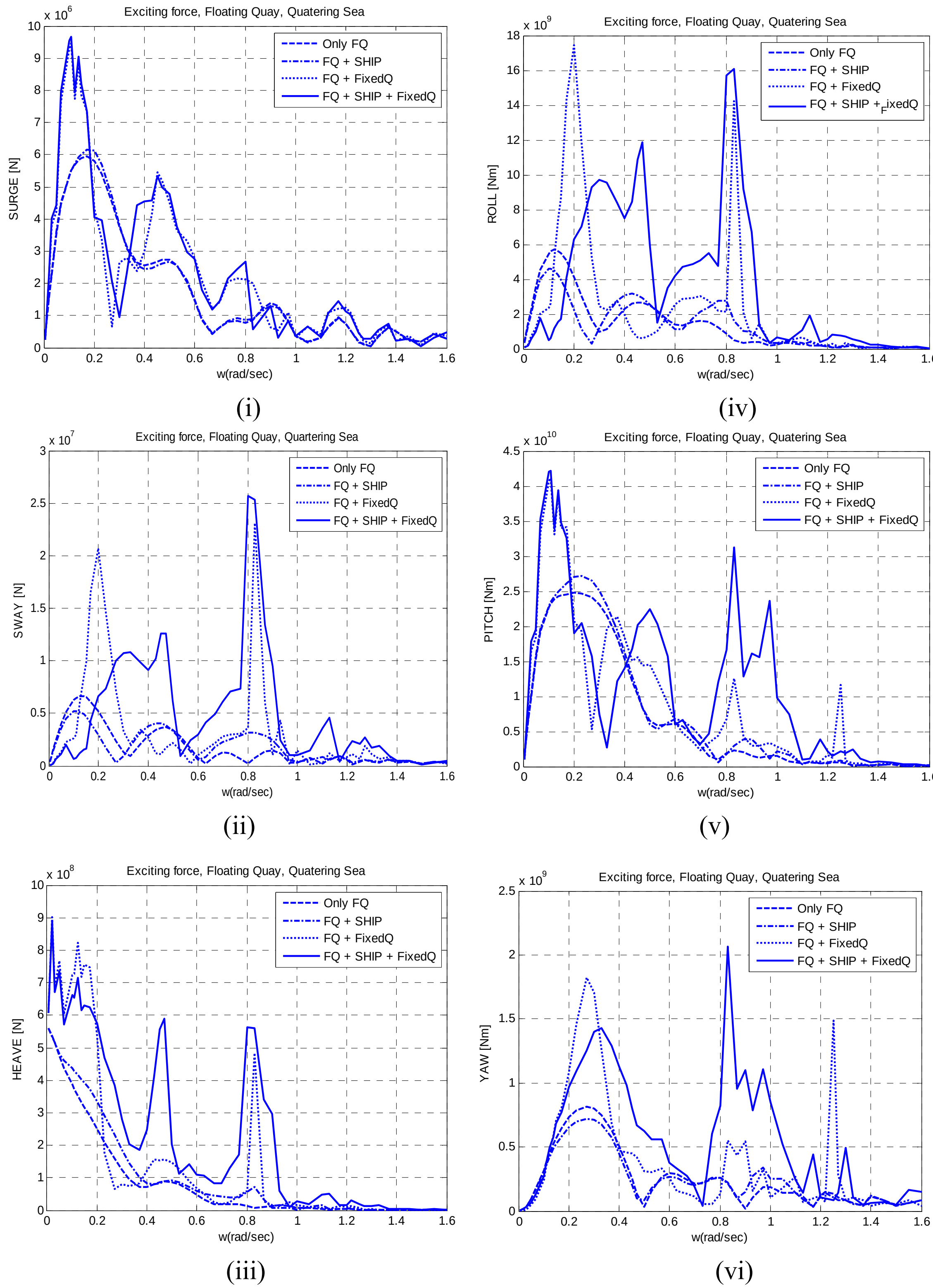

Fig. 3-12. Wave Excitation Forces for Floating Quay for 45 [deg] Wave Heading

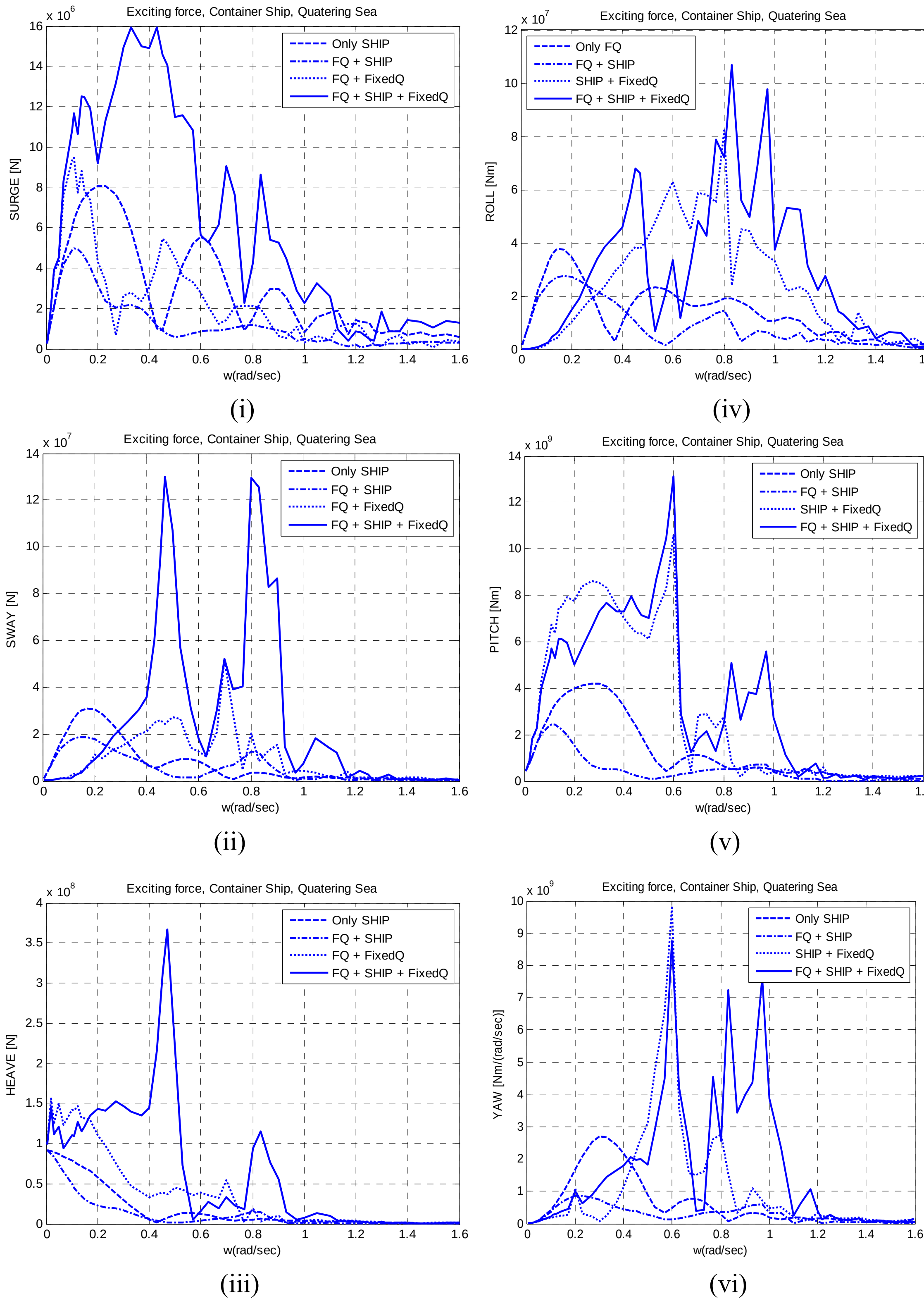

Fig. 3-13. Wave Excitation Forces for Container Ship for 45 [deg] Wave Heading

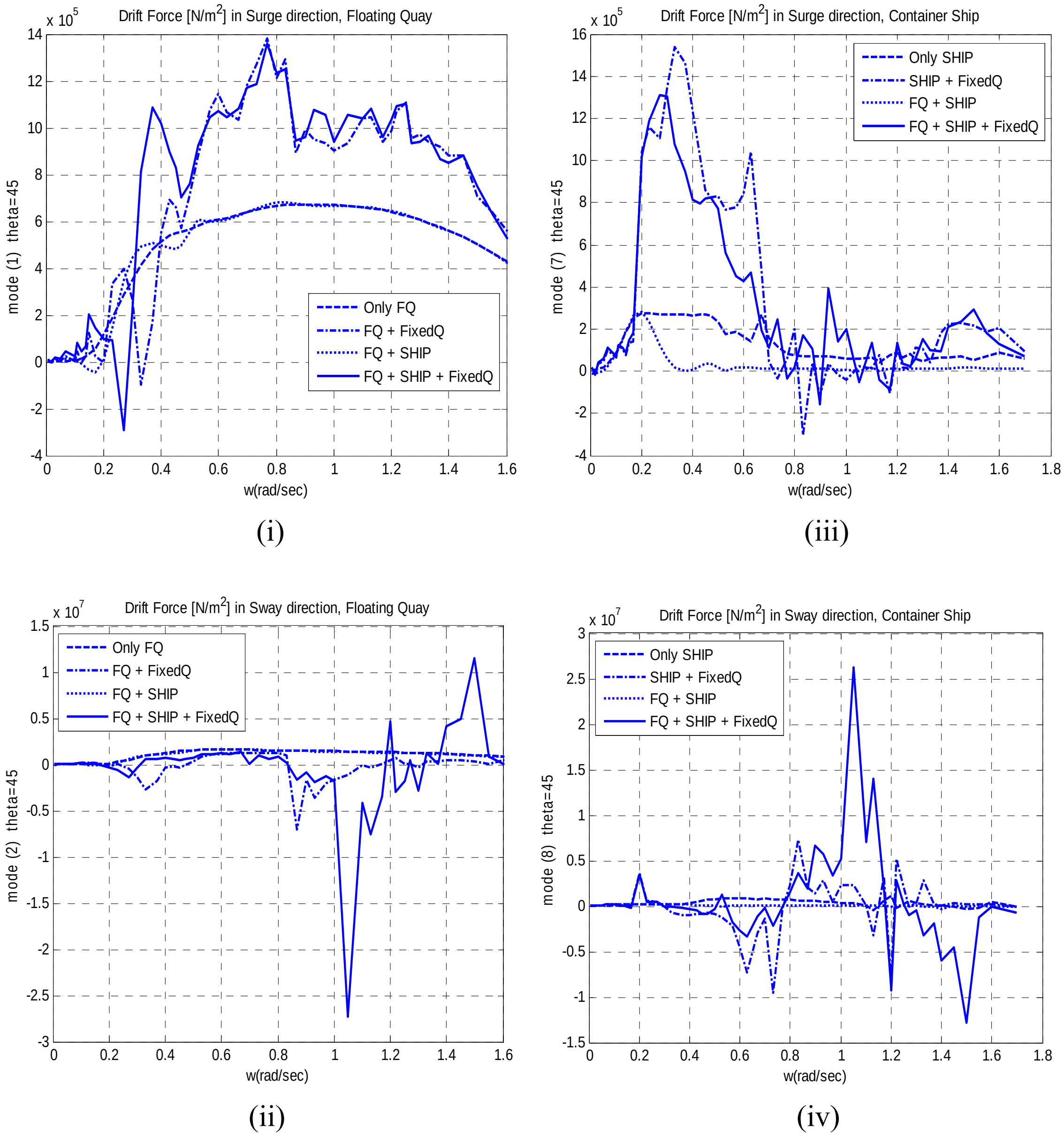

Fig. 3-14. Drift Forces for 45 [deg] Wave Heading

3.1.6 Response Amplitude Operators at 45[deg] of Wave Heading

The incident wave train travels at 45 [deg] of attack angle to side by side arrangement of Floating Quay, Container Ship, and Fixed Quay Wall, the right side of Floating Quay is the weather side. This is the condition in which two dolphins, one on the forward and the other on the aft portion of Floating Quay have been equipped to prevent Floating Quay from surge, sway and yaw motion, even though small motion of surge, sway, and yaw is limitedly allowed. And hawser connections were placed between Fixed Quay Wall and Container Ship for the same purpose.

The resulting response motions of single body case (Only FQ and Only SHIP) and two floating body case (FQ + SHIP) at 45 [deg] of incident wave angle are similar. In Figure 3-15 and Figure 3-16, the response motions of multi-body case are a little greater than those of single body case in floating quay and container ship motion. There are some high peak motions due to the interaction effects and presence of frequency points where they are close to natural frequency points. The ship motion responses of single body case and 2body (FQ + SHIP) case are similar, but the ship motion of single body case is slightly bigger than that of 2 body (FQ + SHIP) case because of shielding effect of Floating Quay. As seen below, the 3 body (FQ + SHIP + FixedQ) response motions are affected by another floating body, but strongly influenced by reflection caused by the presence of Fixed Quay Wall.

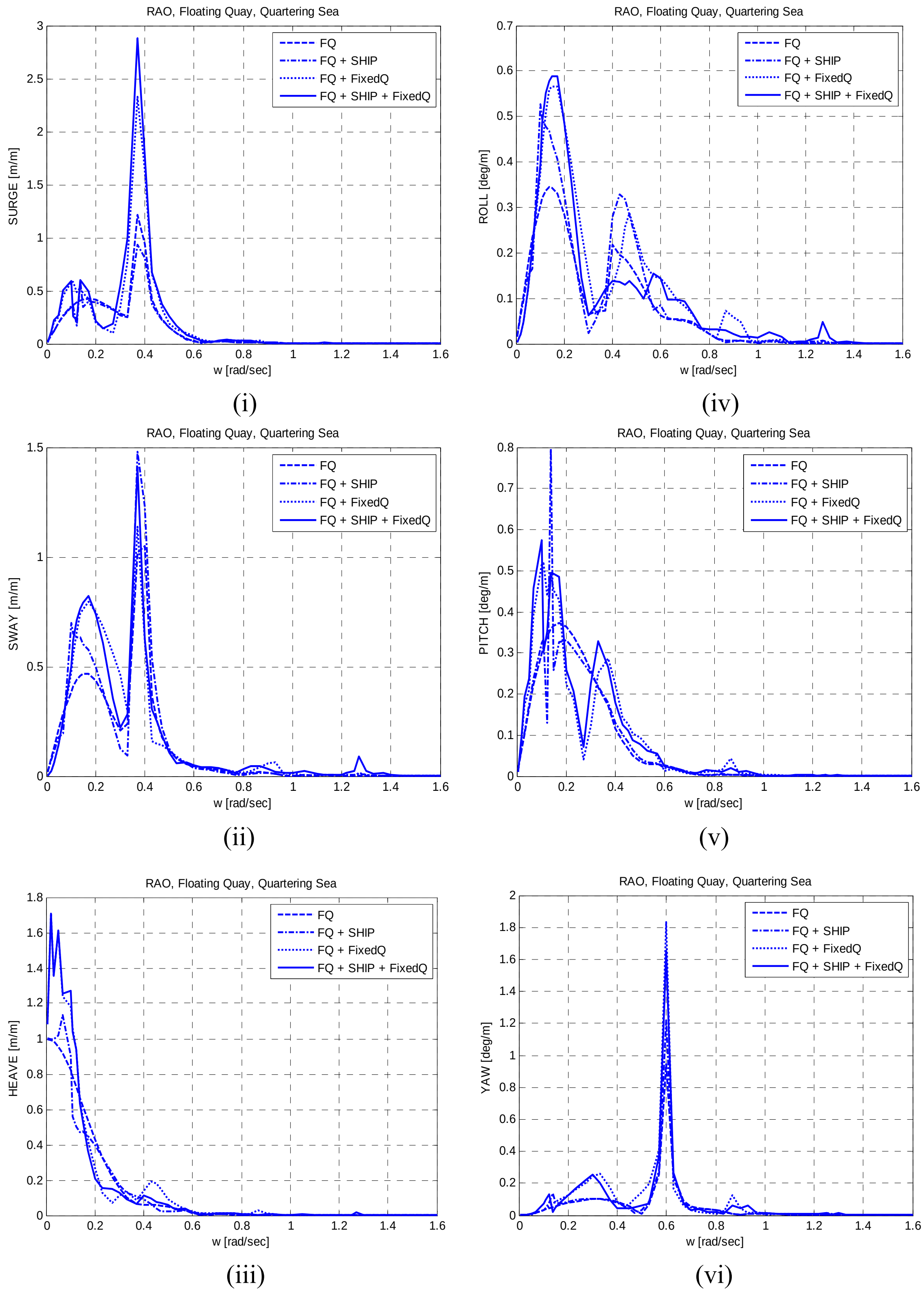

Fig. 3-15. Response Amplitude Operators of Floating Quay for 45 [deg] Wave Heading

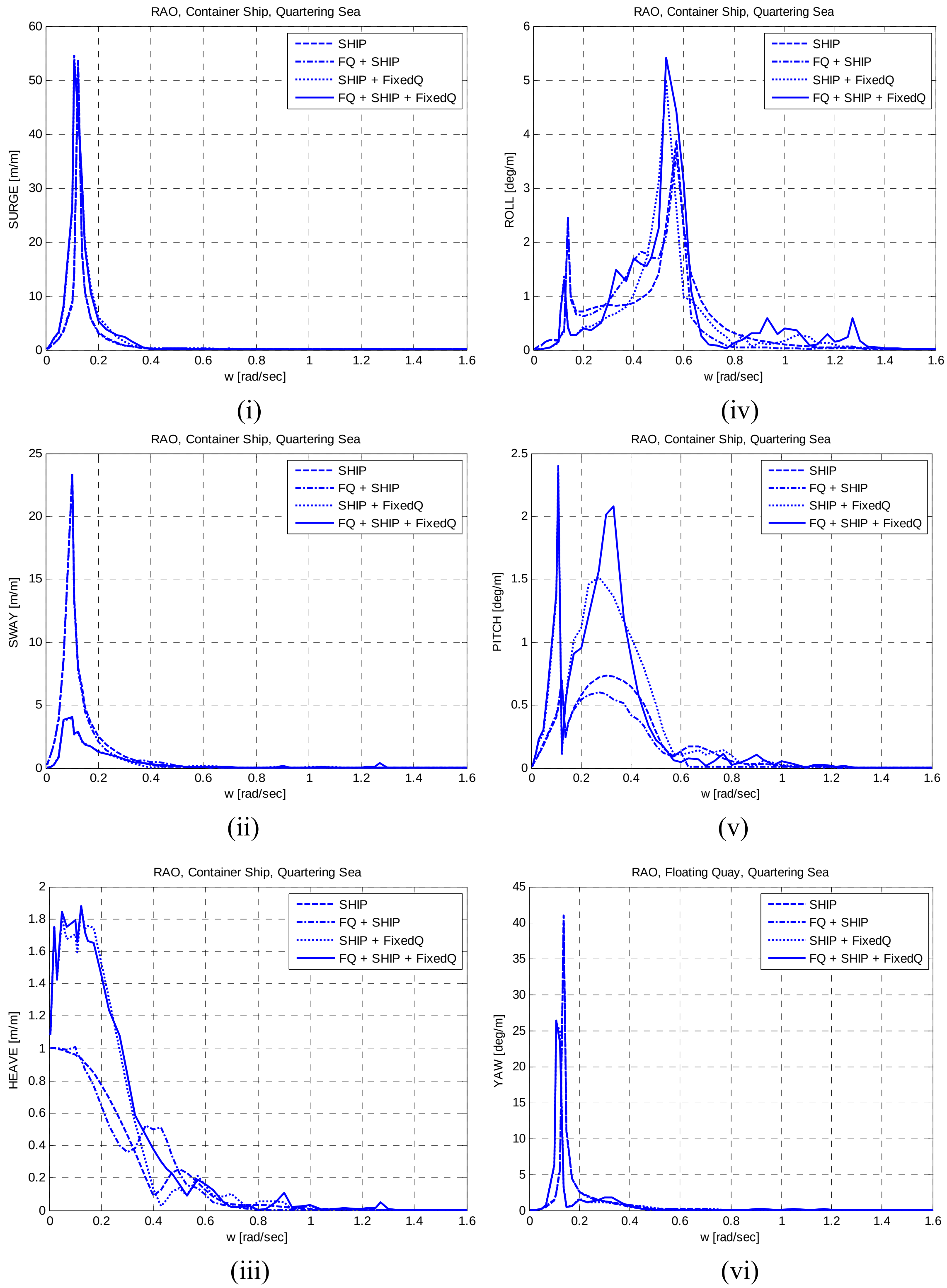

Fig. 3-16. Response Amplitude Operators of Container Ship for 45 [deg] Wave Heading

3.1.7 Wave Elevation in the Gap at 45[deg] of Wave Heading

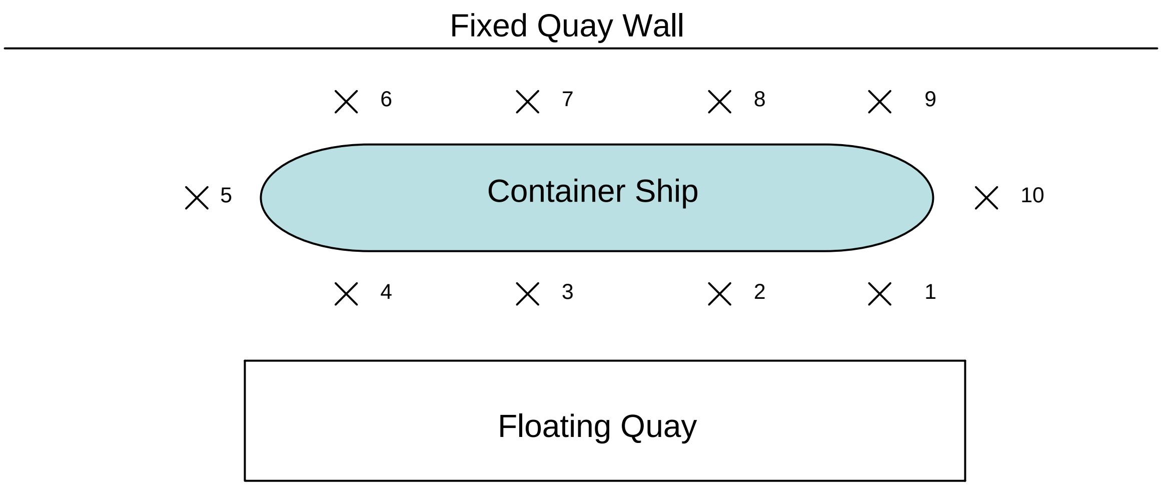

Fig. 3-17. Location of 10 points for wave elevations

Point locations are seen in Fig. 3-17, and frequency domain wave elevations at those points are shown in Fig. 3-18. The 3body case wave elevations are effected by the presence of Fixed Quay Wall, Container Ship, and Floating Quay. The wave elevations at point 1, 5, 9,10 are relatively small, because of closeness to open sea and gap 40 [m] between Floating Quay and Fixed Quay. Those points are less effected by Container Ship, and shielding effect of two floating bodies. The wave elevations at point 4, 6 are bigger than the previous points due to the narrow channel 2.1[m] between Container Ship and Floating Quay, interaction between two floating bodies and reflection from Fixed Quay Wall. The wave elevations at point 2, 3, 7, 8 are biggest because of the narrow channel 2.1[m] and strong reflection effect due to the presence of Fixed Quay and Container Ship. The wave energy is not able to penetrate Fixed Quay Wall, so it was completely bounced back.

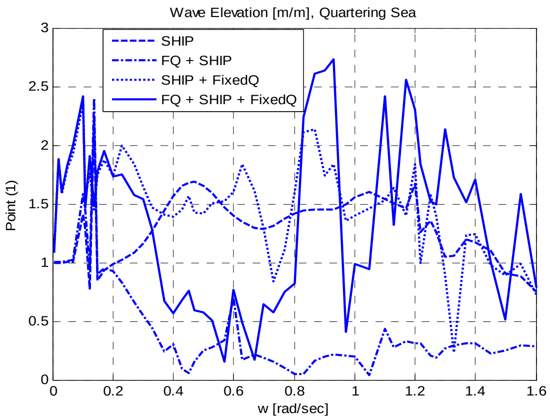

Wave Elevation at Point 1

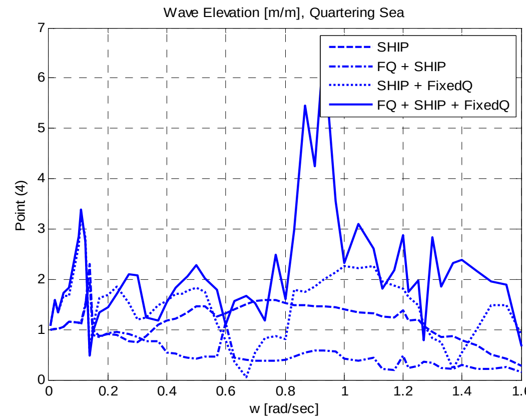

Wave Elevation at Point 4

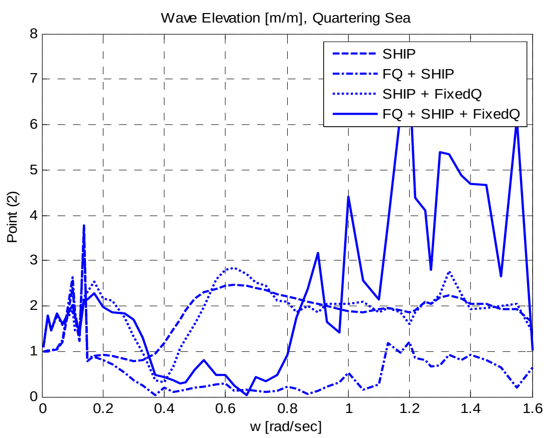

Wave Elevation at Point 2

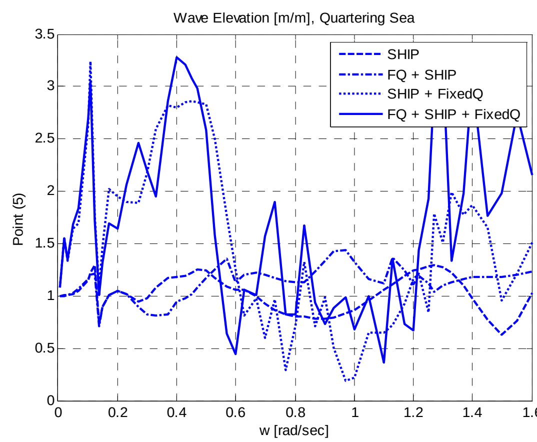

Wave Elevation at Point 5

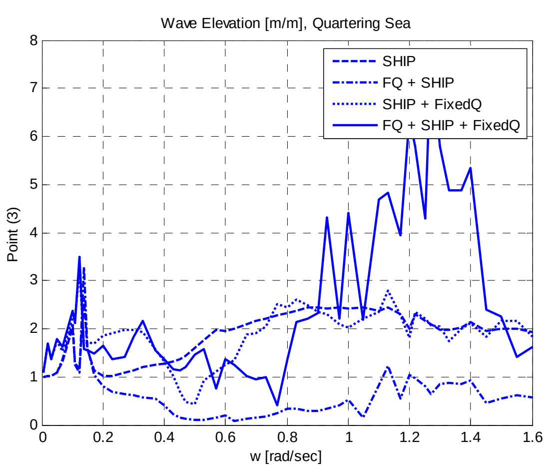

Wave Elevation at Point 3

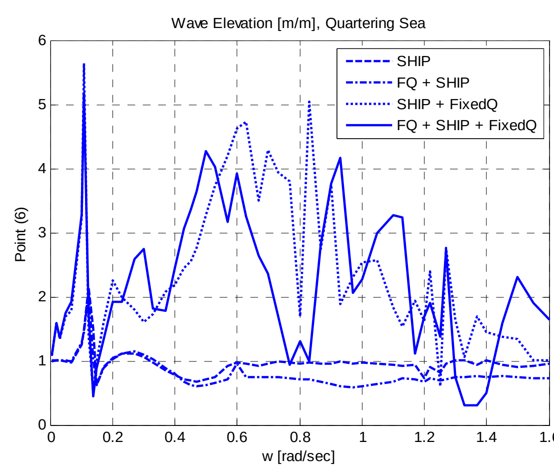

Wave Elevation at Point 6

Fig. 3-18. Wave Elevation at 45[deg] Wave Heading

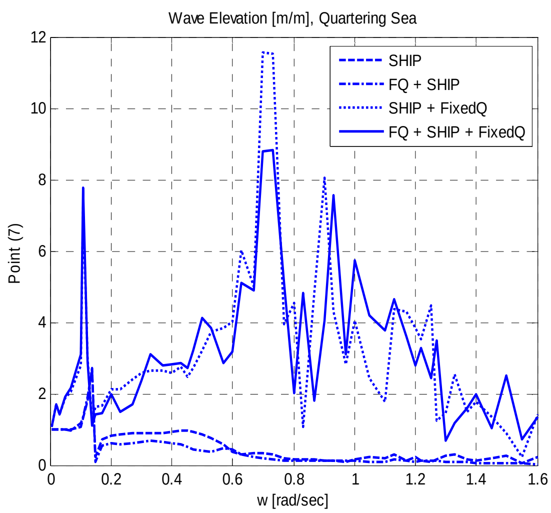

Wave Elevation at Point 7

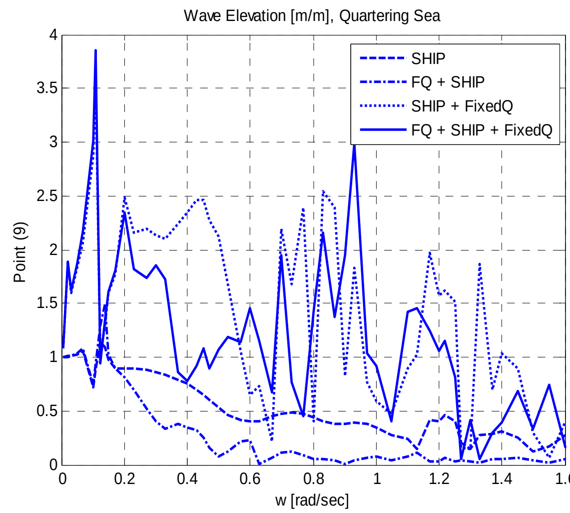

Wave Elevation at Point 9

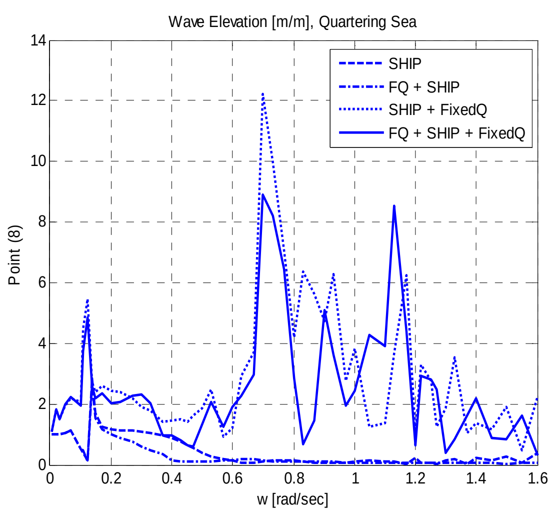

Wave Elevation at Point 1

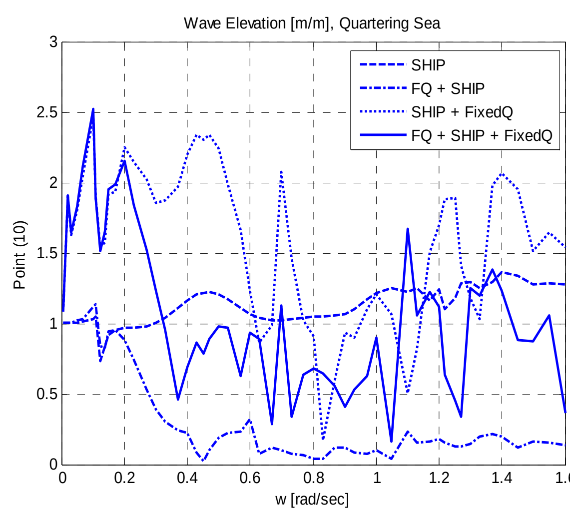

Wave Elevation at Point 10

Fig. 3-18. Continued

3.1.8 Wave Excitation Forces at 90[deg] of Wave Heading

Frequency domain wave exciting forces are given in Fig. 3-19 and Fig. 3-20. Exciting forces of single body (Only FQ and Only SHIP) case and two floating body (FQ + SHIP) case are similar, and Exciting forces of 2body (FQ + FixedQ and SHIP + FixedQ) case and 3 body (FQ + SHIP + FixedQ) case are so. The presence of a Fixed Quay Wall mainly makes a major contribution to formation of exciting forces of 3 body case. The presence of another floating body also effects process of formation of exciting forces of 3 body case relatively weakly. In Fig. 3-19(iii), the multi-body heave exciting force for the floating quay at low frequency is bigger than the single body case heave exciting force due to the additional effects of the reflected waves in the multi-body case.

In Fig. 3-20[(ii), (iii), (iv)], the multi-body case sway, heave, and roll exciting force for the container ship is less than the single body case exciting force on the most of frequency range. There are peak wave exciting forces at 0.6 [rad/sec] in Figure 3-20[(v), (vi)]. and 0.8 [rad/sec] in Figure 3-19[(ii), (iii), (iv), (v), (vi)] and Figure 3-20[(ii), (iv), (v), (vi)]. Figure 3-21 show mean drift forces exerted on the floating quay and the container ship. As the shape of the floating quay is symmetrical about the Y-Z plane, the surge direction drift force for single body is very small and negligible. And the surge drift force for multi-body is also relatively small compared to the sway and heave drift force for multi-body. From Figure 3-21[(ii), (v)], it shows that the sway drift force at 1.05 [rad/sec] is large to make the floating quay and container ship move away from each other. The floating quay tends to move in the opposite direction to the incident wave away from the container ship.

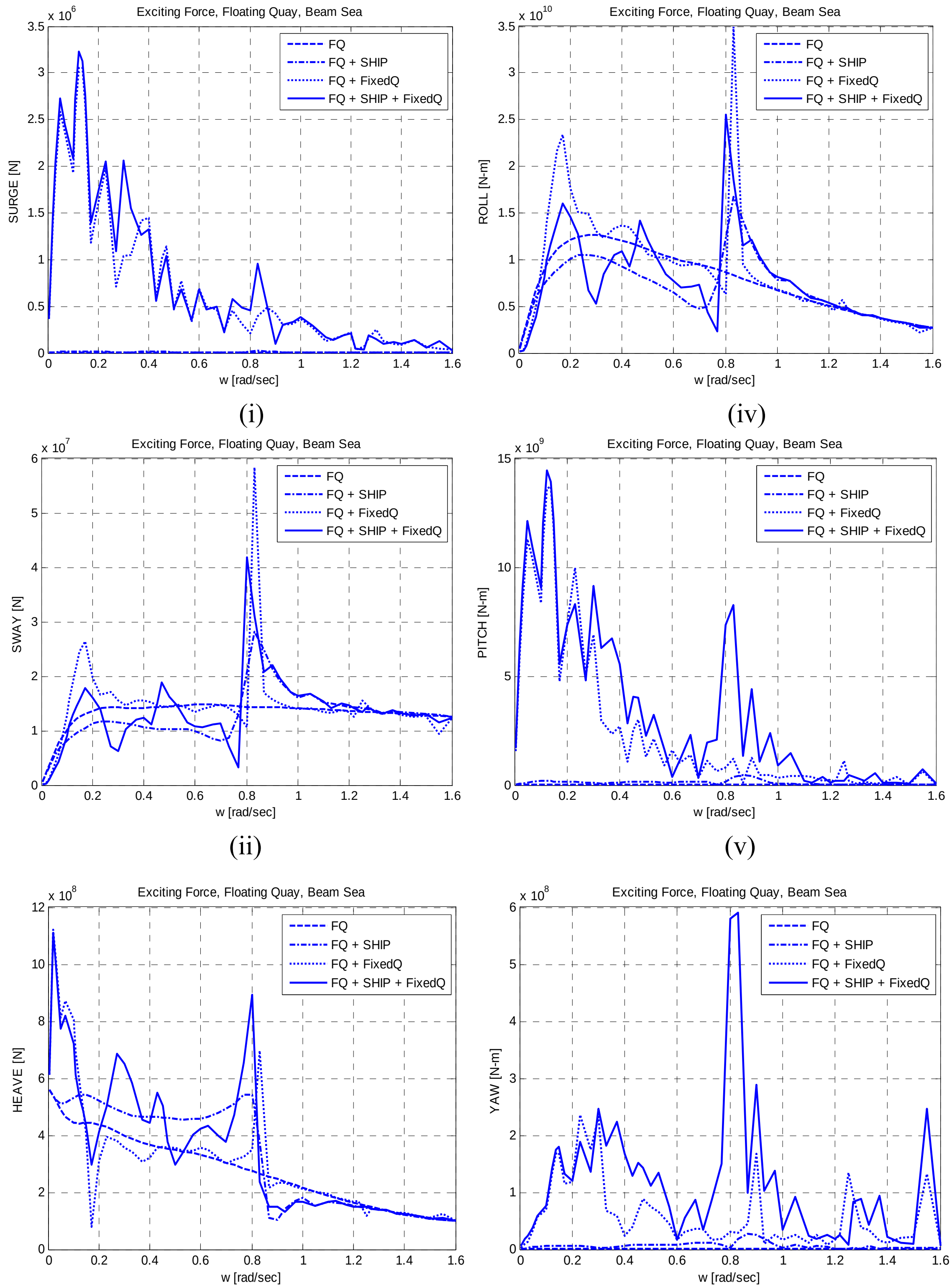

(iii) (vi)

Fig. 3-19. Wave Excitation Forces for Floating Quay for 90 [deg] Wave Heading

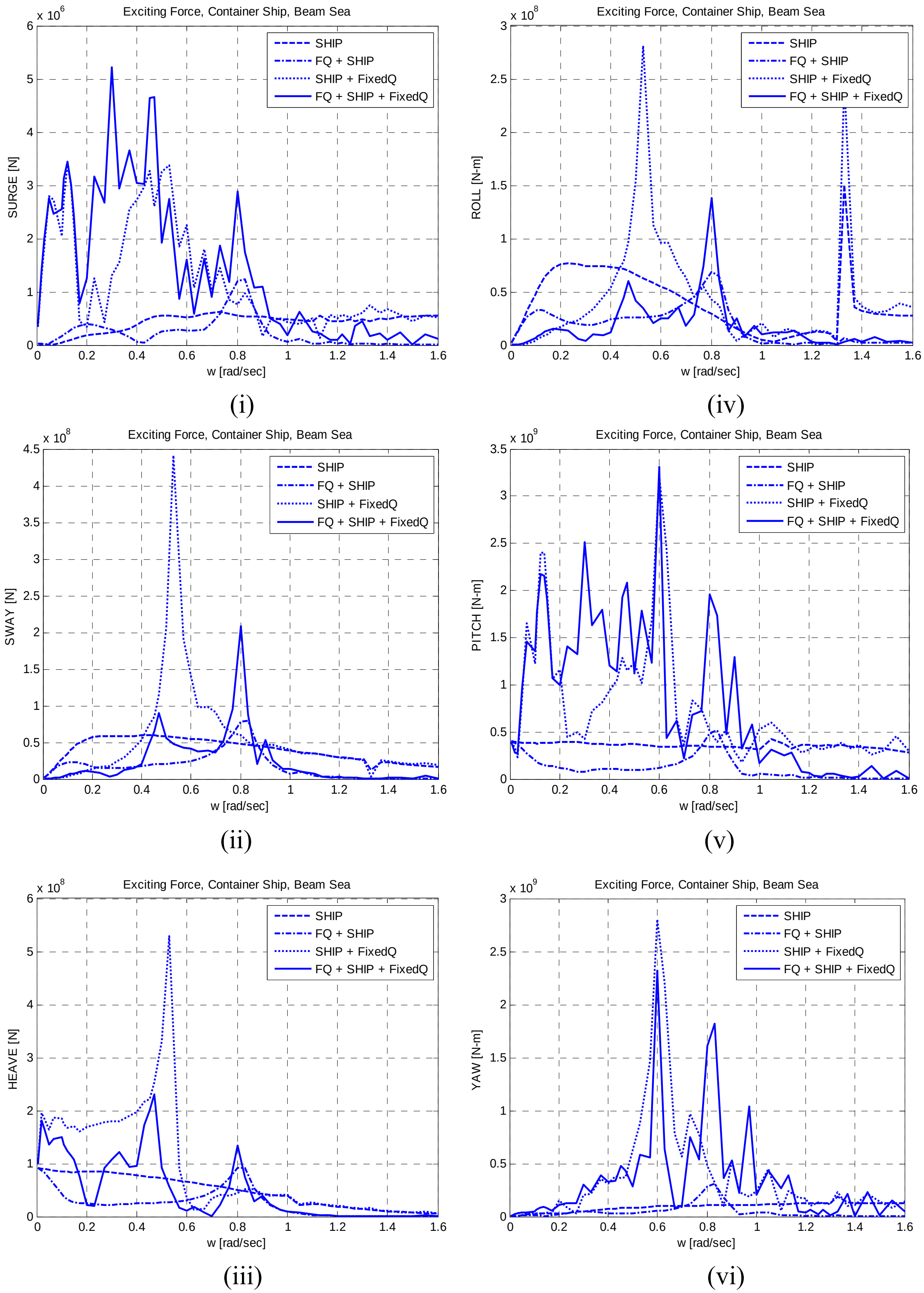

Fig. 3-20. Wave Excitation Forces for Container Ship for 90 [deg] Wave Heading

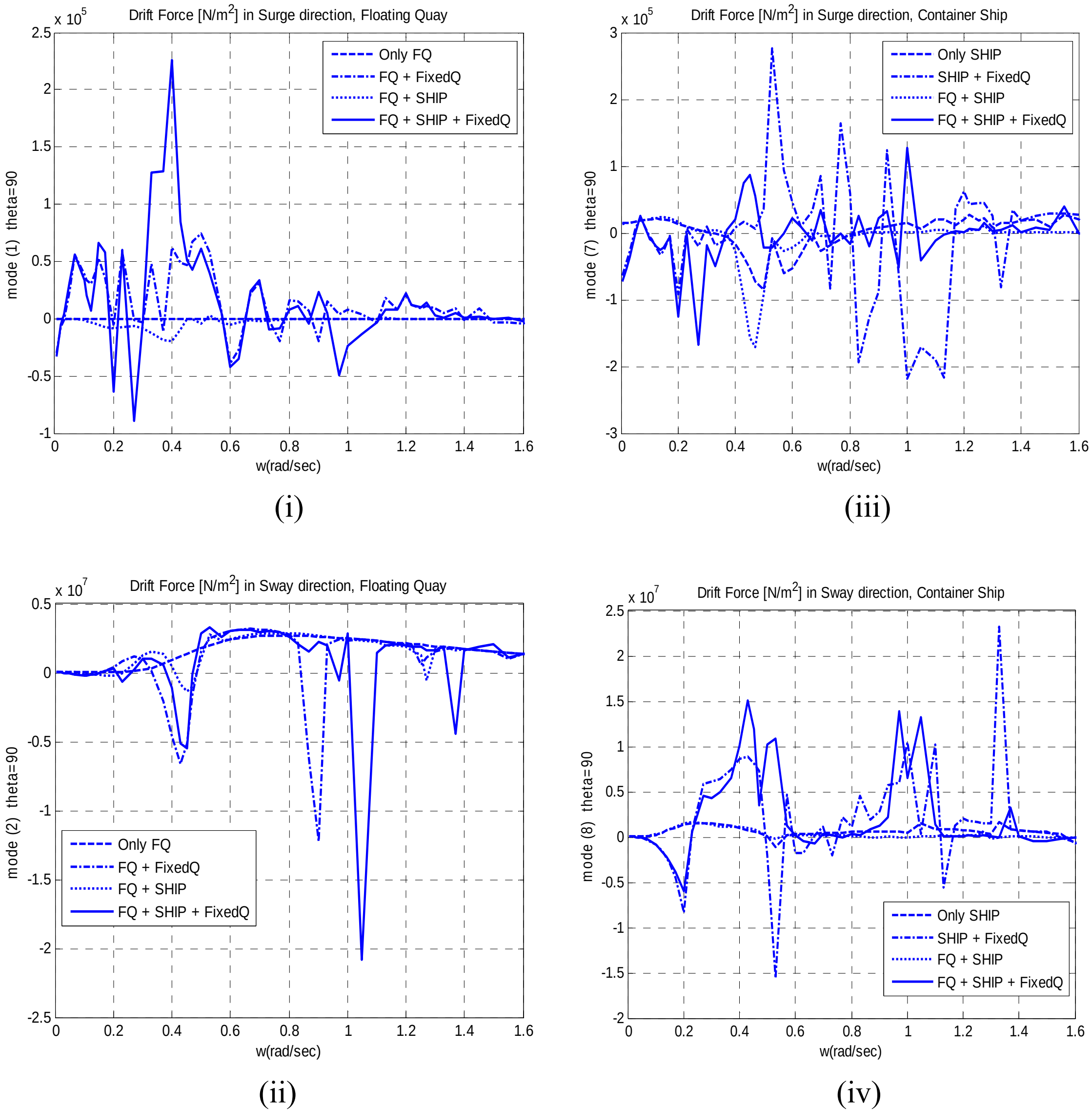

Fig. 3-21. Drift Forces for 90 [deg] Wave Heading

3.1.9 Response Amplitude Operators at 90[deg] of Wave Heading

Figure 3-22 and Figure 3-23 illustrate Response Amplitude Operators of Floating Quay and Container Ship. In this case the incident wave train travels perpendicular to side by side arrangement of Floating Quay, Container Ship, and Fixed Quay Wall i.e. looking to the positive X-direction in the layout, the right side of Floating Quay is the weather side. This is the condition in which two dolphins, one on the forward and the other on the aft portion of Floating Quay have been attached to prevent Floating Quay from surge, sway and yaw motion, even though a little motion of surge, sway, and yaw is allowed limitedly. And hawser connections were placed between Fixed Quay Wall and Container Ship for the same reason. In this case of the wave direction of 90 [deg], wave force contributes little to surge, pitch, and yaw direction motion. Surge, sway, and yaw RAOs are very small compared to other mode motions, and sway, heave, and roll RAOs are comparatively significant due to wave direction and interaction effects between bodies as shown below. Because the three body arrangement is as symmetrical to the incident wave direction, the reflected waves are not equally spread around the floating body surfaces. The interaction effects between the interacting bodies also contribute to sharp peaks at certain frequencies.

As seen in Table 3-1, the frequency points where those incident wave frequencies are close to the natural frequencies are well matched with high peaks in motion Response Amplitude Operator graphs below.

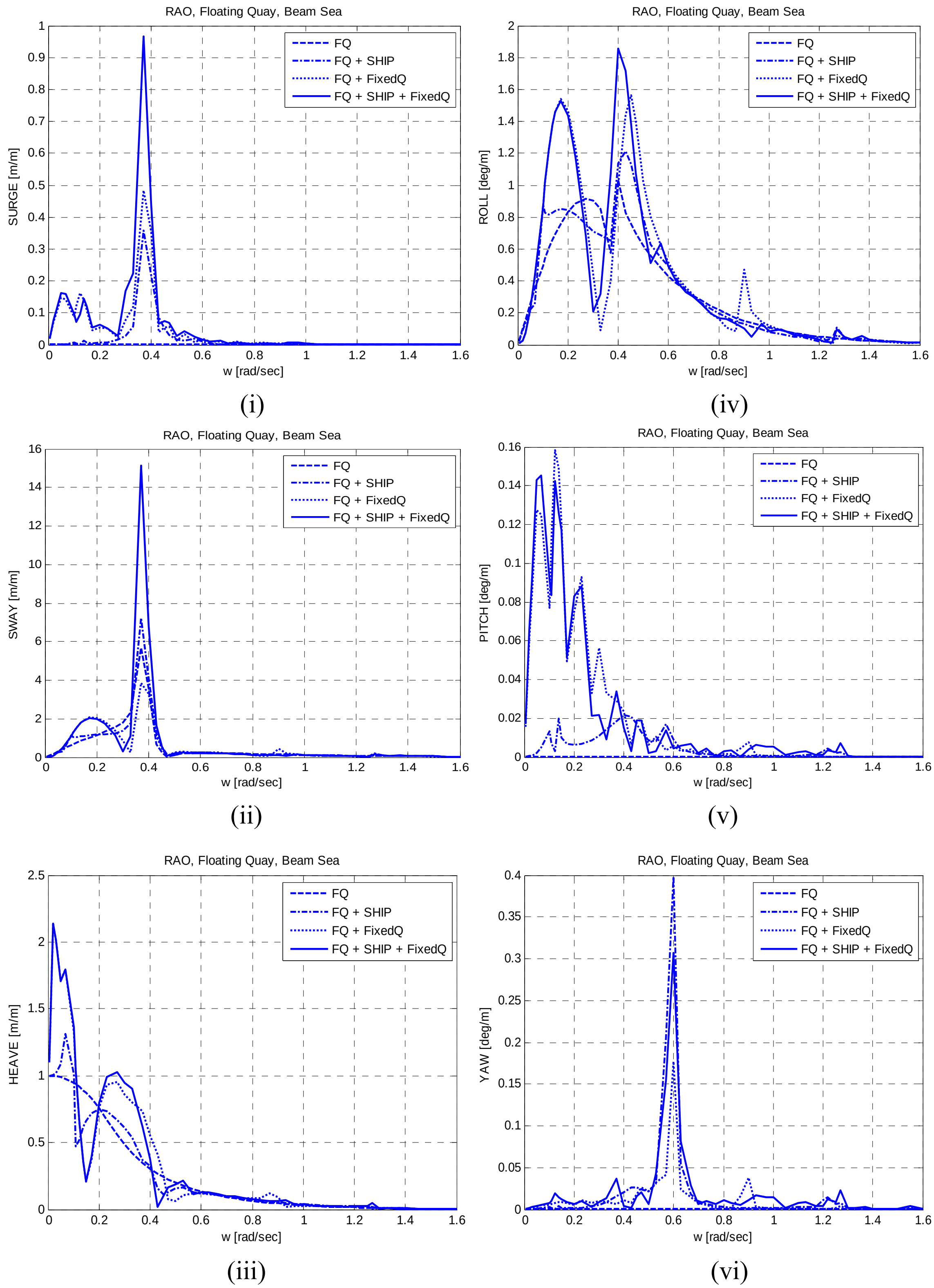

Fig. 3-22. Response Amplitude Operators for Floating Quay for 90 [deg] Wave Heading

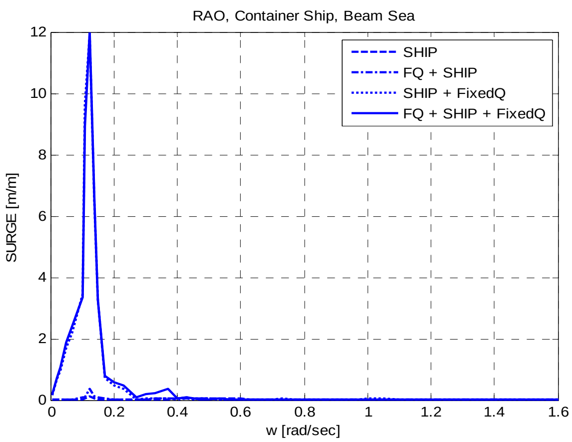

(i)

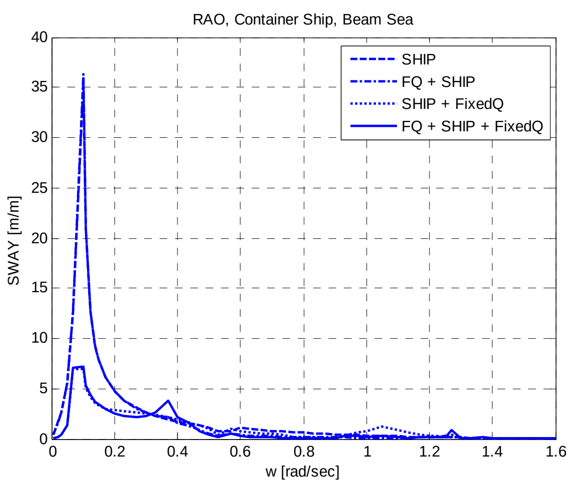

(ii)

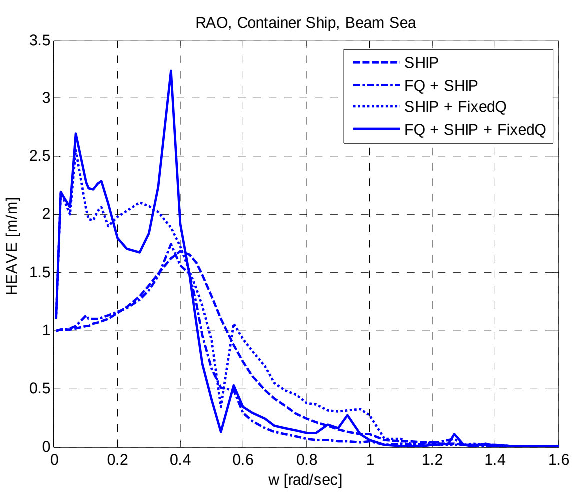

(iii)

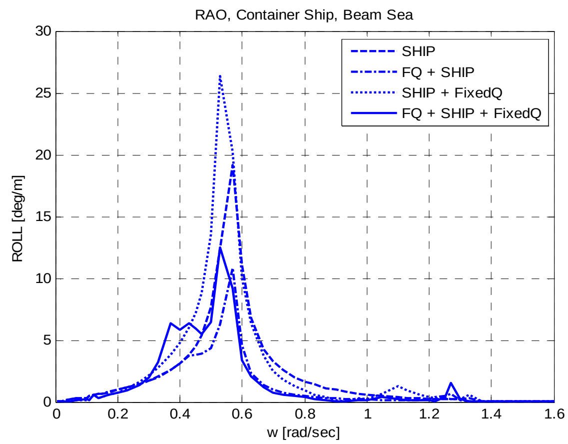

(iv)

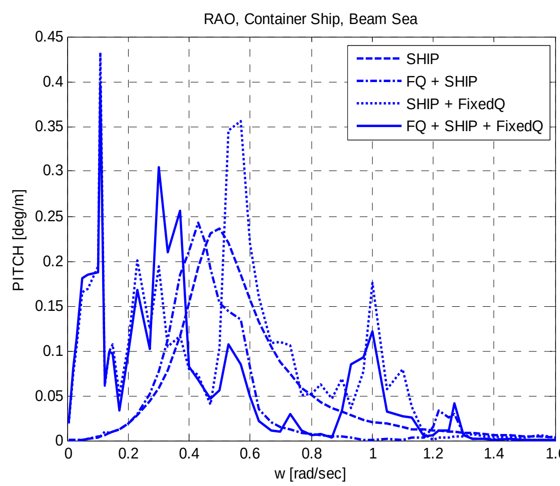

(v)

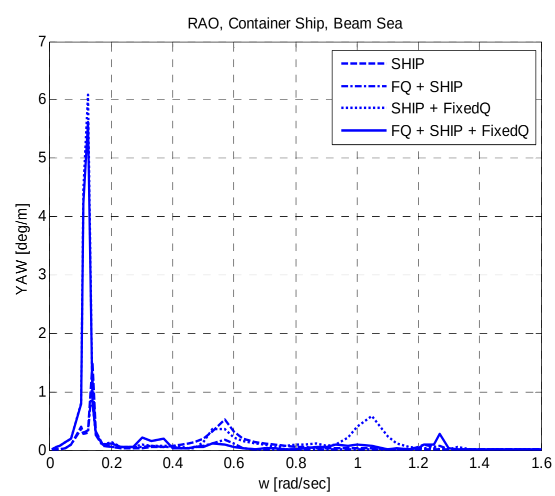

(vi)

Fig. 3-23. Response Amplitude Operators for Container Ship for 90 [deg] Wave Heading

3.1.10 Wave Elevation in the Gap at 90[deg] of Wave Heading

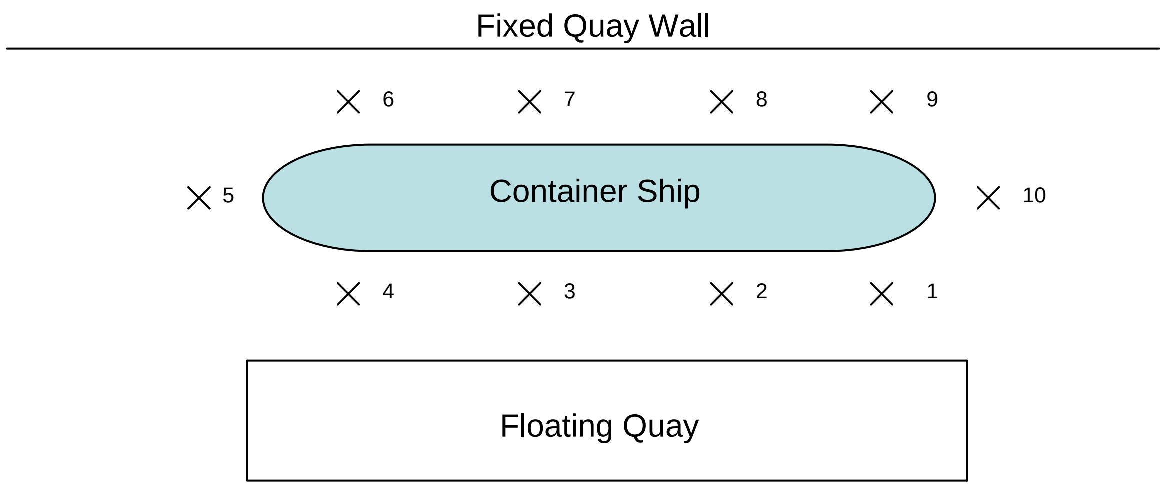

Fig. 3-24. Position of Points for Wave Elevations

Point positions are shown in Fig. 3-24, and frequency domain wave elevations are in Fig. 3-25. The 3 body case wave elevations are effected by the presence of Fixed Quay Wall, Container Ship, and Floating Quay. The wave elevations at point 1, 4, 5, 10 are relatively small, and the wave elevations at point 2, 3 are bigger than the previous points 1, 4, 5, 10 due to interaction effect between two floating bodies. The wave elevations at point 6, 7, 8, 9 are biggest because of reflection effect due to the presence of Fixed Quay and Container Ship. The wave energy is not able to penetrate Fixed Quay Wall, so it was totally bounced back, so this event makes the wave elevations there biggest. And that also makes response motion of multi-body case way bigger than response motion of single body case or multi-body case without Fixed Quay Wall.

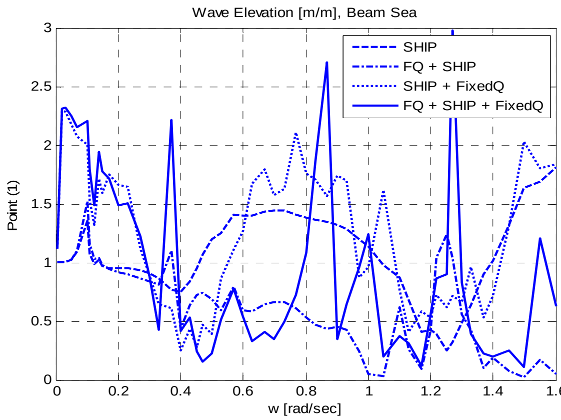

Wave Elevation at Point 1

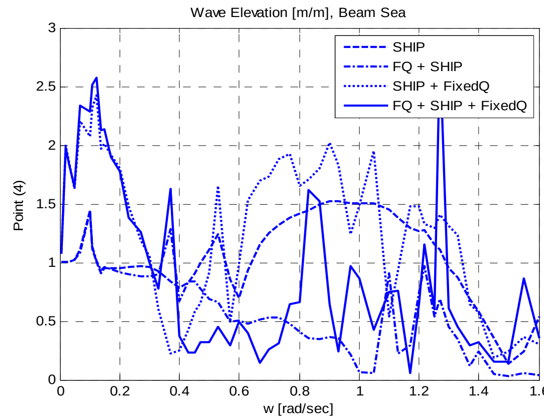

Wave Elevation at Point 4

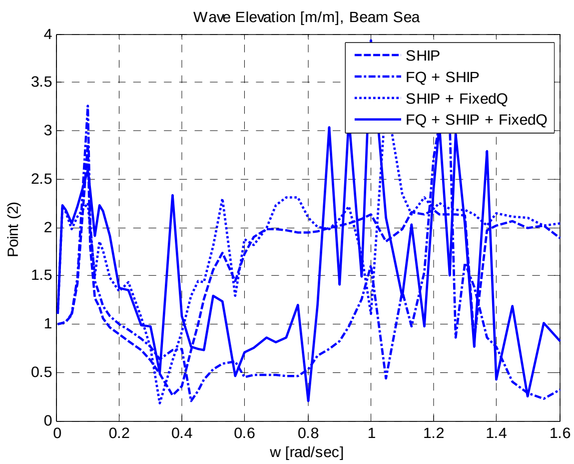

Wave Elevation at Point 2

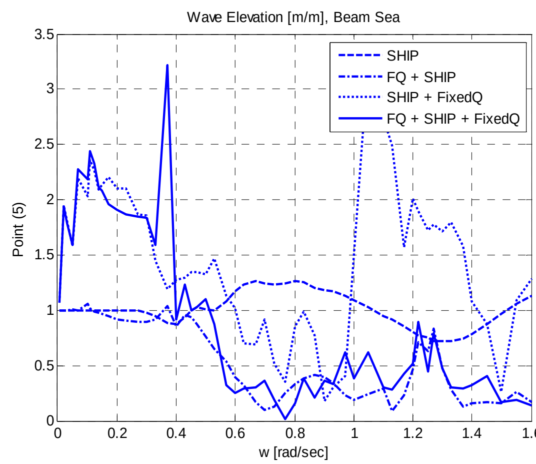

Wave Elevation at Point 5

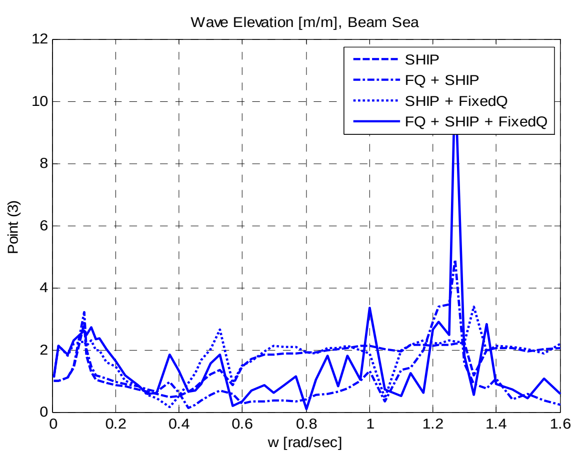

Wave Elevation at Point 3

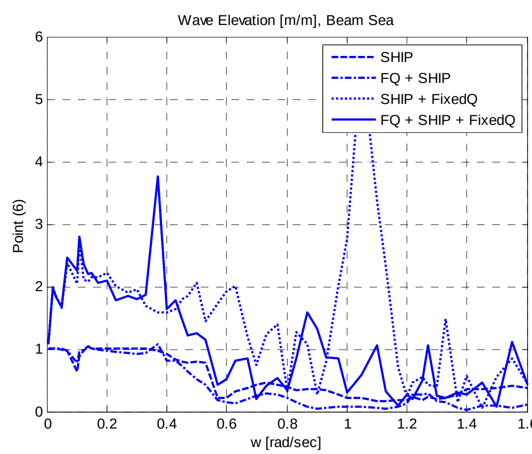

Wave Elevation at Point 6

Fig. 3-25. Wave Elevation at 90[deg] Wave Heading

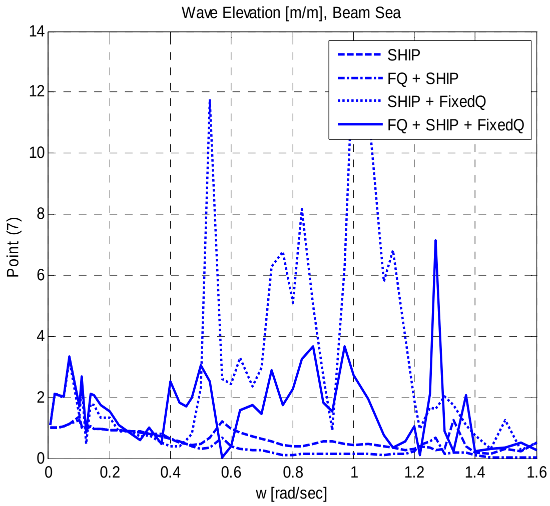

Wave Elevation at Point 7

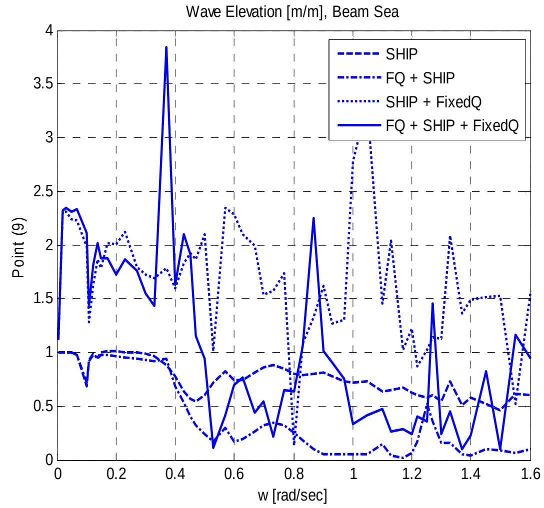

Wave Elevation at Point 9

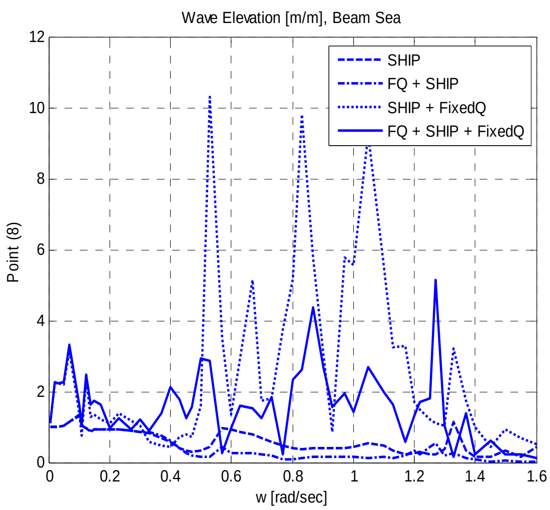

Wave Elevation at Point 8

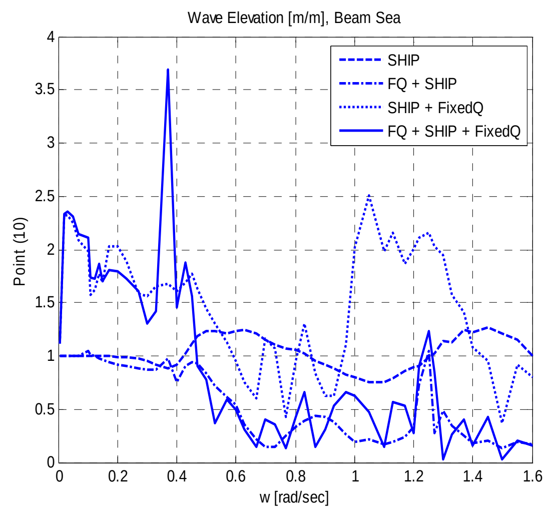

Wave Elevation at Point 10

Fig. 3-25. Continued

3.2 Time Domain Results and Coupled Dynamic Analysis in Time Domain

WINPOST is utilized for the time domain coupled dynamic analysis of moored offshore structures. Hydrodynamic coefficients and forces from WAMIT output (frequency domain data) are converted to time domain data input for WINPOST. Container Ship is moored with four hawser connections, Floating Quay is fixed with two dolphin moorings as shown and fenders are equipped between Container Ship and Fixed Quay Wall to avert collision because of the drift forces mentioned earlier. The dolphin moorings and hawsers restrict the horizontal motions (surge, sway, and, yaw motion) of Floating Quay and the Container Ship. In this research, the hawser connections and dolphin moorings have been modeled with external linear spring. The stiffness of linear spring has been fit in the way that the dolphin moorings and the hawsers strongly restrict horizontal motion (surge, sway, and yaw motion) of Floating Quay and Container Ship, so they provide little horizontal motion. Table 3-2 and Table 3-3 show dolphin mooring and hawser stiffness coefficients (external stiffness).

Table 3-2. Dolphin Mooring Stiffness Coefficients of Floating Quay

SURGE	1.96E+07 [N/m]
SWAY	1.96E+07 [N/m]
YAW	6.1E+11 [N-m/rad]

Table 3-3. Hawser Stiffness Coefficients of Container Ship

SURGE	2.0E+06 [N/m]
SWAY	4.0E+06 [N/m]
YAW	3.0E+10 [N-m/rad]

Wave Spectrum, Operational Condition

WINPOST generates time domain wave elevation based on Jonswap spectrum. The wave elevation for the operational condition is in Fig. 3-26, and comparison of theoretical Jonswap spectrum and recovered spectrum is in Fig. 3-27.

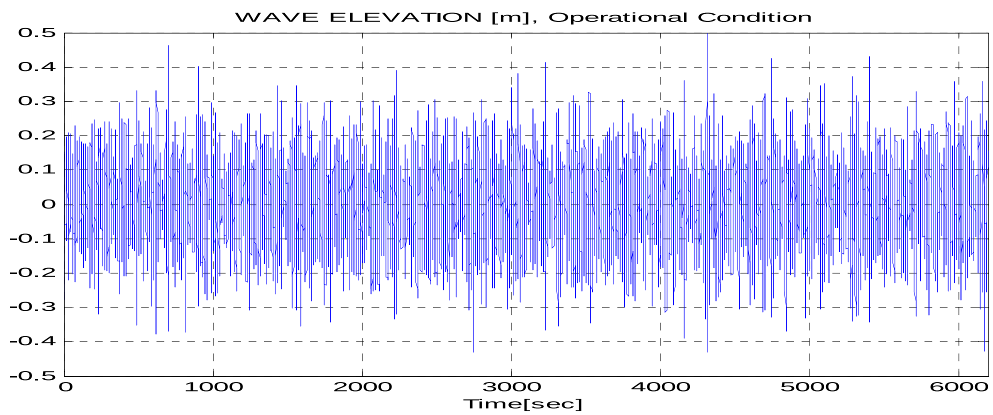

Fig. 3-26. Wave Elevation Time History, Operational Condition

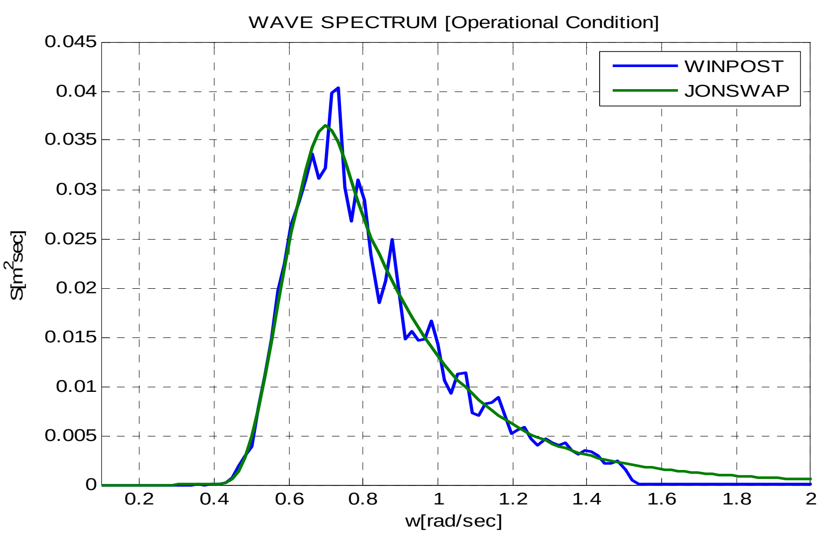

Hs = 0.5 [m]   Tp = 9 [sec]   Gamma, the peak parameter = 1.2

Current profile = 0.115 [m/sec] on the surface at 45 [deg] direction following 1/7th power method

Fig. 3-27. Wave Spectrum, Operational Condition

Wave Spectrum, Survival Condition

The wave elevation for the survival condition is in Fig. 3-28, and comparison of theoretical Jonswap spectrum and recovered spectrum is in Fig. 3-29.

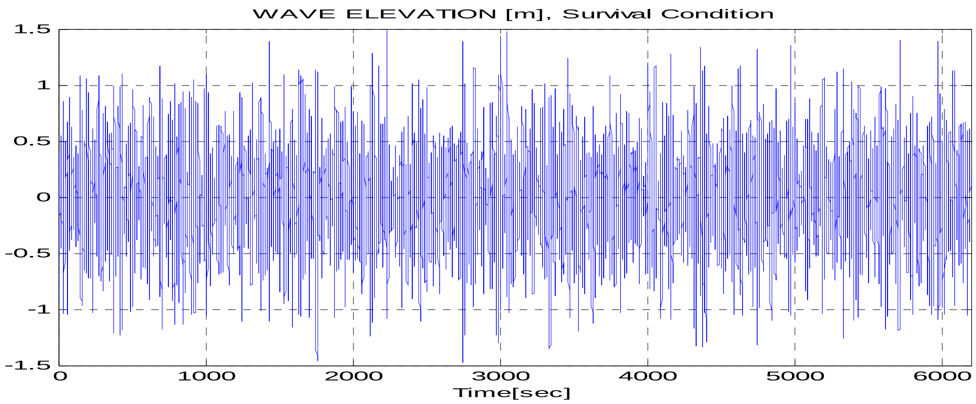

Fig. 3-28. Wave Elevation Time History, Survival Condition

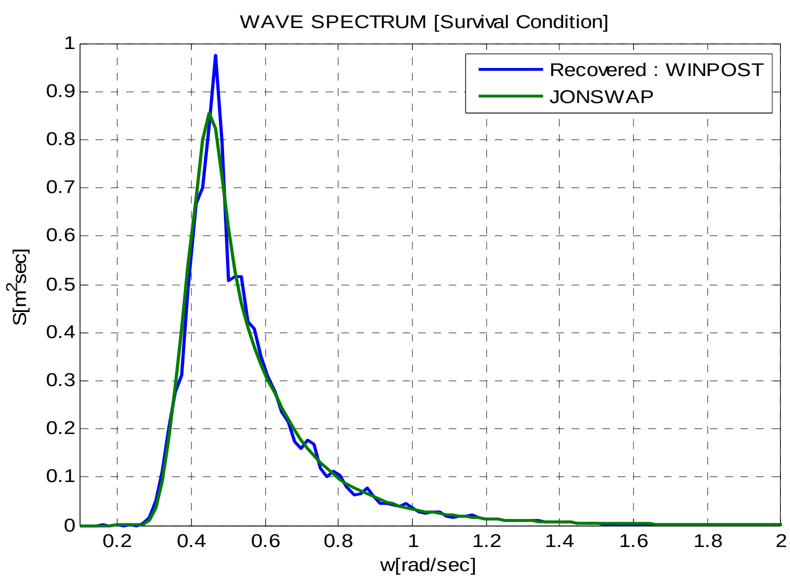

Hs = 1.8 [m] Tp = 14[sec] Gamma, the peak parameter = 1.5

Current profile = 0.23 [m/sec] on the surface at 45 [deg] direction following 1/7th power method

Fig. 3-29. Wave Spectrum, Survival Condition

Wind Spectrum

API Spectrum is used to generate wind force time history. Comparisons of theoretical API spectrum and recovered spectrum from generated wind velocity time history are shown in Fig. 3-30.

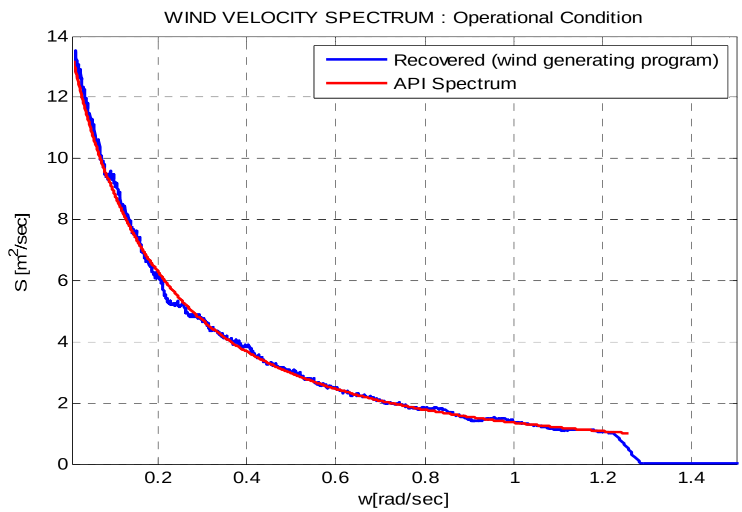

(Operational Condition)

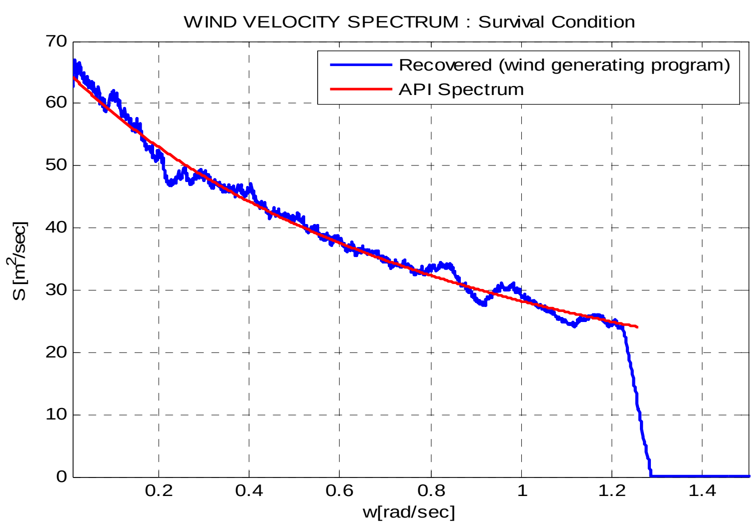

(Survival Condition)

Fig.3-30. Wind Spectrum

Numerical Wave Test, Head Sea, 3body case (Wave Heading: 0[deg])

Frequency domain results from WAMIT are identical with time domain results from WINPOST. WAMIT RAO is compared with WINPOST RAO in Fig. 3-31, Fig. 3-32, and Fig. 3-33.

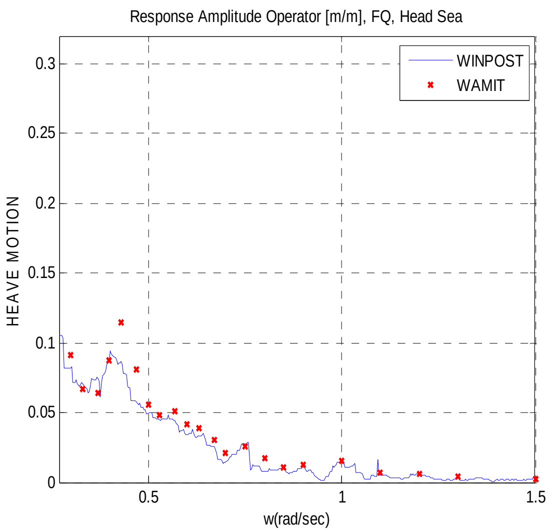

(i)

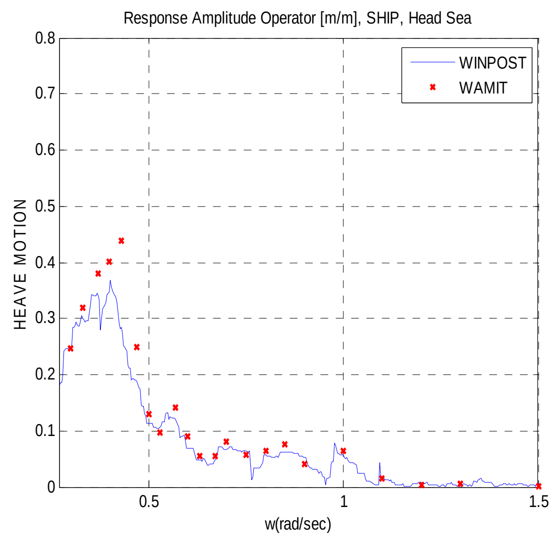

(iii)

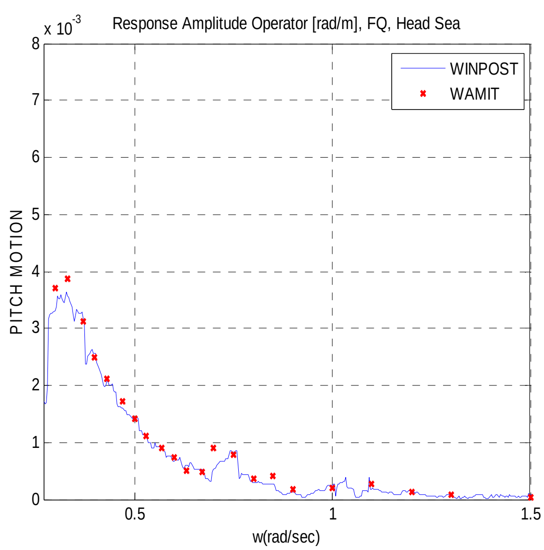

(ii)

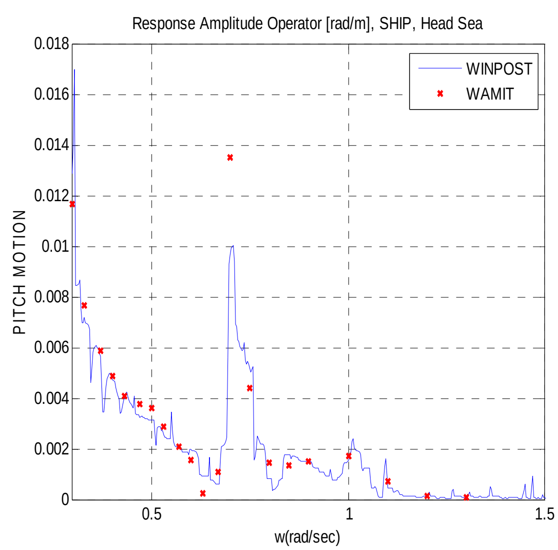

(iv)

Fig. 3-31. Numerical Irregular Wave Test, Head Sea Wave

Numerical Wave Test, Quartering Sea, 3body case (Wave Heading: 45[deg])

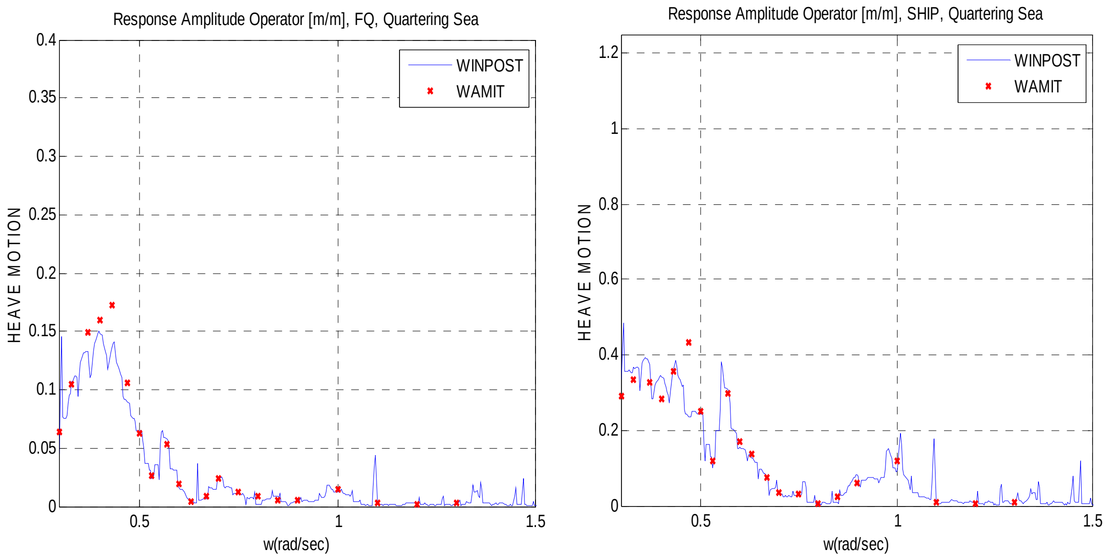

(i)

(iii)

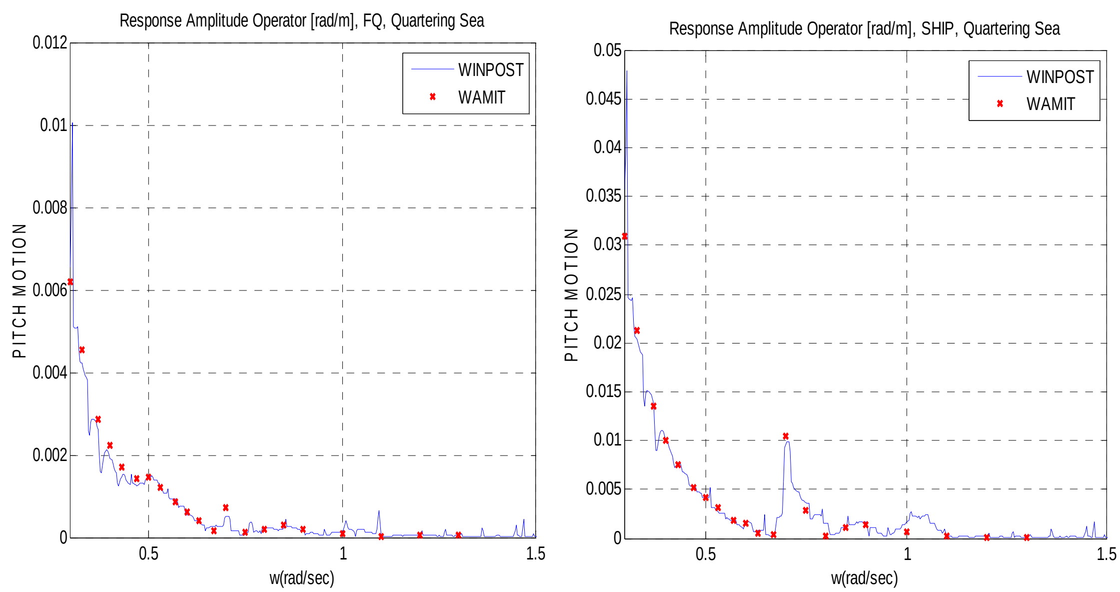

(ii)

(iv)

Fig. 3-32. Numerical Irregular Wave Test, Quartering Sea Wave

Numerical Wave Test, Beam Sea,3body case (Wave Heading: 90[deg])

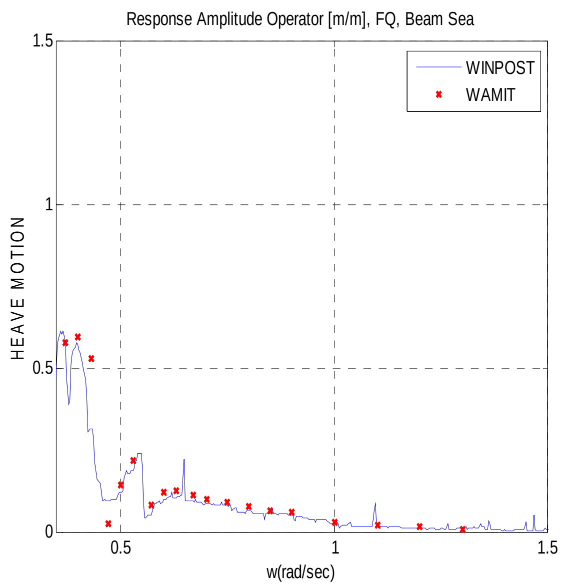

(i)

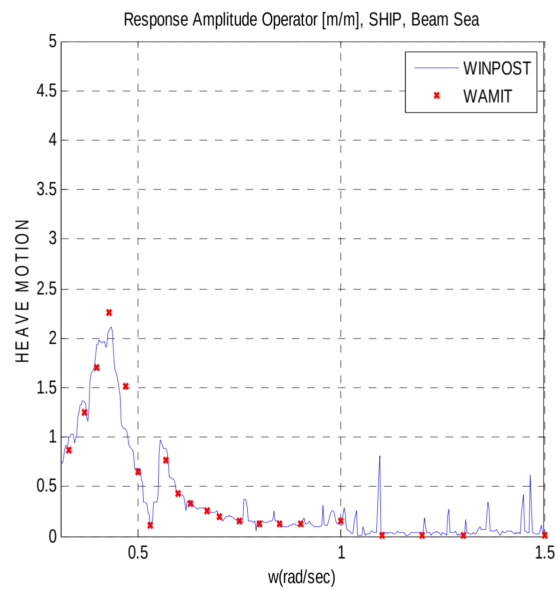

(ii)

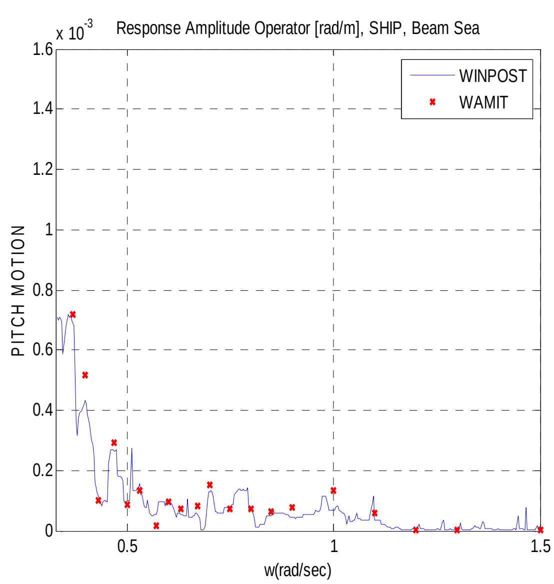

(iii)

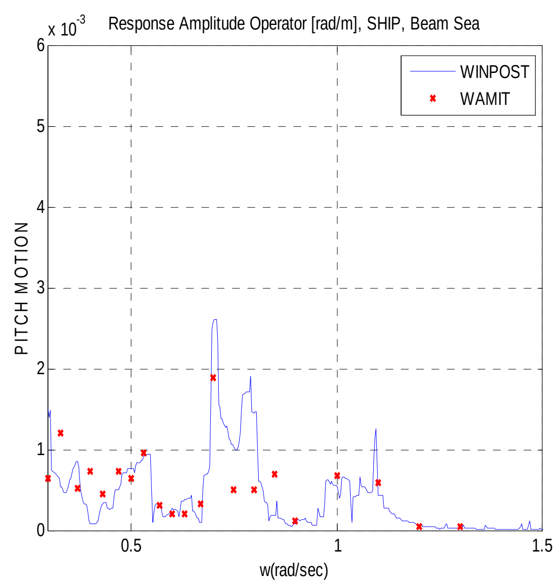

(iv)

Fig. 3-33. Numerical Irregular Wave Test, Beam Sea Wave

3.2.1 Head Sea Case (0 [deg] of Wave Heading)

Wave train propagates in positive x direction. Wave energy is not trapped in the gaps between those interacting bodies, and huge reflection against Fixed Quay Wall will not occur at the area of Floating Quay and Container Ship due to wave direction and normal direction of Fixed Quay Wall. Surge and pitch motions are relatively big, and sway, roll, yaw motions are smaller than those in Quadrant and Beam Sea wave cases.

Table 3-4 and Table 3-5 show statistics of pure mode response motion and relative motions between Floating Quay and Container Ship. Fig. 3-34, Fig. 3-35, and Fig. 3-36 show motion response spectrum, motion time history, and relative motion time history for operational condition, respectively. Fig. 3-37, Fig. 3-38, and Fig. 3-39 also show motion response spectrum, motion time history, and relative motion time history for survival condition, respectively.

Tables and figures show all motions look acceptable at operational condition with 0[deg] wave heading. Loading and Offloading operation between Floating Quay, Container Ship, and Fixed Quay Wall is possible at operational condition. But loading and offloading operation at survival condition looks impossible. The gap between the floating bodies and the fixed body is 2.1[m], and the limitation of operation is 1 to 2 [m] at most. The container ships must be moved or strongly tied. Table 3-6 illustrates statistics of force on Dolphin moorings for 0 [deg] wave heading case.

3.2.1.1 Head Sea Case, Operational Condition

Motion Response Spectrum of Floating Quay, Head Sea, Operational Condition

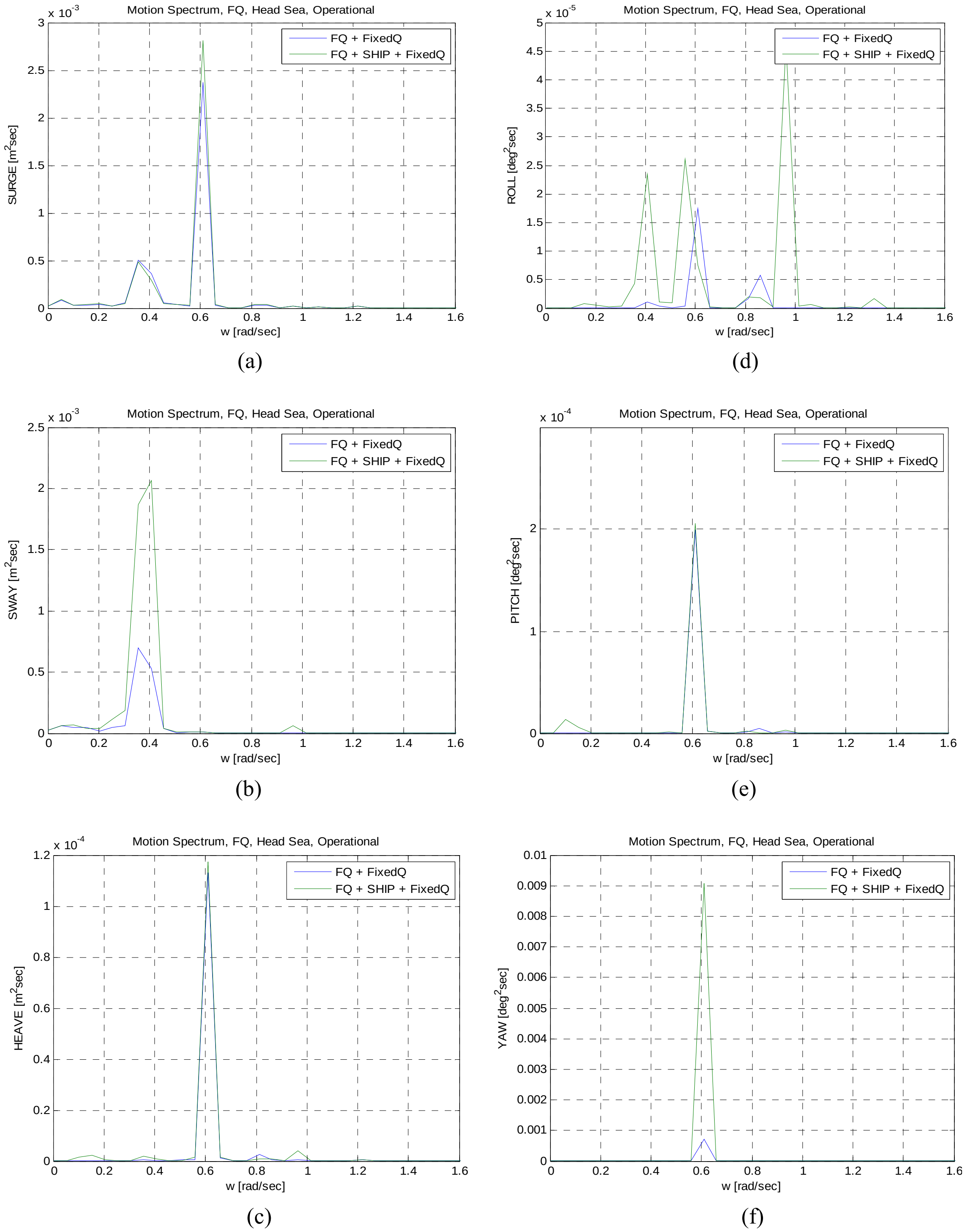

Fig. 3-34. Motion Response Spectrum, Head Sea, Operational

Motion Response Spectrum of Container Ship, Head Sea, Operational Condition

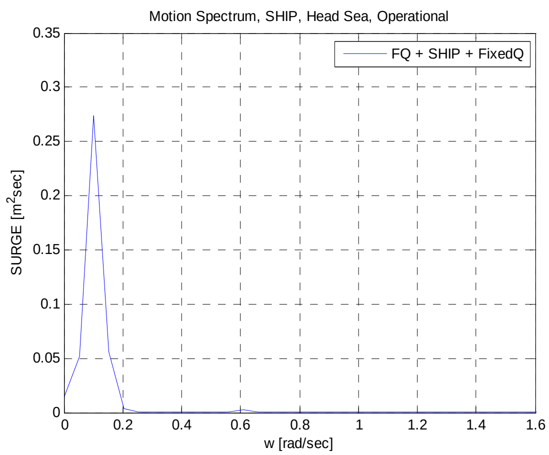

(g)

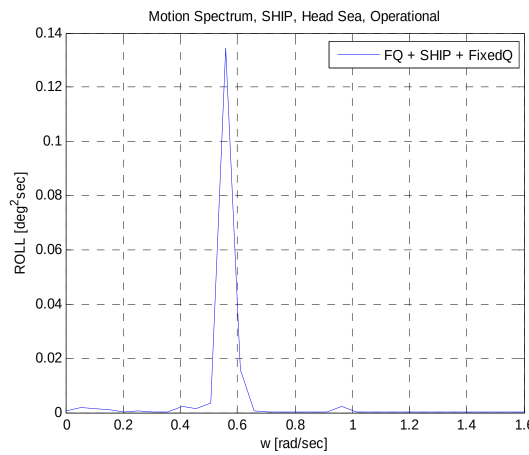

(j)

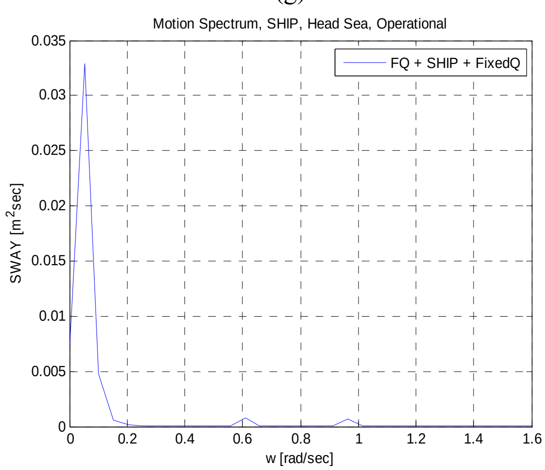

(h)

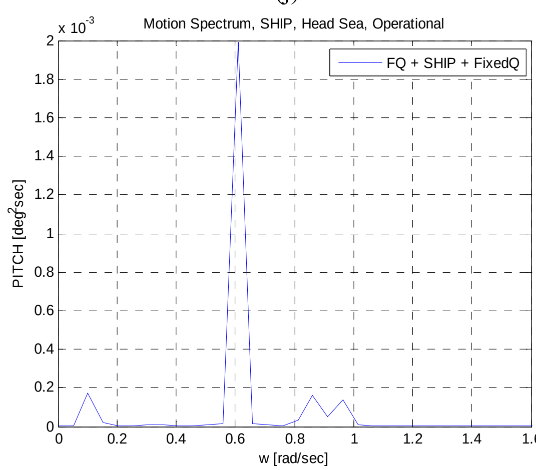

(k)

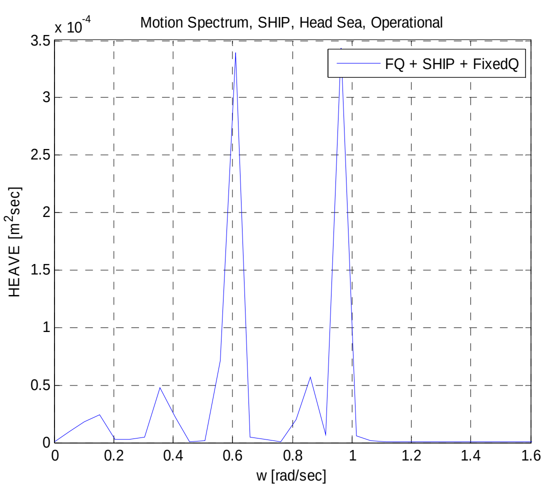

(i)

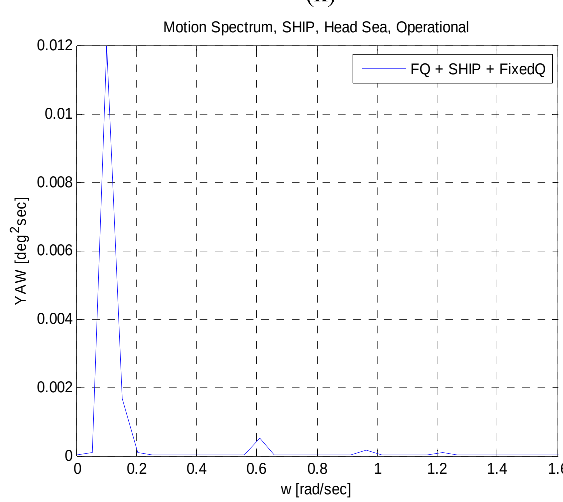

(l)

Fig. 3-34. Continued

Motion Time History of Floating Quay and Container Ship, Operational

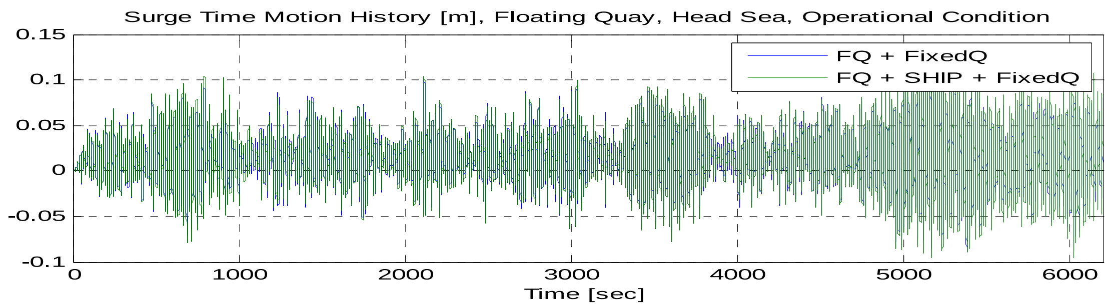

(a)

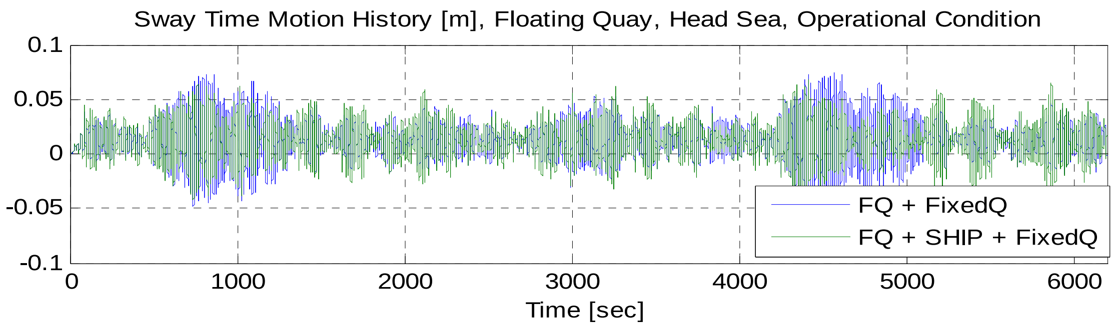

(b)

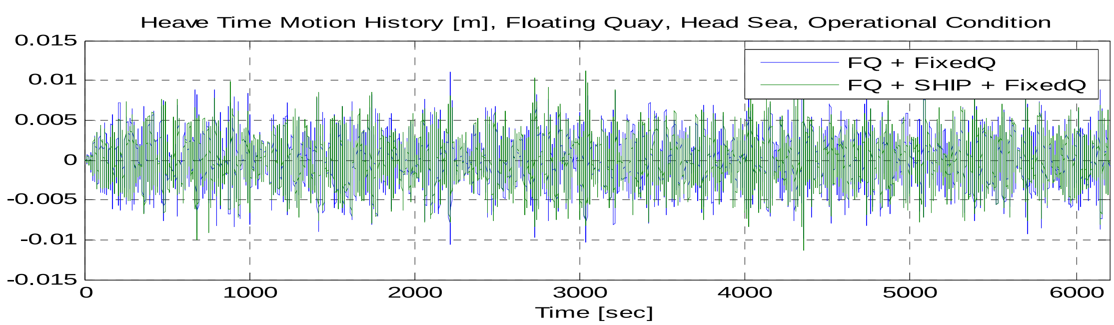

(c)

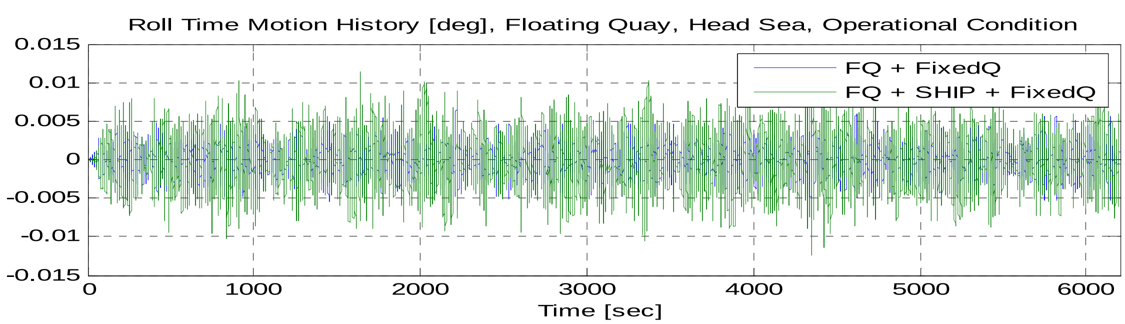

(d)

Fig. 3-35. Time Motion History, Head Sea, Operational

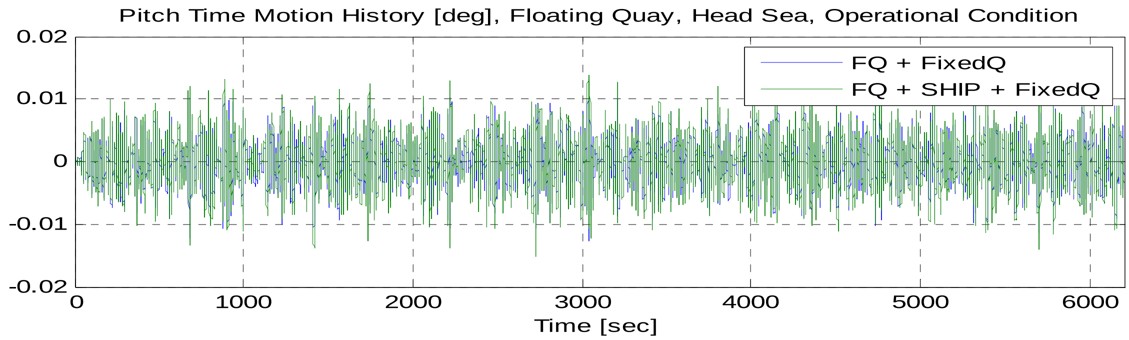

(e)

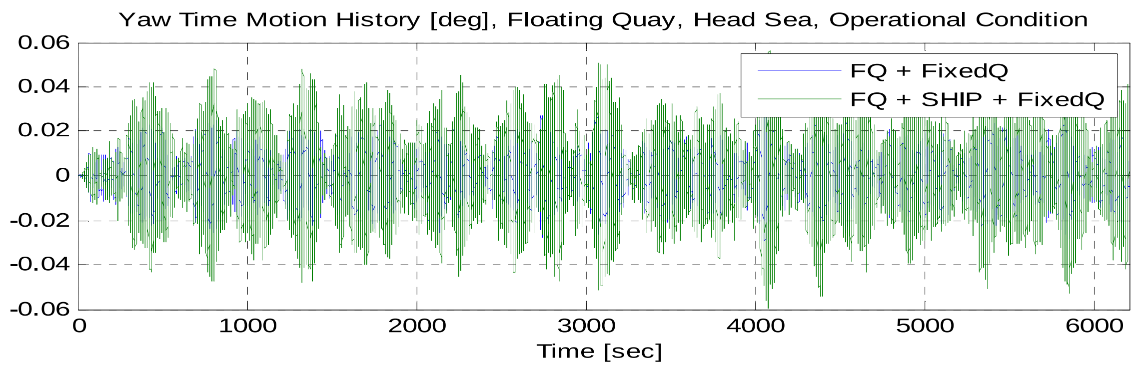

(f)

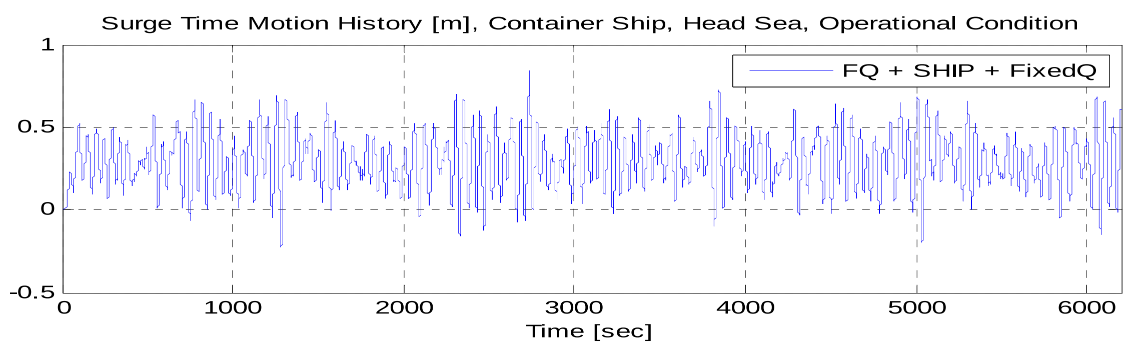

(g)

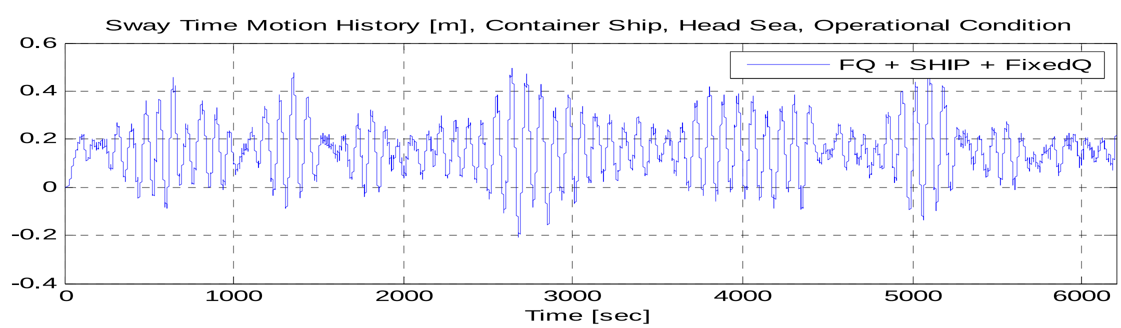

(h)

Fig. 3-35. Continued

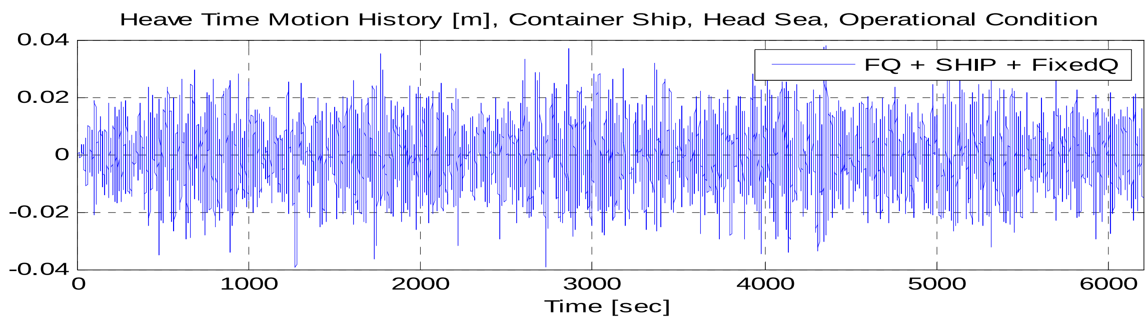

(i)

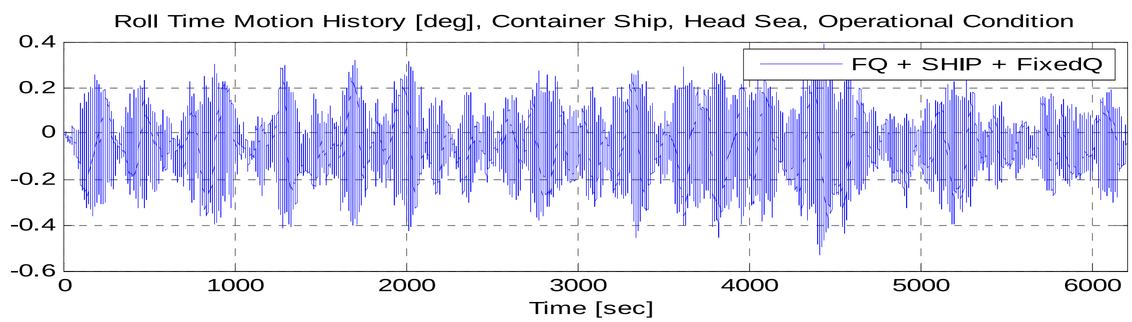

(j)

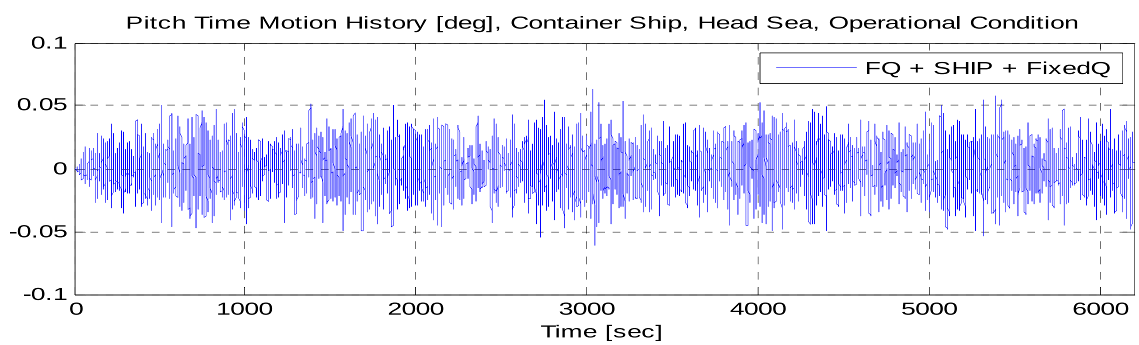

(k)

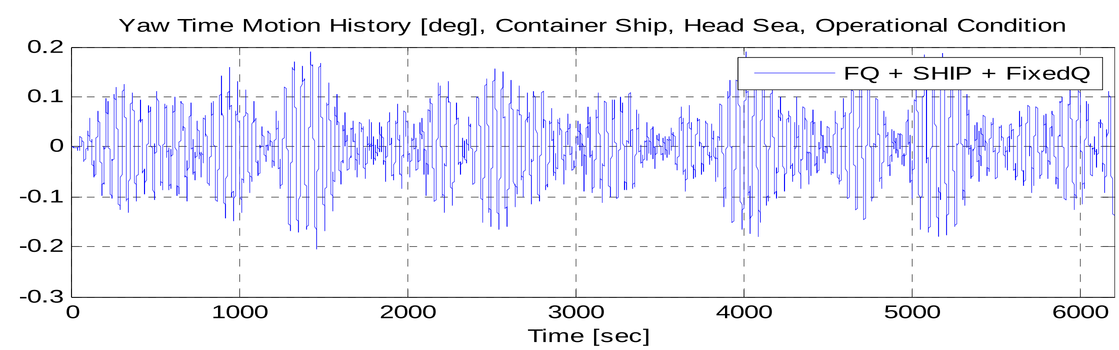

(l)

Fig. 3-35. Continued

Relative Motion Time History, Operational Condition, Head Sea

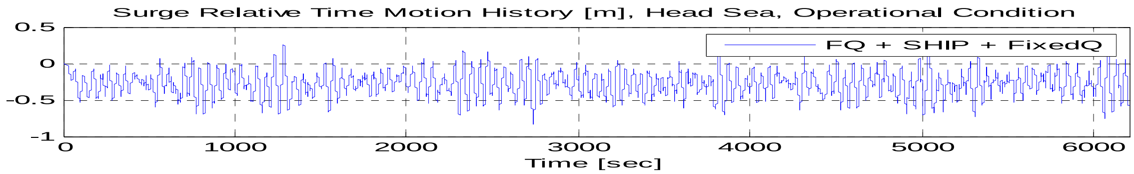

(a)

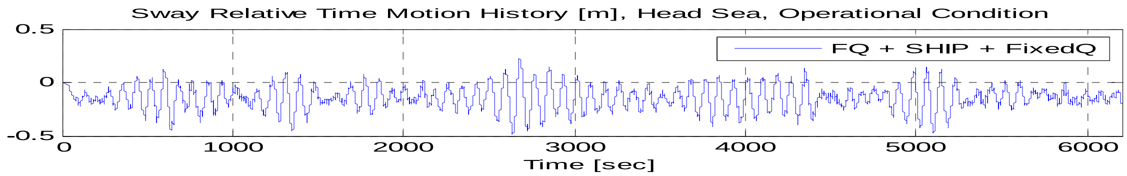

(b)

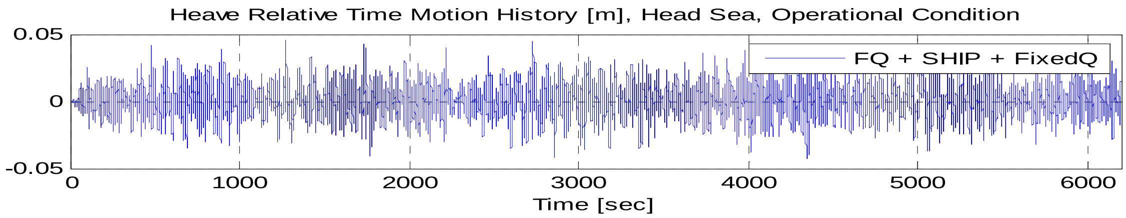

(c)

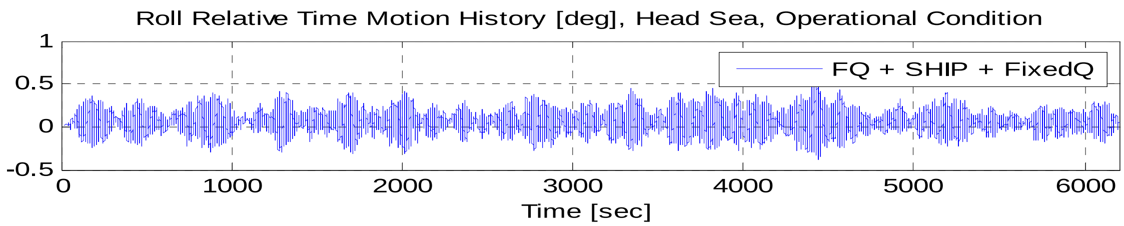

(d)

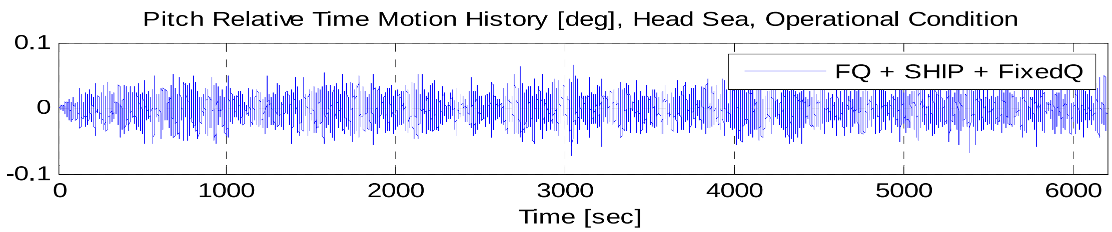

(e)

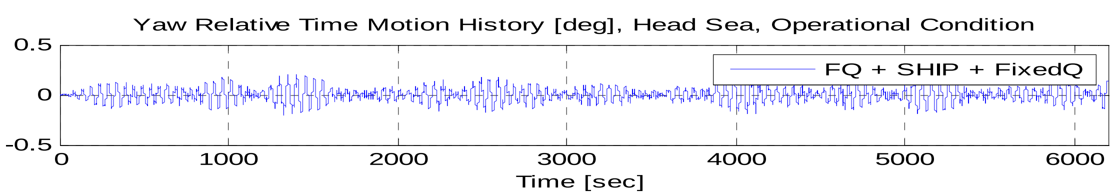

(f)

Fig. 3-36. Relative Motion Time History, Head Sea, Operational

3.2.1.2 Head Sea Case, Survival Condition

Motion Response Spectrum of Floating Quay, Head Sea, Survival Condition

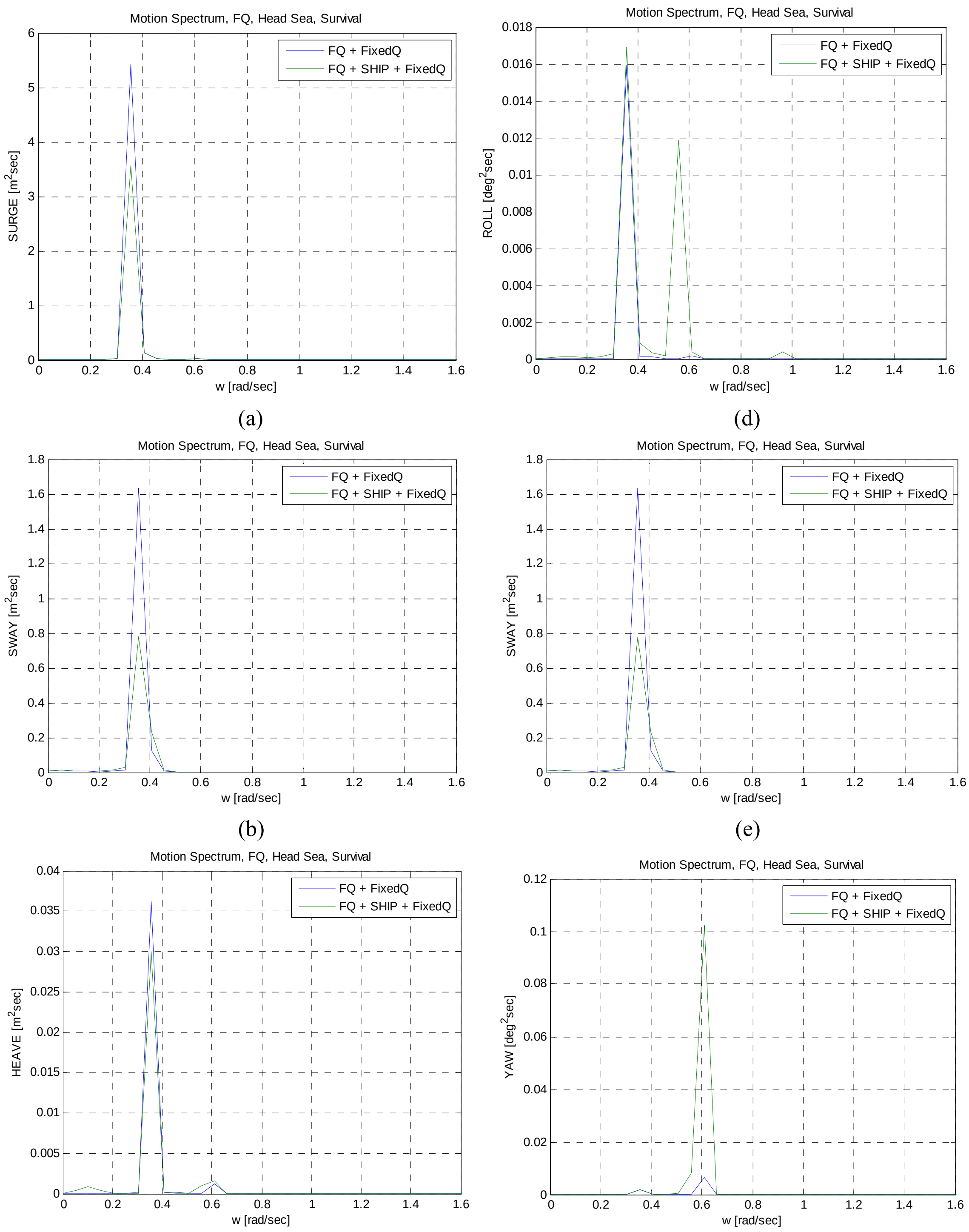

(a) (d) (b) (e) (c) (f)

Fig. 3-37. Motion Response Spectrum, Head Sea, Survival

Motion Response Spectrum of Container Ship, Head Sea, Survival Condition

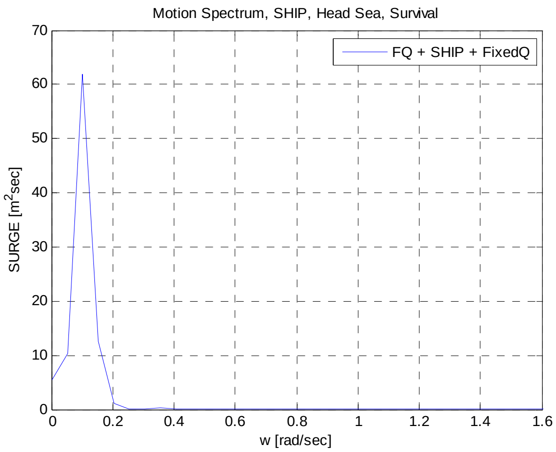

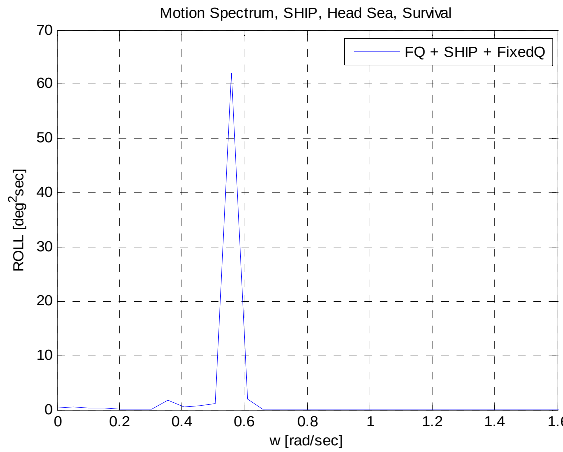

(g) (j)

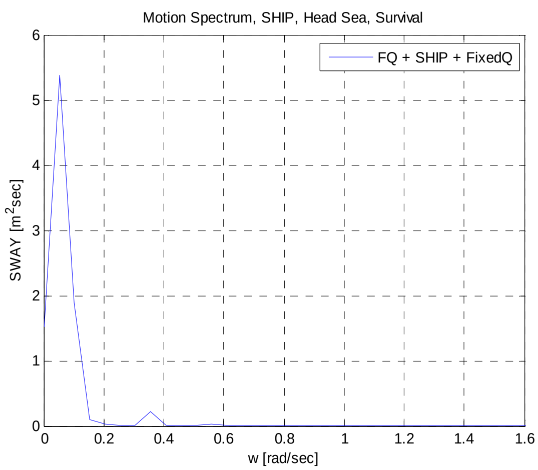

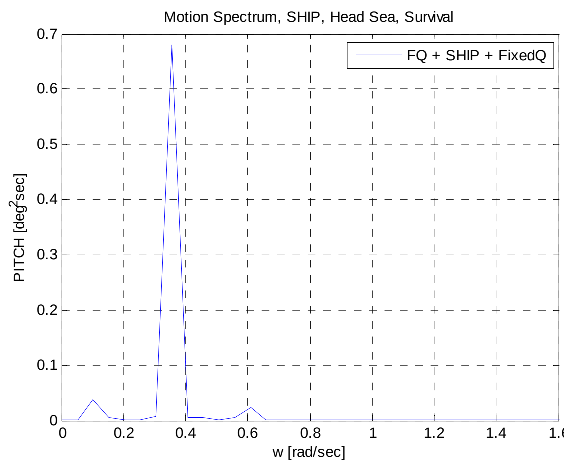

(h) (k)

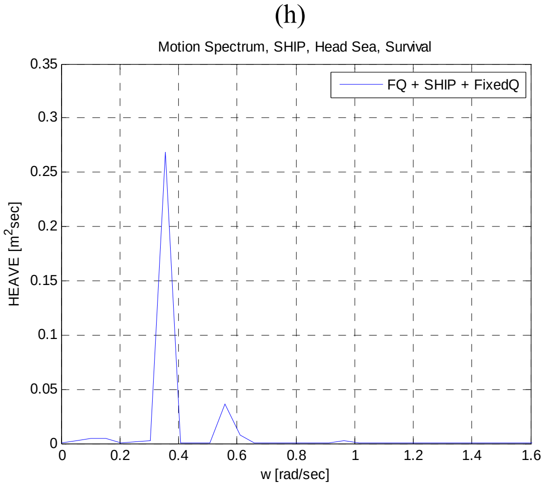

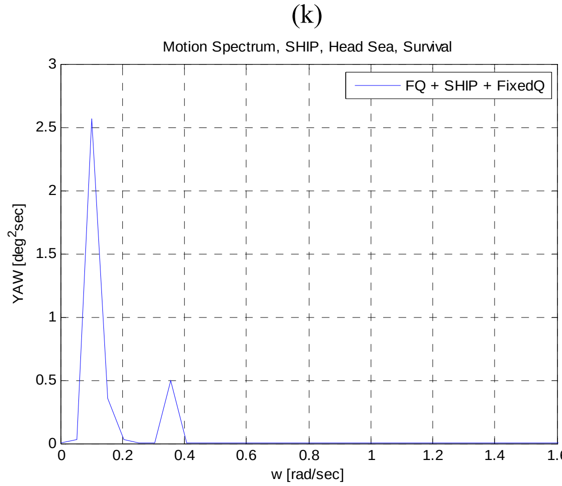

(i) (l)

Fig. 3-37. Continued

Motion Time History of Floating Quay and Container Ship, Survival

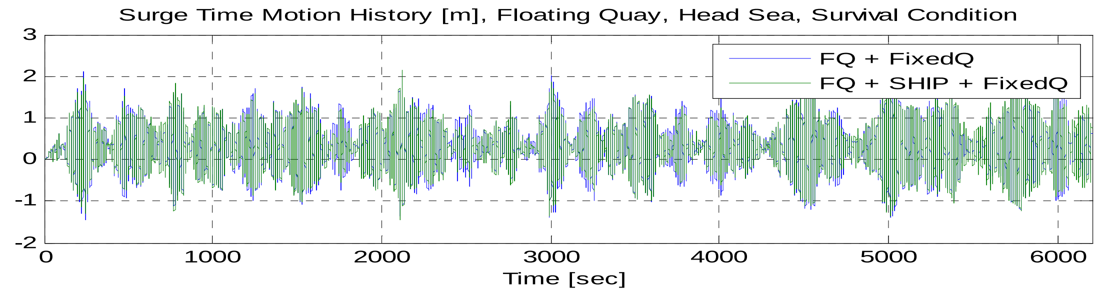

(a)

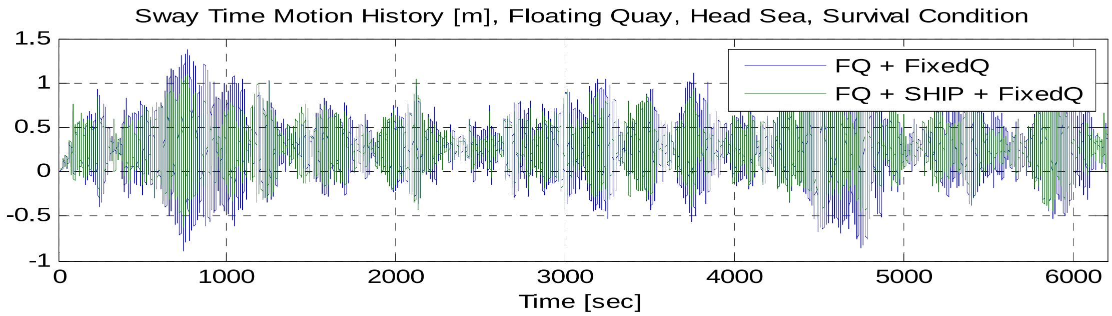

(b)

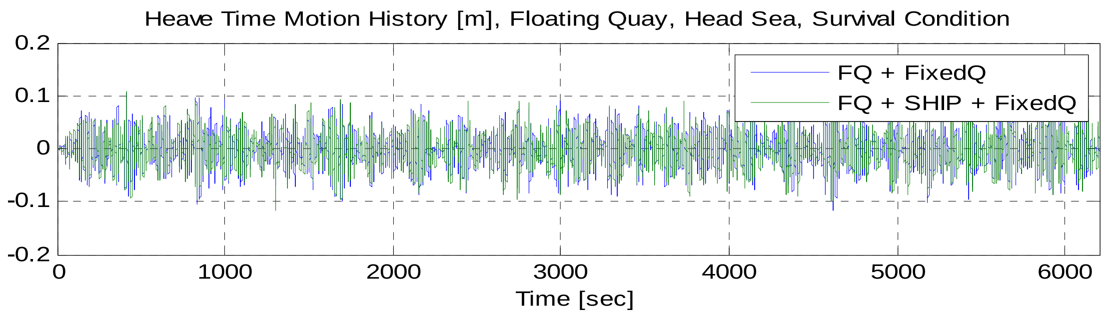

(c)

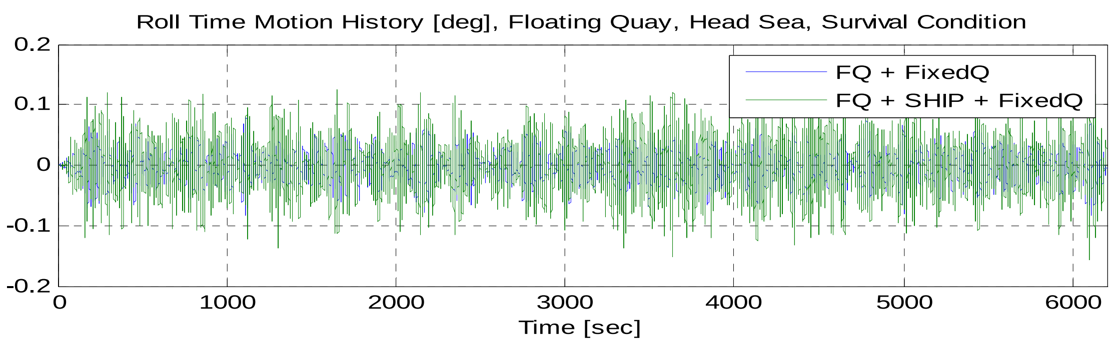

(d)

Fig. 3-38. Time Motion History, Head Sea, Survival

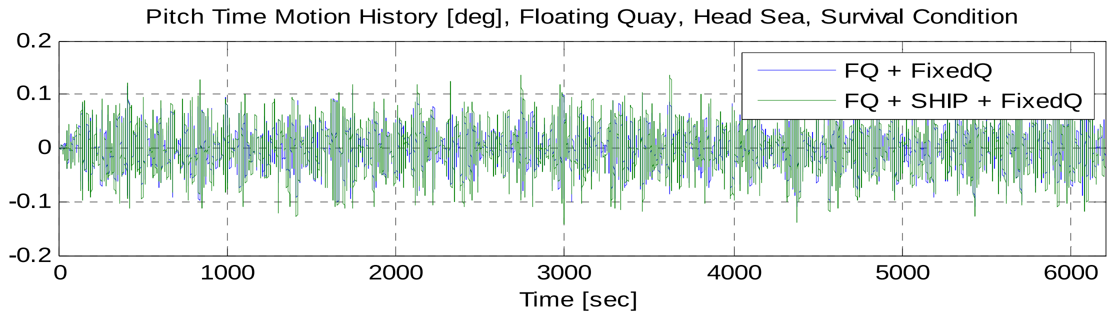

(e)

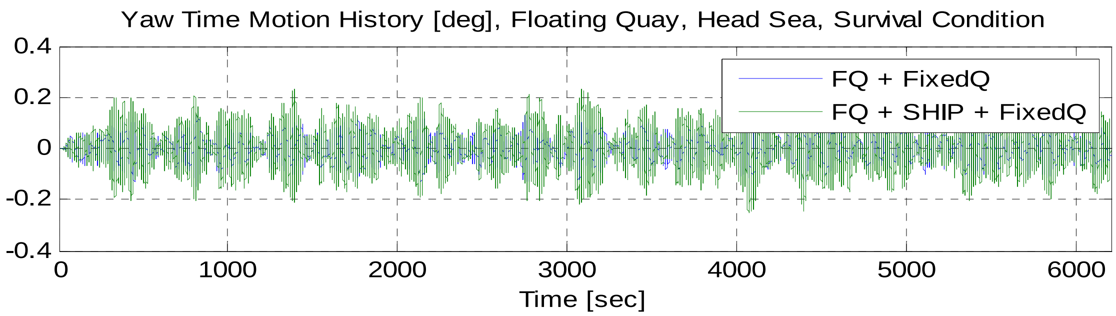

(f)

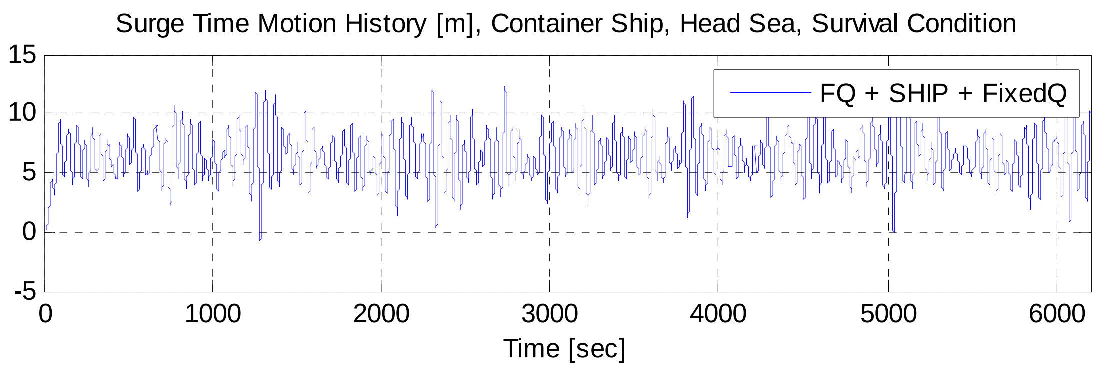

(g)

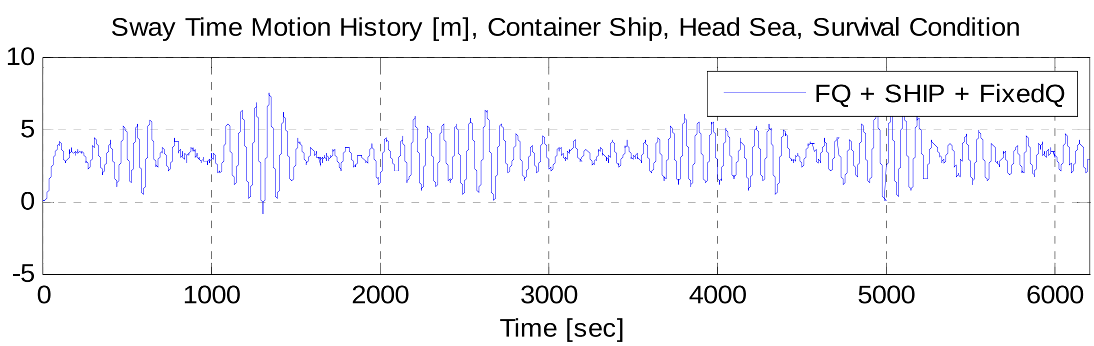

(h)

Fig. 3-38. Continued

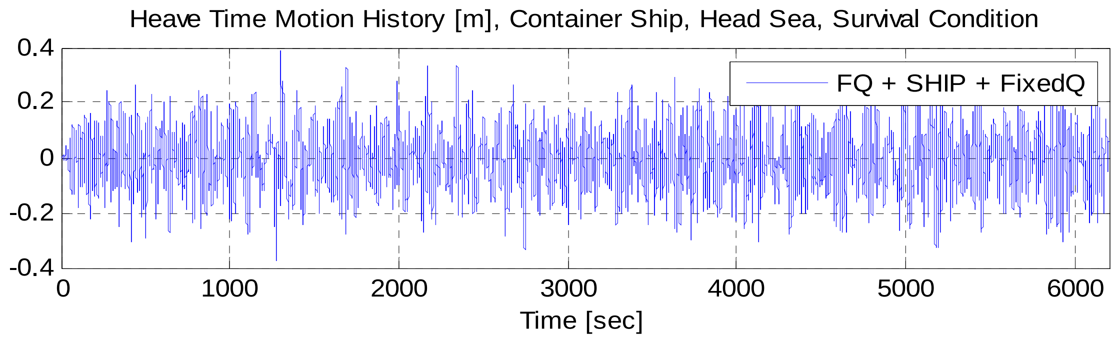

(i)

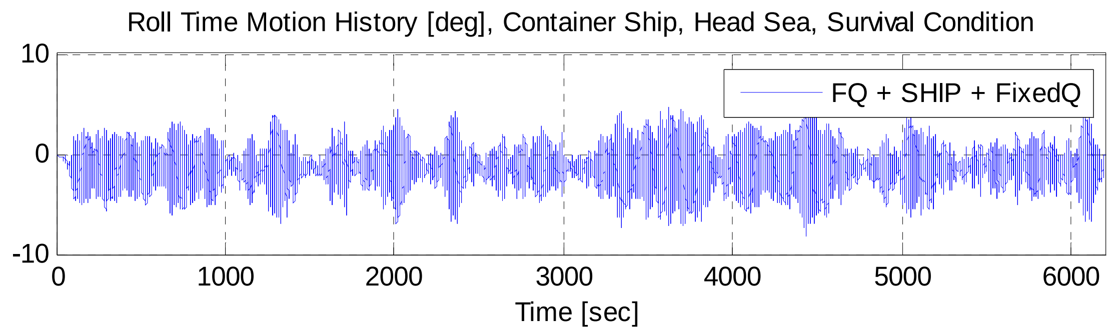

(j)

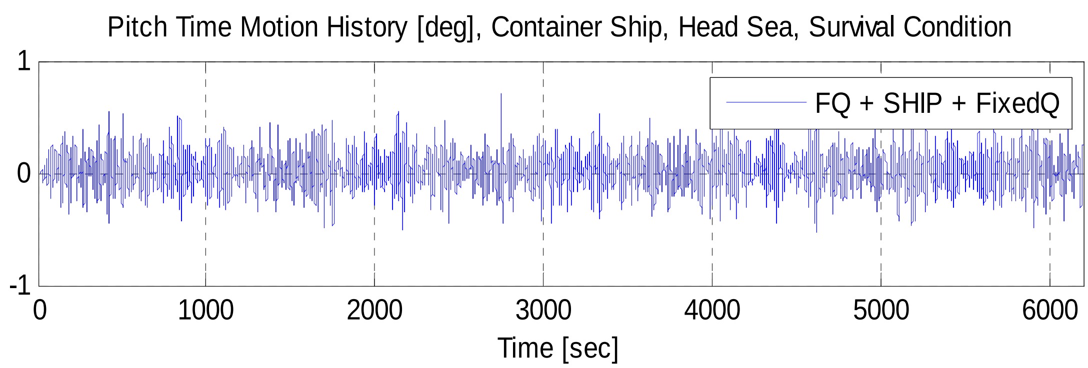

(k)

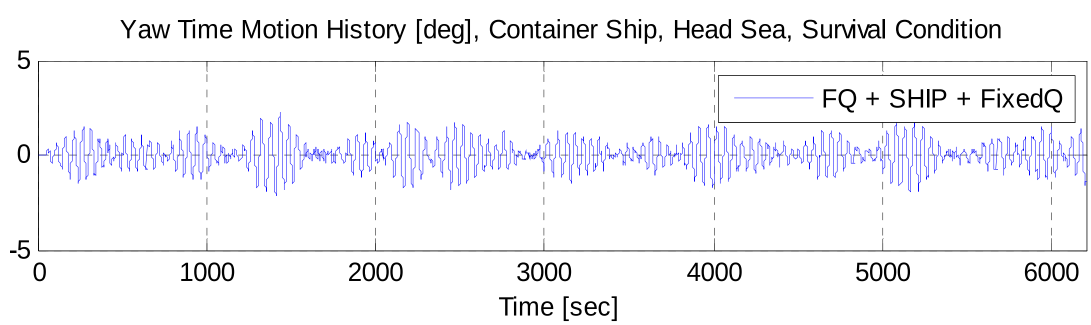

(l)

Fig. 3-38. Continued

Relative Motion Time History, Survival Condition, Head Sea

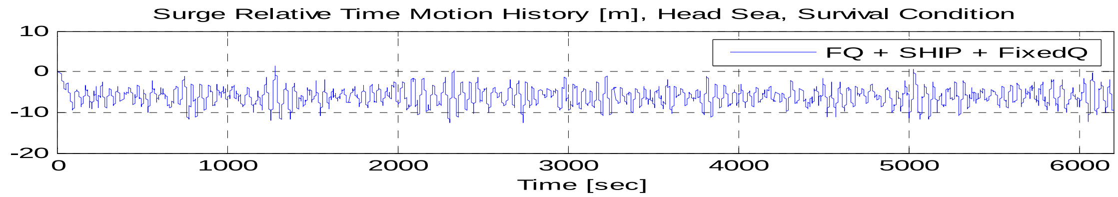

(a)

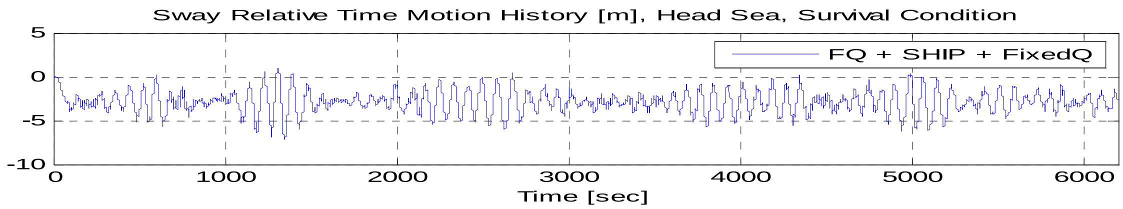

(b)

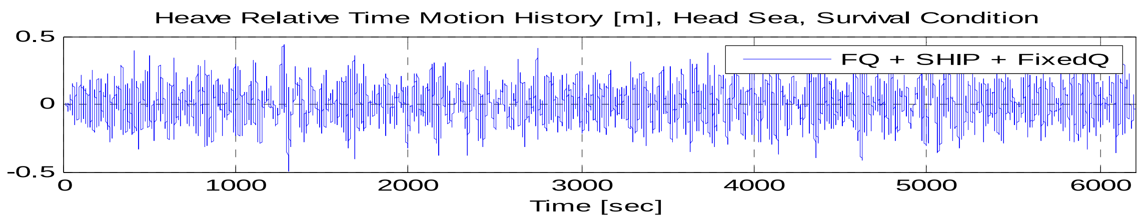

(c)

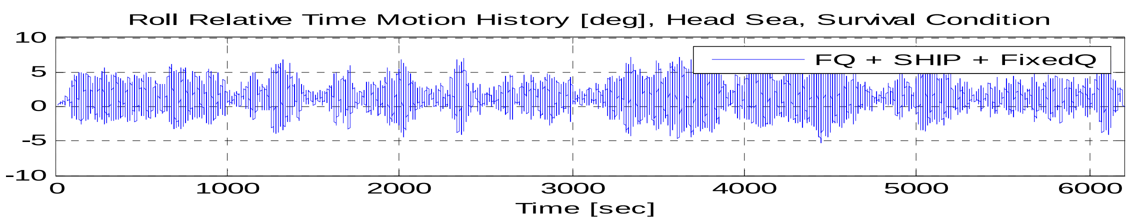

(d)

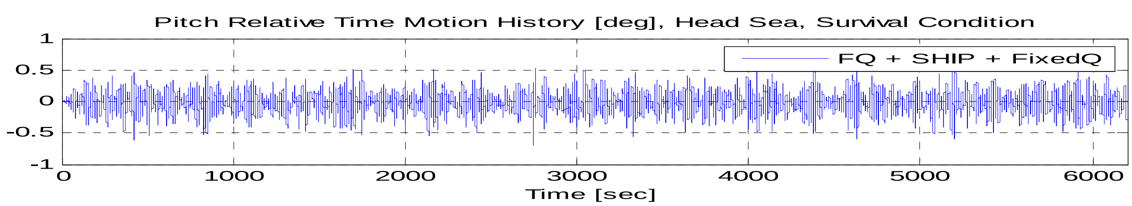

(e)

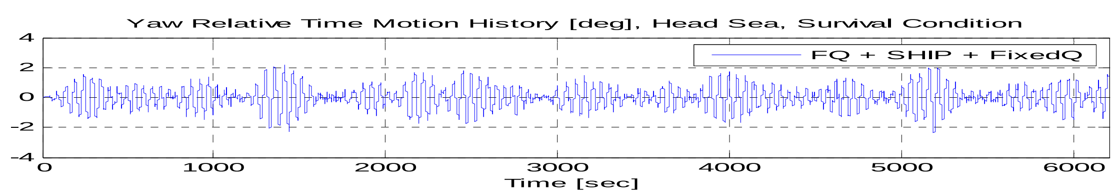

(f)

Fig. 3-39. Relative Motion Time History, Head Sea, Survival

Table 3-4. Motion Statistics, Head Sea

Motion	**Floating Quay, 3body Head Sea Operational Con't**	**Container Ship 3body Head Sea Operational Con't**	**Floating Quay 3body Head Sea Survival Con't**	**Container Ship 3body Head Sea Survival Con't**	**Floating Quay, 2body (FQ + FixedQ) Head Sea Survival Con't**
SURGE [m]	Max = 0.1235 Min = -0.0953 Mean = 0.0146 Std. Dev. = 0.0341	Max = 0.8403 Min = -0.2246 Mean = 0.2940 Std. Dev. = 0.1643	Max = 2.139 Min = -1.4493 Mean = 0.297 Std. Dev. = 0.564	Max = 12.22 Min = -0.759 Mean = 6.3626 Std. Dev. = 2.0624	Max = 2.1236 Min = -1.4485 Mean = 0.2976 Std. Dev. = 0.5821
SWAY [m]	Max = 0.06768 Min = -0.038 Mean = 0.01233 Std. Dev. = 0.0169	Max = 0.4947 Min = -0.2114 Mean = 0.1564 Std. Dev. = 0.111	Max = 1.11539 Min = -0.6285 Mean = 0.273 Std. Dev. = 0.2685	Max = 7.4924 Min = -0.8214 Mean = 3.15 Std. Dev. = 1.2421	Max = 1.3779 Min = -0.88938 Mean = 0.2695 Std. Dev. = 0.35261
HEAVE [m]	Max = 0.01125 Min = -0.01132 Mean = -4.995E-05 Std. Dev. = 0.0029	Max = 0.03794 Min = -0.03932 Mean = -5.89E-04 Std. Dev. = 0.0107	Max = 0.1263 Min = -0.1178 Mean = -0.0012 Std. Dev. =0.0334	Max = 0.3867 Min = -0.3762 Mean = -0.0064 Std. Dev. = 0.109	Max = 0.11157 Min = -0.11736 Mean = -0.001498 Std. Dev. = 0.0336
ROLL [deg]	Max = 0.01146 Min = -0.01243 Mean = -7.5E-05 Std. Dev. = 0.0033	Max = 0.3903 Min = -0.5331 Mean = -0.0564 Std. Dev. =0.13586	Max = 0.1491 Min = -0.1567 Mean = -0.0014 Std. Dev. = 0.045	Max = 5.316 Min = -8.2297 Mean = -1.325 Std. Dev. = 2.1084	Max = 0.07753 Min = -0.08332 Mean = -0.00241 Std. Dev. = 0.02587
PITCH [deg]	Max = 0.0139 Min = -0.0156 Mean = -1.221E-05 Std. Dev. = -0.004	Max = 0.0628 Min = -0.0606 Mean = 8.576E-04 Std. Dev. = 0.0173	Max = 0.1636 Min = -0.1426 Mean = -2.34E-06 Std. Dev. = 0.0438	Max = 0.718 Min = -0.5228 Mean = 0.01917 Std. Dev. = 0.167	Max = 0.1145 Min = -0.1099 Mean = 1.9432E-04 Std. Dev. = 0.03576
YAW [deg]	Max = 0.0567 Min = -0.059 Mean = 3.78095 Std. Dev.= 0.0196	Max = 0.1907 Min = -0.2048 Mean = -7.2E-04 Std. Dev. =0.0652	Max = 0.2636 Min = -0.2513 Mean = 6.094E-04 Std. Dev. = 0.0813	Max = 2.36 Min = -2.12 Mean = -0.00937 Std. Dev. = 0.6937	Max = 0.14387 Min = -0.14855 Mean = -7.5385E-04 Std. Dev.= 0.0453

Table 3-5. Relative Motion Statistics, Head Sea

Relative Motion	Head Sea, 3body Operational Condition	Head Sea, 3body Survival Condition
SURGE [m]	Max = 0.2586 Min = -0.8372 Mean = -0.2794 Std. Dev. = 0.1681	Max = 1.34 Min = -12.482 Mean = -6.065 Std. Dev. = 2.13
SWAY [m]	Max = 0.2244 Min = -0.48258 Mean = -0.1441 Std. Dev. = 0.1122	Max = 1.0504 Min = -7.225 Mean = -2.8775 Std. Dev.= 1.264
HEAVE [m]	Max = 0.04569 Min = -0.0428 Mean = 5.39E-04 Std. Dev. = 0.01235	Max = 0.4432 Min = -0.4981 Mean = 0.00524 Std. Dev. = 0.13315
ROLL [deg]	Max = 0.5292 Min = -0.3855 Mean = 0.0564 Std. Dev. = 0.13427	Max = 8.1832 Min = -5.26 Mean = 1.324 Std. Dev. = 2.087
PITCH [deg]	Max = 0.0663 Min = -0.0729 Mean = -8.6981E-04 Std. Dev. = 0.01907	Max = 0.55739 Min = -0.7013 Mean = -0.0191 Std. Dev. = 0.18068
YAW [deg]	Max = 0.209 Min = -0.1986 Mean =7.311E-04 Std. Dev.= 0.067	Max = 2.1768 Min = -2.3637 Mean = -0.00876 Std. Dev.= 0.6956

Table 3-6. Statistics of Force on Dolphin Moorings, Head Sea

3body	Forward Dolphin Head Sea Operational Condition	Afterward Dolphin Head Sea Operational Condition	2body (FQ+FixedQ)	Forward Dolphin Head Sea Survival Condition	Afterward Dolphin Head Sea Survival Condition
FORCE [N]	Max =2.122E+06 Mean = 6.2133E+05 Std. Dev. = 3.43E+05	Max = 2.25E+06 Mean = 6.213E+05 Std. Dev. = 3.395E+05	FORCE [N]	Max = 2.385E+07 Mean = 6.864E+06 Std. Dev. = 3.8458E+06	Max = 2.325E+07 Mean = 6.861E+06 Std. Dev. = 3.827E+06

3.2.2 Quadrant Sea Case (45 [deg] of Wave Heading)

Wave train propagates in quartering sea wave direction. Waves are trapped in the gaps between those interacting bodies, and standing wave formation happens in this wave direction. Big reflection against Fixed Quay Wall will take place around Floating Quay and Container Ship, and shielding effect by Floating Quay and Container Ship also occur. These interaction effects, wave heading angle, and shielding effect, which are combined, make motions of certain modes bigger and motions of other modes less.

Table 3-7 and Table 3-8 illustrate statistics of pure mode response motion and relative motions between Floating Quay and Container Ship. Fig. 3-40, Fig. 3-41, and Fig. 3-42 show motion response spectrum, motion time history, and relative motion time history for operational condition, respectively. Fig. 3-43, Fig. 3-44, and Fig. 3-45 also show motion response spectrum, motion time history, and relative motion time history for survival condition, respectively.

Figures and tables show motions at operational condition with 45[deg] wave heading are small enough to make possible loading and Offloading operation between Floating Quay, Container Ship, and Fixed Quay Wall. But loading and offloading operation at survival condition is impossible. The gap between the floating bodies and the fixed body is 2.1[m]. Therefore, Floating Harbor, Container Ship, and Fixed Quay Wall will be damaged. Ships should be removed or must be moored strongly. Statistics of force on Dolphin moorings for 45 [deg] wave heading case is shown in Table 3-9.

3.2.2.1 Quadrant Sea Case, Operational Condition

Motion Response Spectrum of Floating Quay, Quartering Sea, Operational

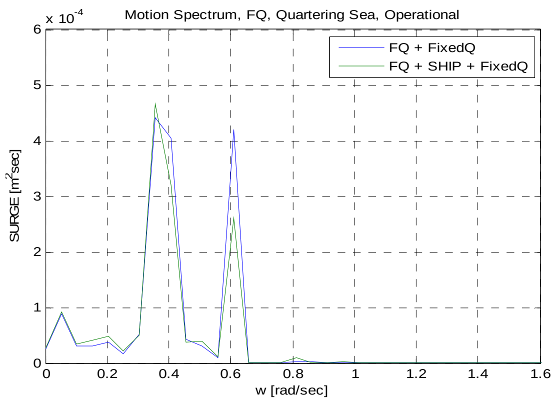

(a)

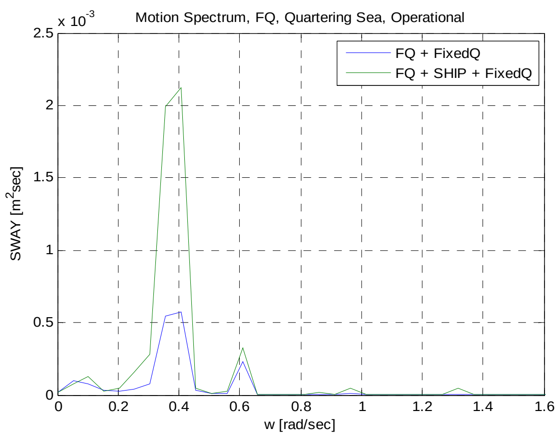

(b)

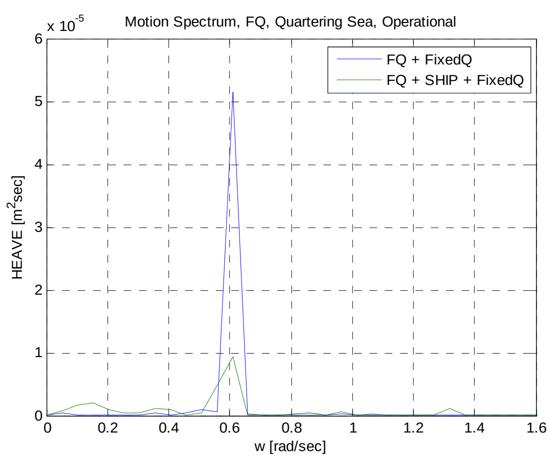

(c)

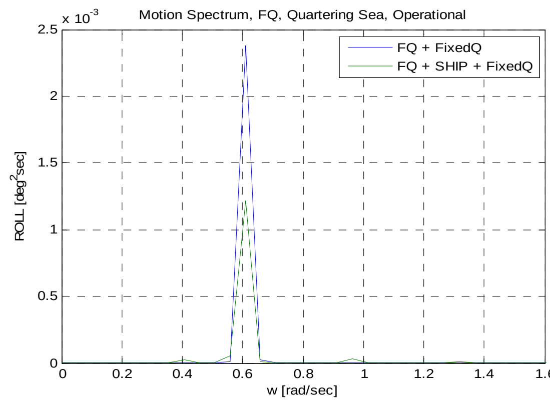

(d)

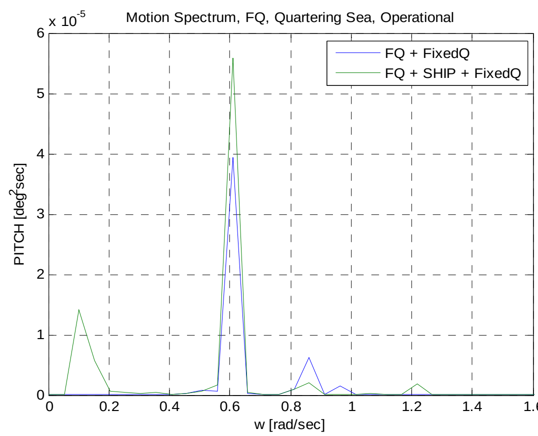

(e)

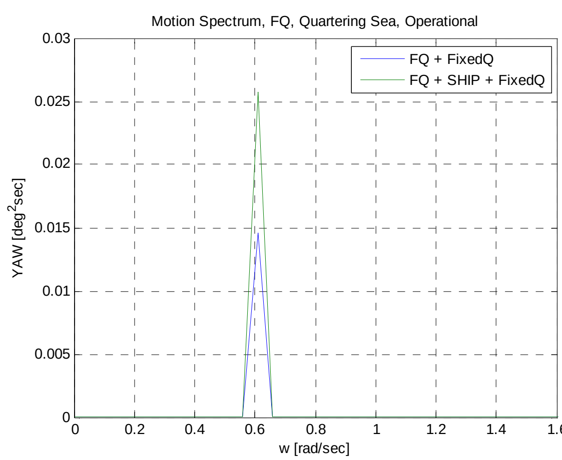

(f)

Fig. 3-40. Motion Response Spectrum, Quartering Sea, Operational

Motion Response Spectrum of Container Ship, Quartering Sea, Operational

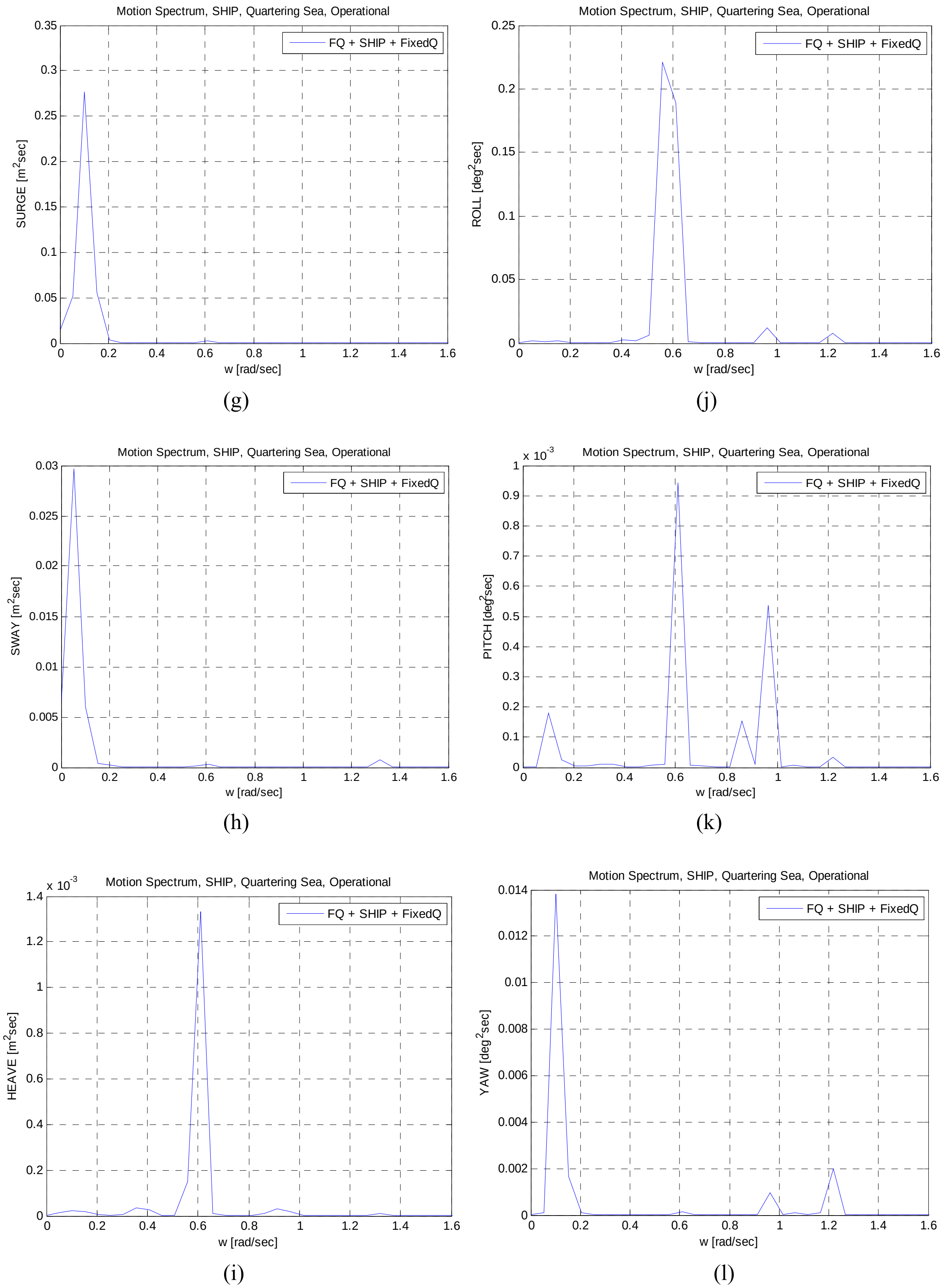

Fig. 3-40. Continued

Motion Time History of Floating Quay and Container Ship, Operational

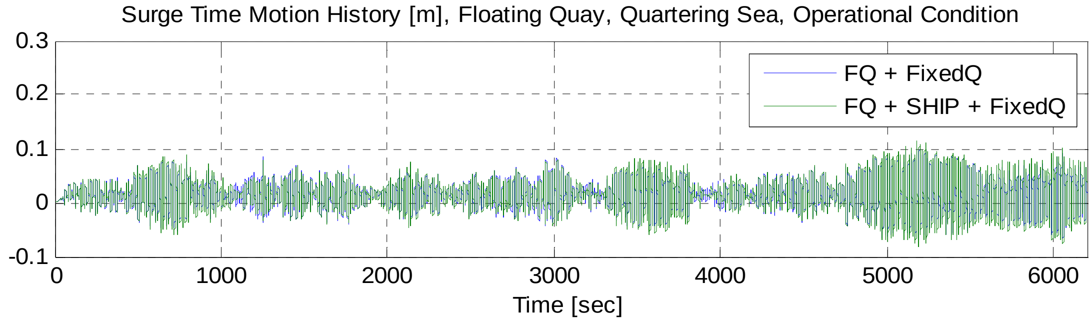

(a)

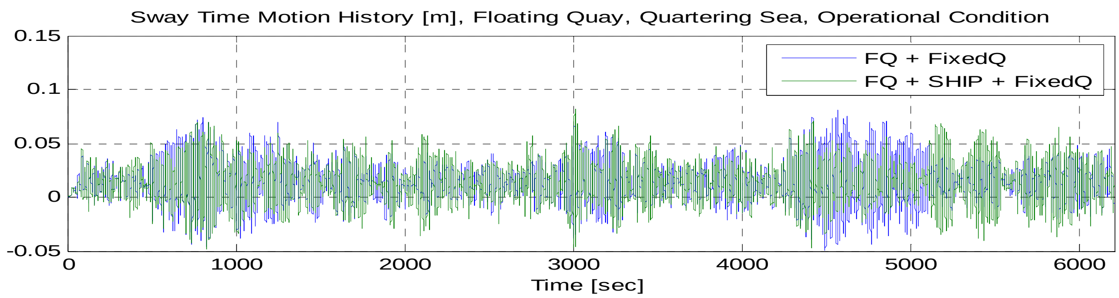

(b)

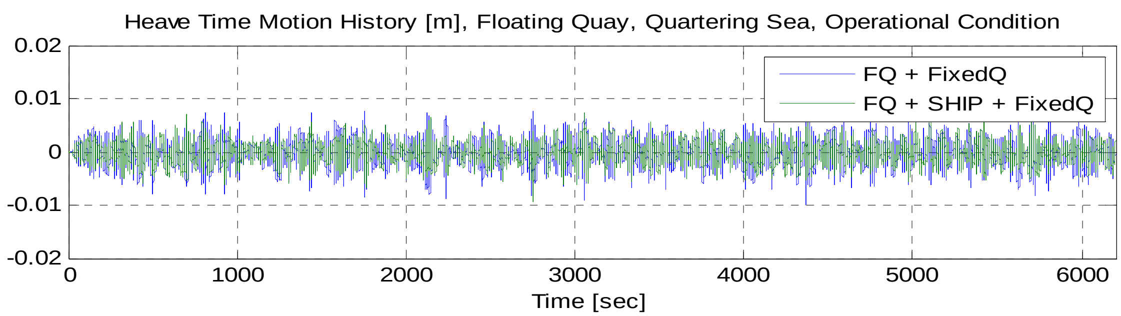

(c)

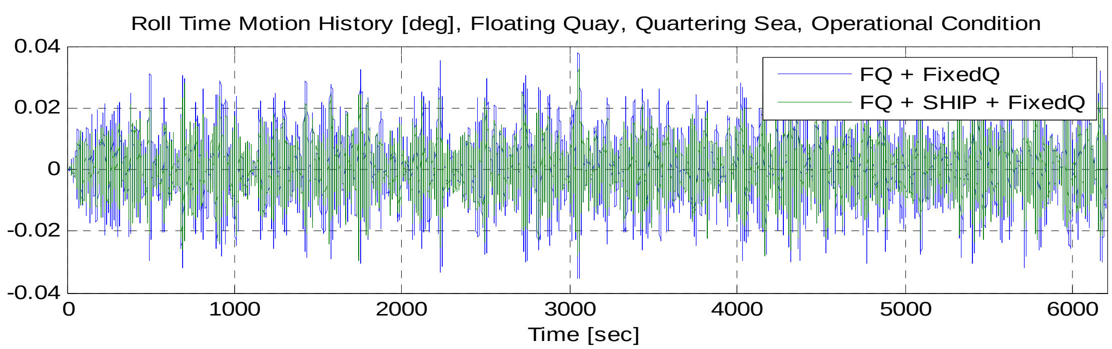

(d)

Fig. 3-41. Time Motion History, Quartering Sea, Operational

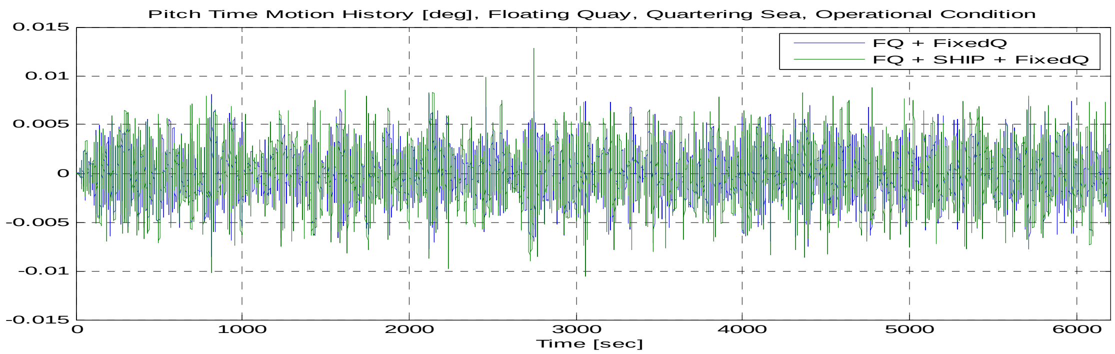

(e)

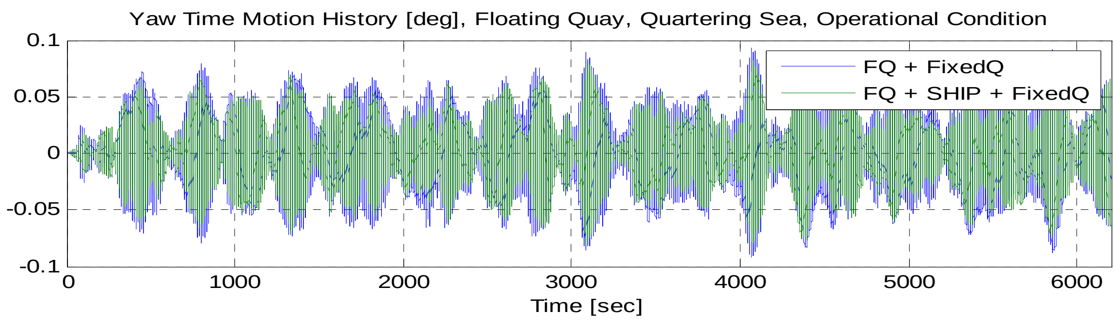

(f)

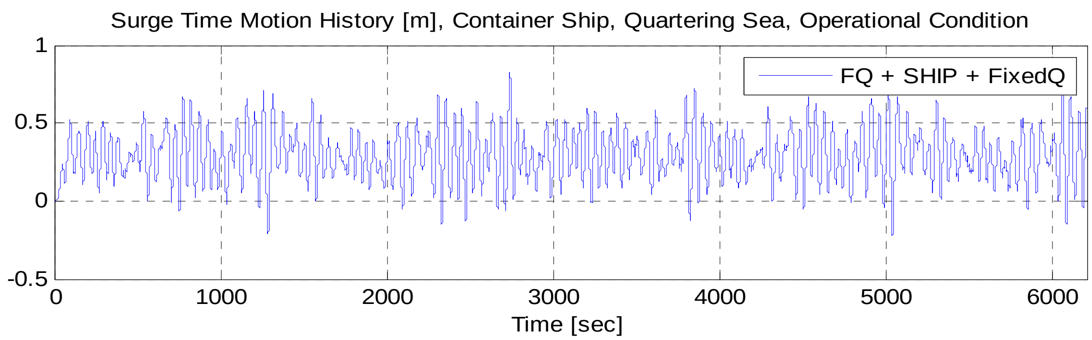

(g)

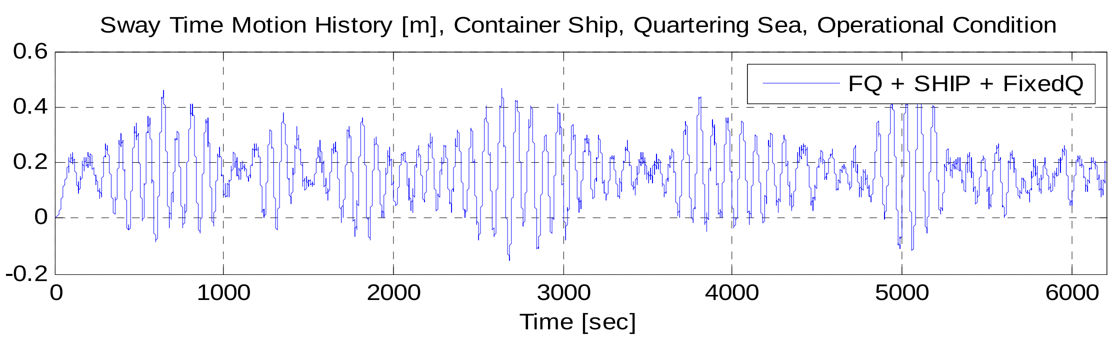

(h)

Fig. 3-41. Continued

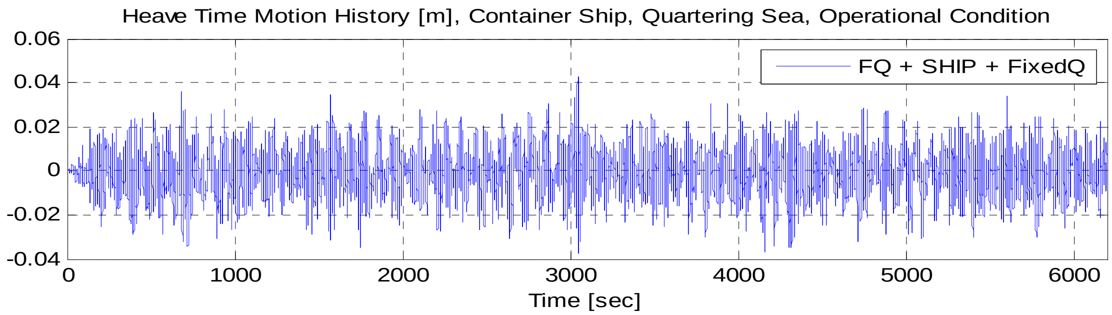

(i)

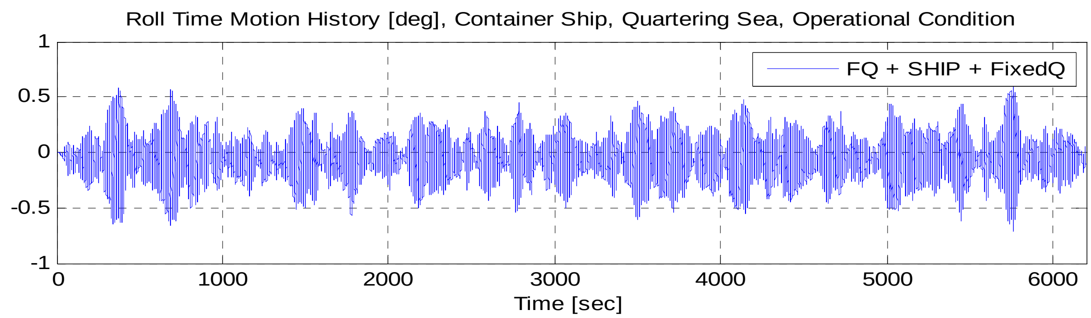

(j)

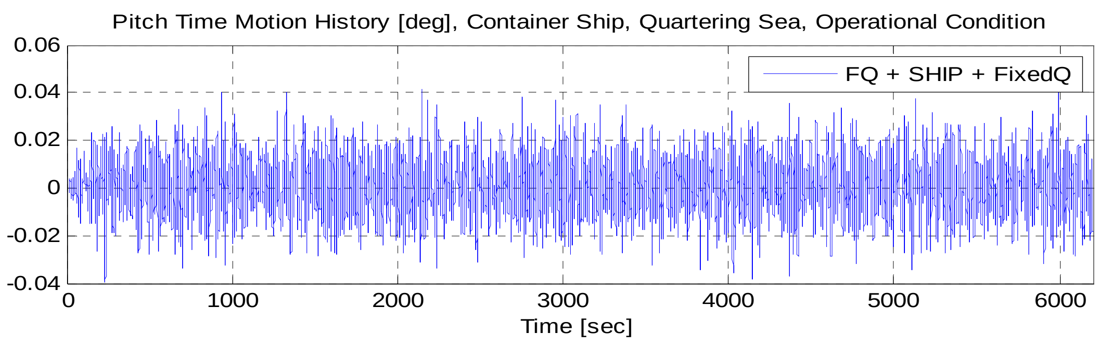

(k)

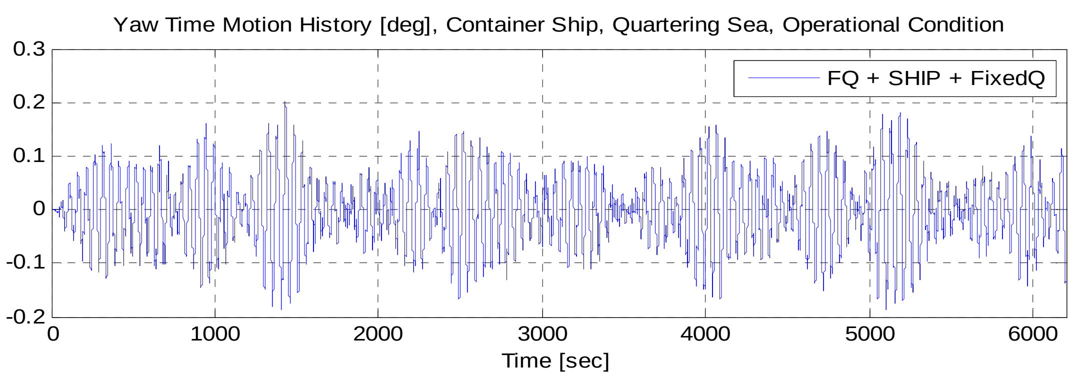

(l)

Fig. 3-41. Continued

Relative Motion Time History, Quartering Sea, Operational Condition

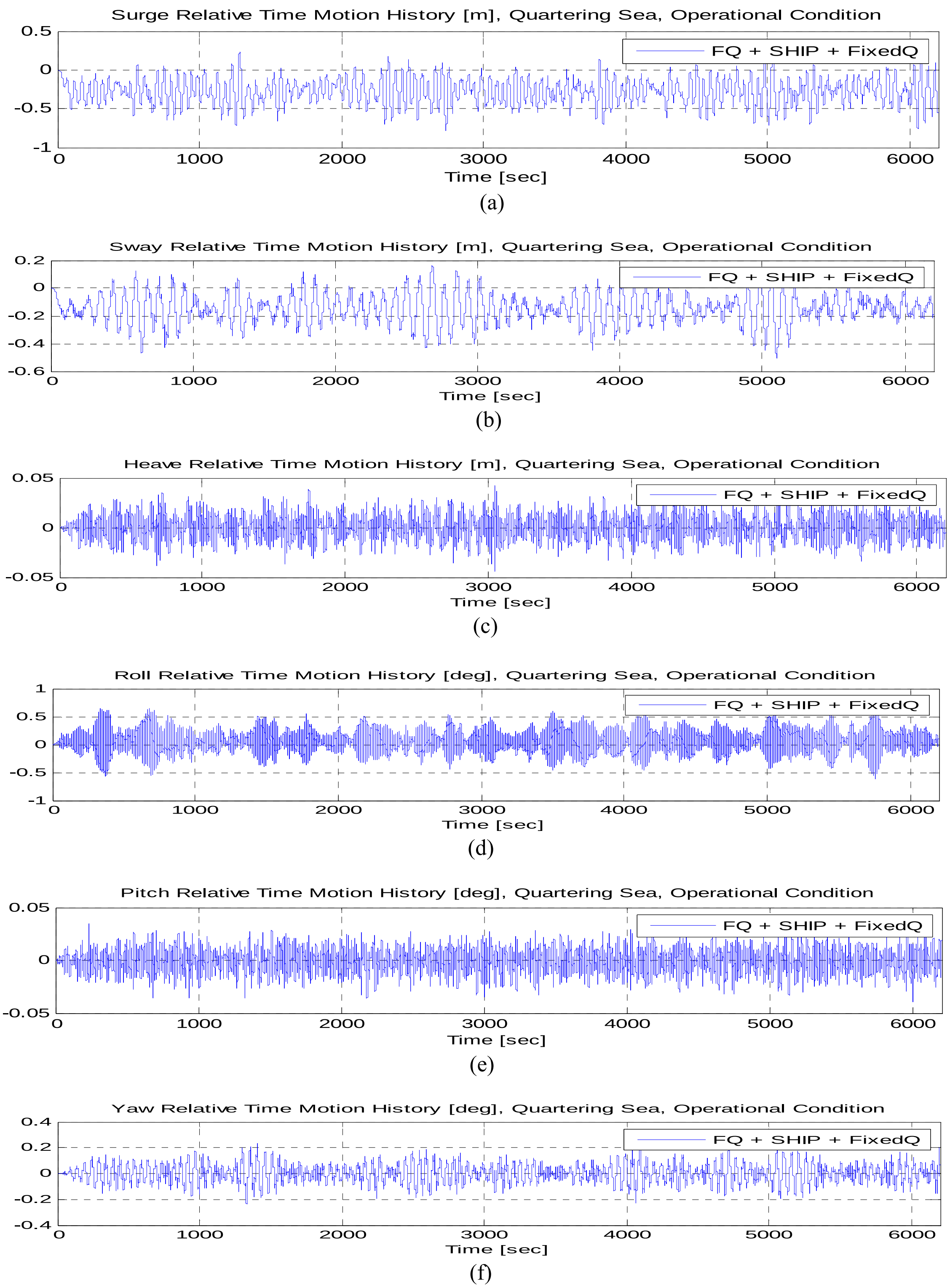

Fig. 3-42. Relative Motion Time History, Quartering Sea, Operational

3.2.2.2 Quadrant Sea Case, Survival Condition

Motion Time History of Floating Quay, Quartering Sea, Survival

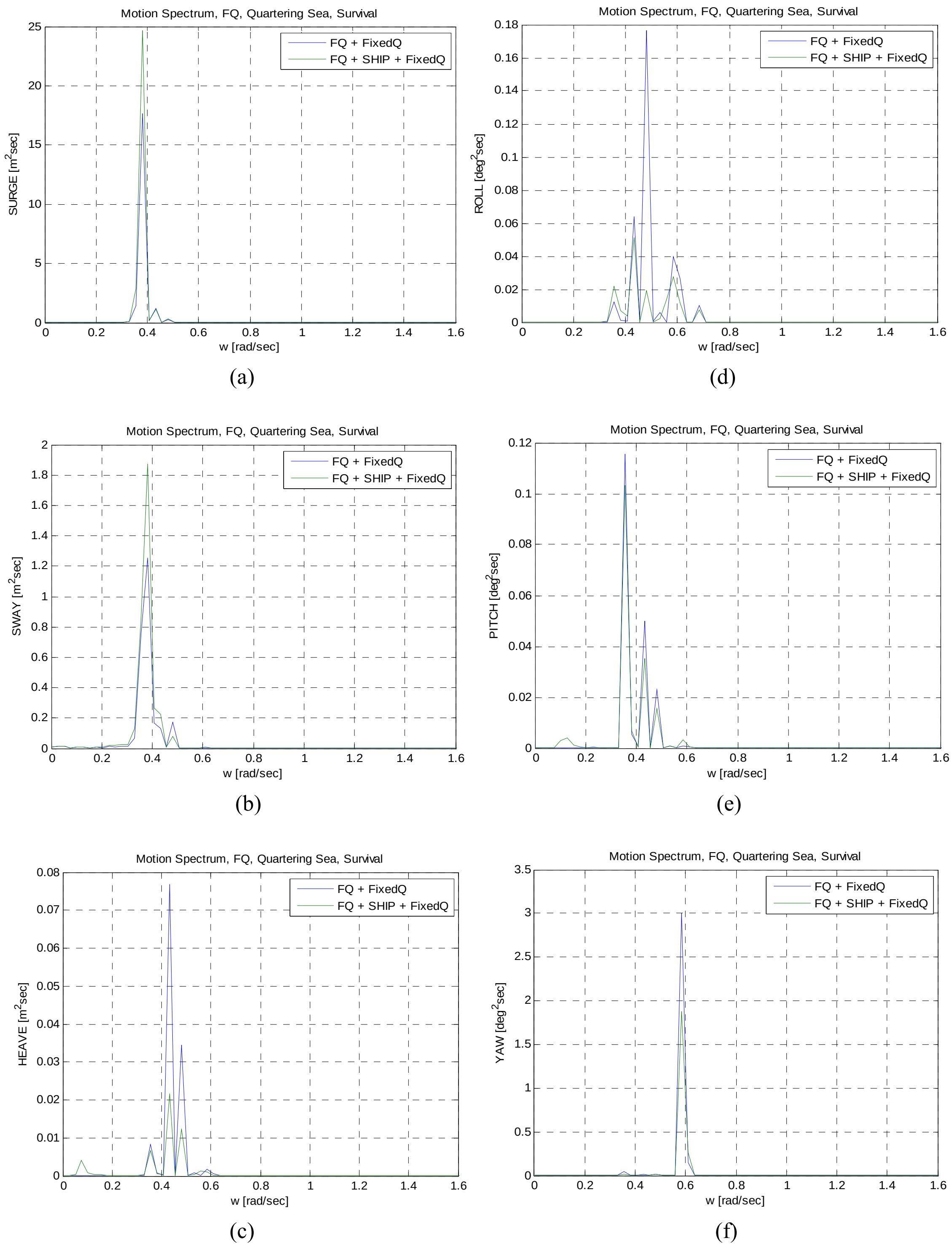

Fig. 3-43. Motion Response Spectrum, Quartering Sea, Survival

Motion Time History of Container Ship, Quartering Sea, Survival

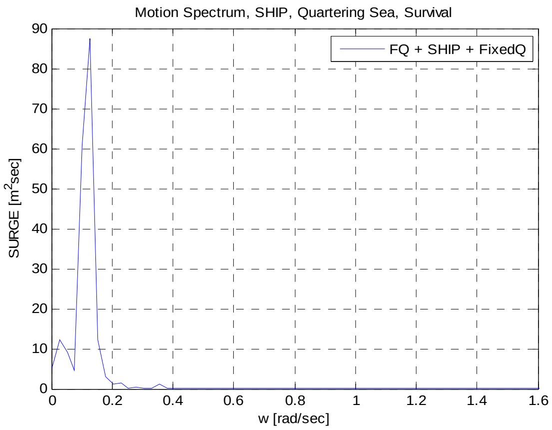

(g)

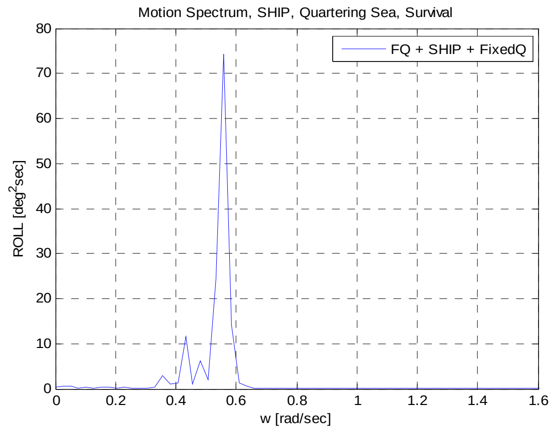

(j)

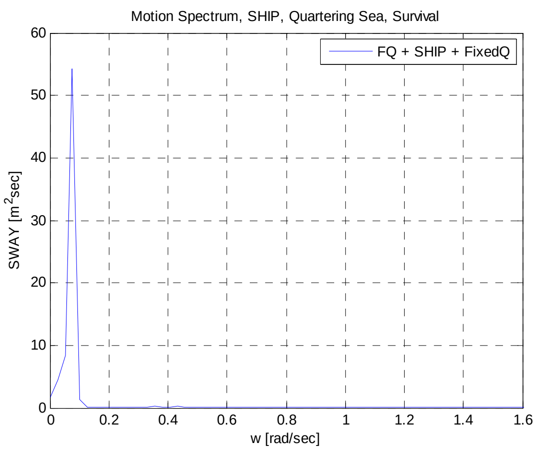

(h)

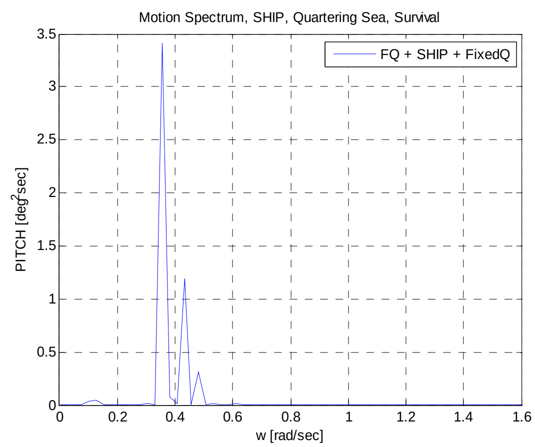

(k)

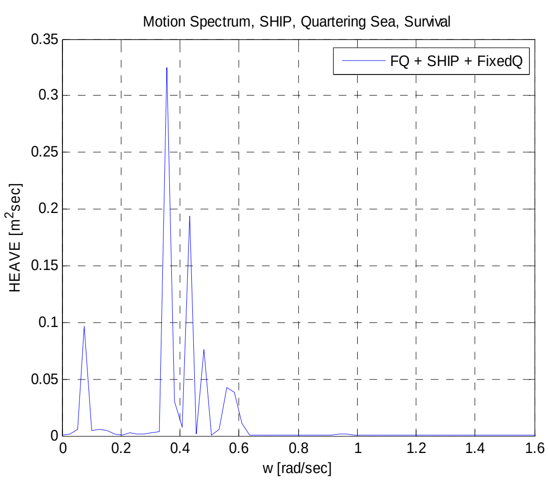

(i)

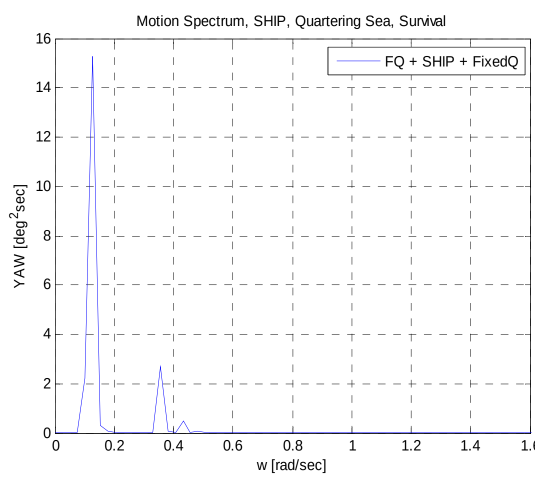

(l)

Fig. 3-43. Continued

Motion Time History of Floating Quay and Container Ship, Survival

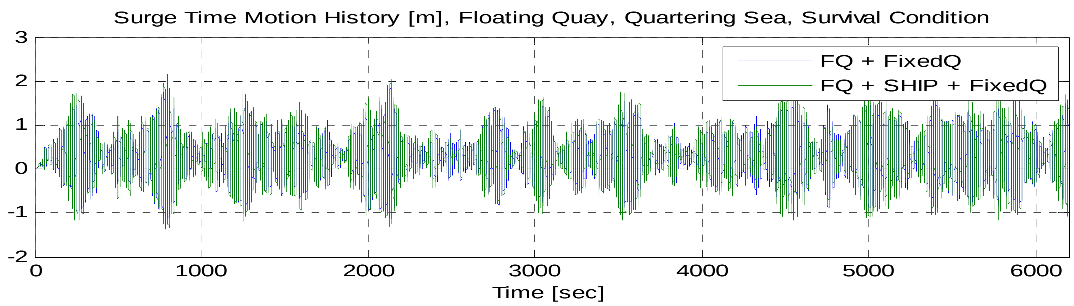

(a)

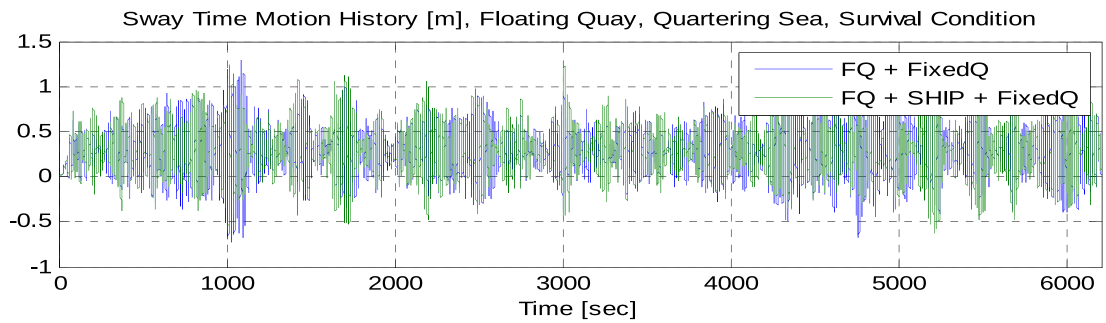

(b)

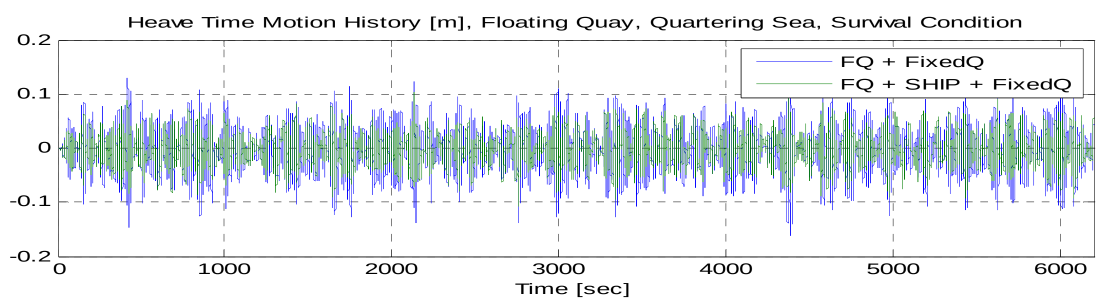

(c)

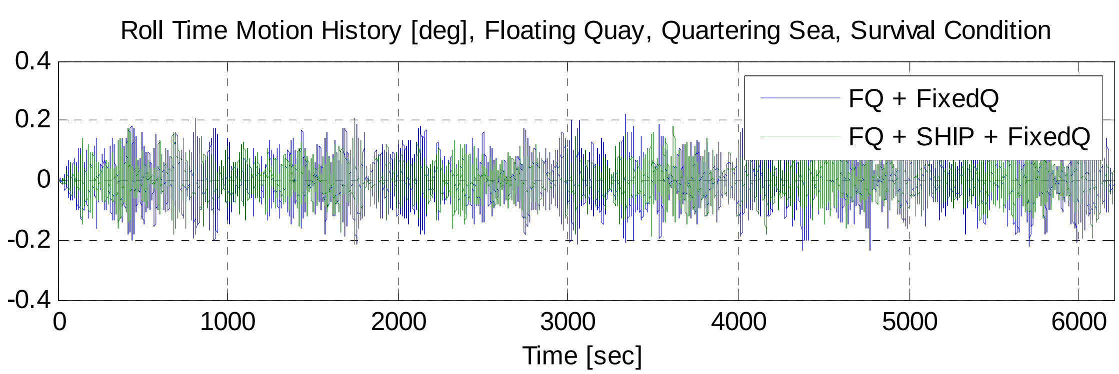

(d)

Fig. 3-44. Time Motion History, Quartering Sea, Survival

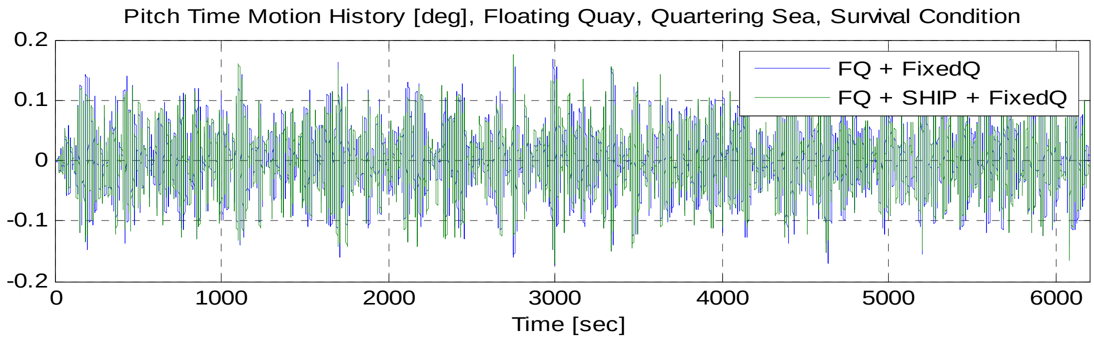

(e)

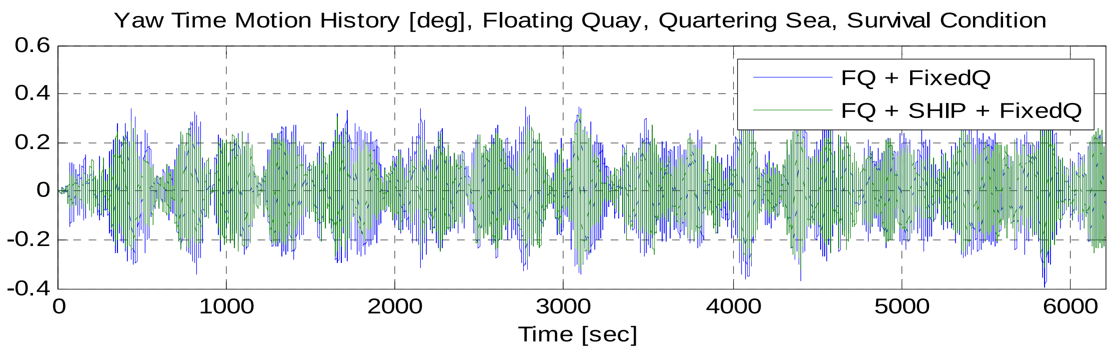

(f)

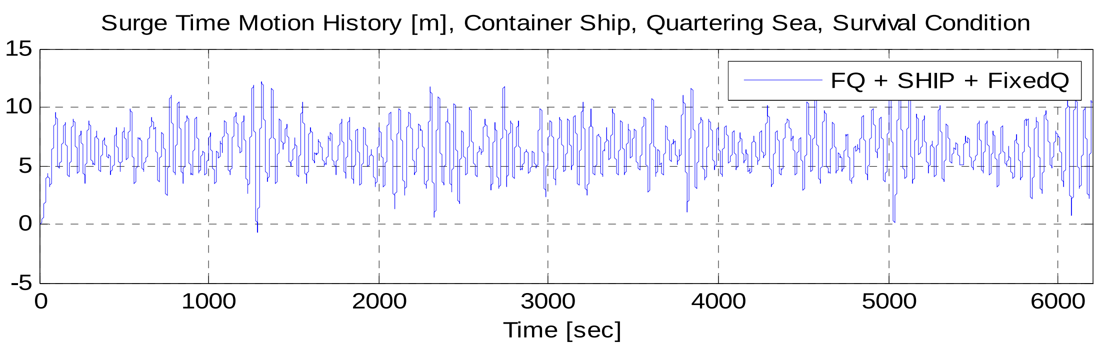

(g)

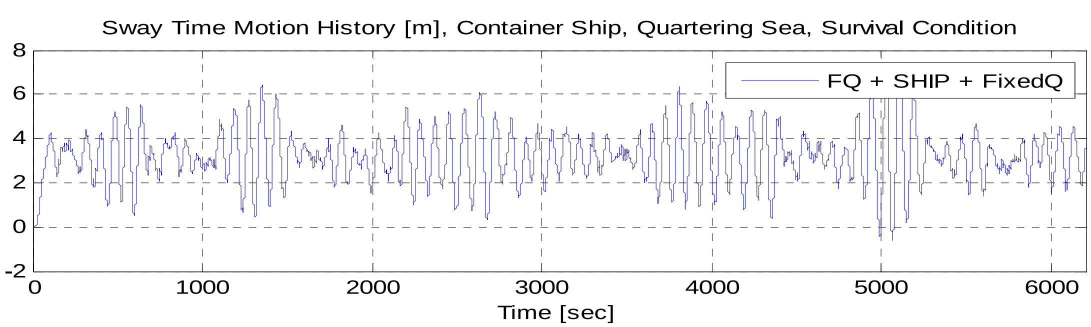

(h)

Fig. 3-44. Continued

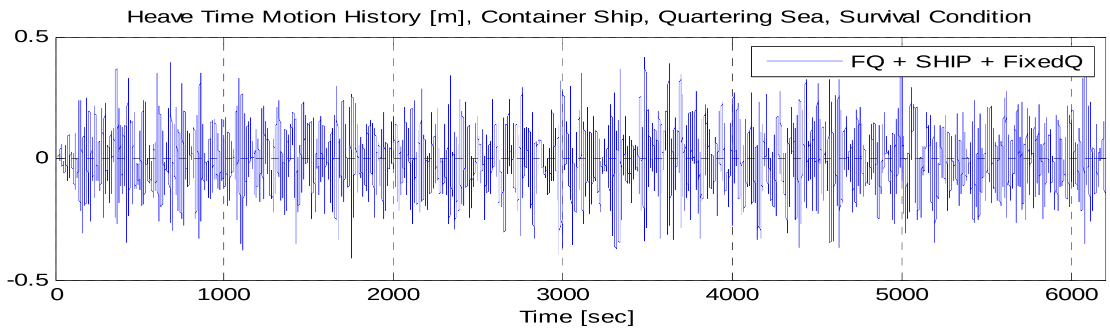

(i)

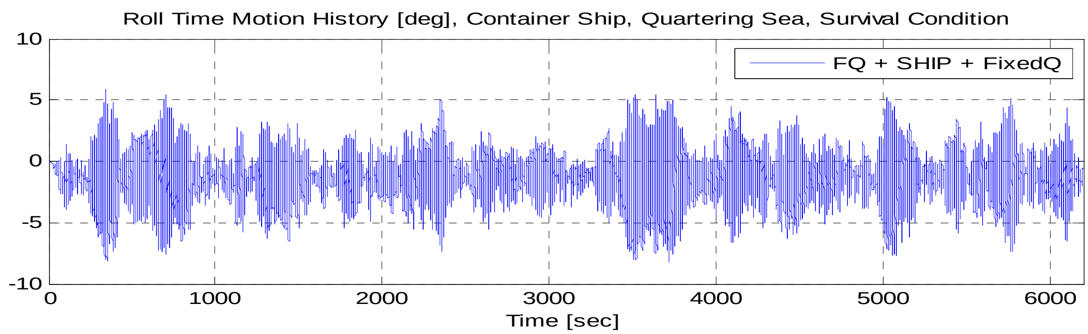

(j)

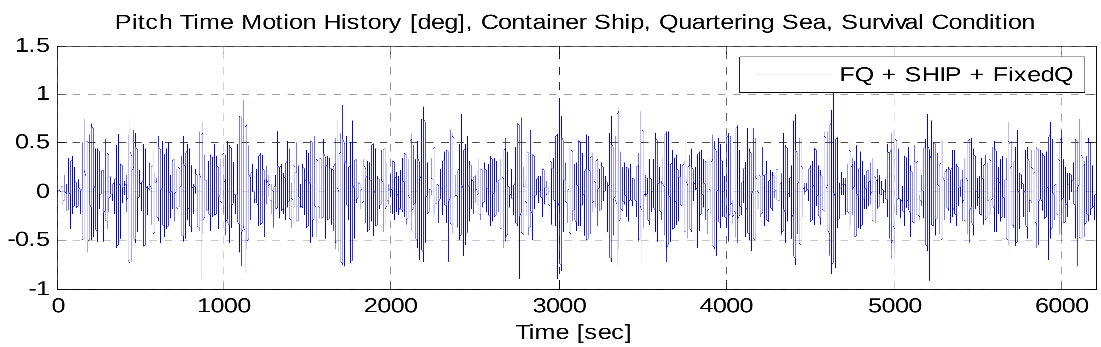

(k)

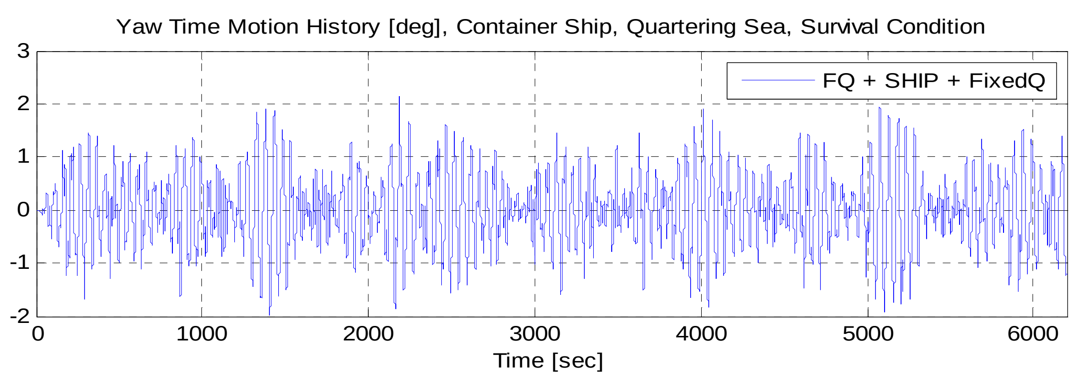

(l)

Fig. 3-44. Continued

Relative Motion Time History, Quartering Sea, Survival Condition

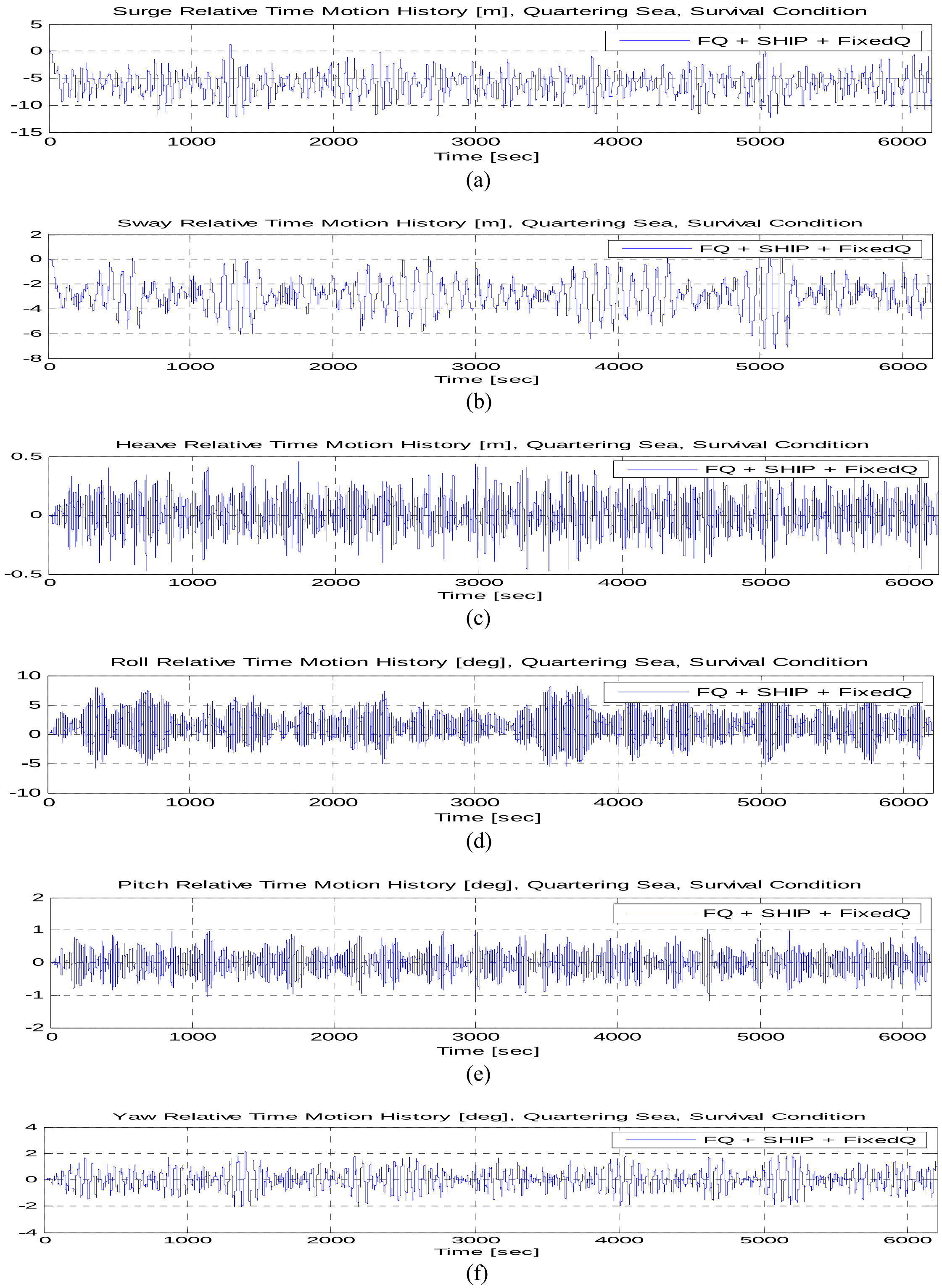

Fig. 3-45. Relative Motion Time History, Quartering Sea, Survival

Table 3-7. Motion Statistics, Quartering Sea

Motion	Floating Quay 3body Quartering Sea Operational Con't	Container Ship 3body Quartering Sea Operational Con't	Floating Quay 3body Quartering Sea Survival Con't	Container Ship 3body Quartering Sea Survival Con't	Floating Quay, 2body (FQ + FixedQ) Quartering Sea Survival Con't
SURGE [m]	Max = 0.114 Min = -0.0809 Mean = 0.0145 Std. Dev. = 0.0317	Max = 0.8250 Min = -0.2169 Mean = 0.2932 Std. Dev. = 0.1662	Max = 2.1709 Min = -1.3678 Mean = 0.2957 Std. Dev. = 0.5850	Max = 12.1468 Min = -0.6987 Mean = 6.3671 Std. Dev. = 2.0597	Max = 1.9348 Min = -1.2016 Mean = 0.2945 Std. Dev. = 0.5167
SWAY [m]	Max = 0.0825 Min = -0.0469 Mean = 0.0133 Std. Dev. = 0.0188	Max = 0.5121 Min = -0.1512 Mean = 0.1611 Std. Dev. = 0.1039	Max = 1.3062 Min = -0.6592 Mean = 0.2934 Std. Dev. = 0.2893	Max = 7.4172 Min = -0.6506 Mean = 3.1796 Std. Dev. = 1.2088	Max = 1.2927 Min = -0.7304 Mean = 0.2847 Std. Dev. = 0.2864
HEAVE [m]	Max = 0.0074 Min = -0.0094 Mean = -2.01E-04 Std. Dev. = 0.002	Max = 0.0430 Min = -0.0374 Mean = -6.73E-04 Std. Dev. = 0.0106	Max = 0.1042 Min = -0.1076 Mean = -0.003 Std. Dev. =0.0303	Max = 0.4180 Min = -0.4109 Mean = -0.0102 Std. Dev. = 0.1234	Max = 0.1351 Min = -0.1619 Mean = -0.0038 Std. Dev. = 0.0426
ROLL [deg]	Max = 0.0328 Min = -0.0296 Mean = -2.17E-05 Std. Dev. = 0.0082	Max = 0.6106 Min = -0.7134 Mean = -0.0576 Std. Dev. =0.1901	Max = 0.2012 Min = -0.2166 Mean = -0.8E-04 Std. Dev. = 0.0566	Max = 5.9257 Min = -8.2768 Mean = -1.311 Std. Dev. = 2.2194	Max = 0.2226 Min = -0.2374 Mean = -0.002 Std. Dev. = 0.0727
PITCH [deg]	Max = 0.0128 Min = -0.0106 Mean = -2.47E-05 Std. Dev. = 0.0029	Max = 0.0414 Min = -0.0386 Mean = 9.038E-04 Std. Dev. = 0.0118	Max = 0.1813 Min = -0.1718 Mean = -1.04E-04 Std. Dev. = 0.0524	Max = 1.0878 Min = -0.9111 Mean = 0.0176 Std. Dev. = 0.2942	Max = 0.1714 Min = -0.1731 Mean = 1.65E-04 Std. Dev. = 0.0543
YAW [deg]	Max = 0.0827 Min = -0.0826 Mean = 2.225E-04 Std. Dev.= 0.0287	Max = 0.2033 Min = -0.1865 Mean = -0.0021 Std. Dev. = 0.0652	Max = 0.3516 Min = -0.3246 Mean = 0.0026 Std. Dev. = 0.1108	Max = 2.1503 Min = -1.9944 Mean = 0.0064 Std. Dev. = 0.6831	Max = 0.4090 Min = -0.3960 Mean = 0.0022 Std. Dev.= 0.1305

Table 3-8. Relative Motion Statistics, Quartering Sea

Relative Motion	Quartering Sea, 3body Operational Condition	Quartering Sea, 3body Survival Condition
SURGE [m]	Max = 0.2616 Min = -0.7902 Mean = -0.2786 Std. Dev. = 0.1688	Max = 1.3562 Min = -12.2825 Mean = -6.0714 Std. Dev. = 2.1333
SWAY [m]	Max = 0.1627 Min = -0.5052 Mean = -0.1479 Std. Dev. = 0.1055	Max = 1.1684 Min = -7.2563 Mean = -2.8861 Std. Dev.= 1.2436
HEAVE [m]	Max = 0.0425 Min = -0.0442 Mean = 4.7238E-04 Std. Dev. = 0.0114	Max = 0.4572 Min = -0.4691 Mean = 0.0072 Std. Dev. = 0.1406
ROLL [deg]	Max = 0.7058 Min = -0.6108 Mean = 0.0576 Std. Dev. = 0.1873	Max = 8.2078 Min = -5.8980 Mean = 1.3103 Std. Dev. = 2.2026
PITCH [deg]	Max = 0.0387 Min = -0.0392 Mean = -9.2857E-04 Std. Dev. = 0.0106	Max = 1.0237 Min = -1.1898 Mean = -0.0177 Std. Dev. = 0.3307
YAW [deg]	Max = 0.2306 Min = 0.0711 Mean = 0.0023 Std. Dev.= 0.0711	Max = 2.1450 Min = -2.0542 Mean = -0.0038 Std. Dev.= 0.6937

Table 3-9. Statistics of Force on Dolphin Moorings, Quartering Sea

3body	Forward Dolphin Quartering Sea Operational Condition	Afterward Dolphin Quartering Sea Operational Condition	2body (FQ+ FixedQ)	Forward Dolphin Quartering Sea Survival Condition	Afterward Dolphin Quartering Sea Survival Condition
FORCE [N]	Max = 2.778E+06 Mean = 8.01E+05 Std. Dev. = 4.7788E+05	Max = 2.999E+06 Mean = 8.0137E+05 Std. Dev. = 4.757E+05	**FORCE [N]**	Max = 2.394E+07 Mean = 7.068E+06 Std. Dev. = 3.735E+06	Max = 2.2382E+07 Mean = 7.165E+06 Std. Dev. = 3.809E+06

3.2.3 Beam Sea Case (90 [deg] of Wave Heading)

Sway, heave, and roll response motions are largest in 90 [deg] wave direction. Wave train propagates in the positive y direction. Waves will be trapped in the gaps between those interacting bodies, and huge reflection against Fixed Quay Wall and shielding effect by Floating Quay happen around the floating bodies and the fixed body. Surge and pitch motions are relatively small, and sway, roll motions are greater than those in 0[deg] and 45[deg] wave direction cases.

Table 3-10 and table 3-11 show statistics of pure mode response motion and relative motions between Floating Quay and Container Ship. Fig. 3-46, Fig. 3-47, and Fig. 3-48 show motion response spectrum, motion time history, and relative motion time history for operational condition, respectively. Fig. 3-49, Fig. 3-50, and Fig. 3-51 also show motion response spectrum, motion time history, and relative motion time history for survival condition, respectively.

As shown in tables and figures, responses at operational condition with 90[deg] wave heading are not great. Loading and Offloading operation between Floating Quay, Container Ship, and Fixed Quay Wall is definitely possible at operational condition. But loading and offloading operation at survival condition are impossible. This wave direction makes biggest reflection due to the presence of Fixed Quay Wall and normal direction of Fixed Quay Wall. This situation makes sway, heave, roll responses way bigger than those of other wave directions. Table 3-12 illustrates statistics of force on Dolphin moorings for 90 [deg] wave heading case.

3.2.3.1 Beam Sea Case, Operational Condition

Motion Response Spectrum of Floating Quay, Beam Sea, Operational

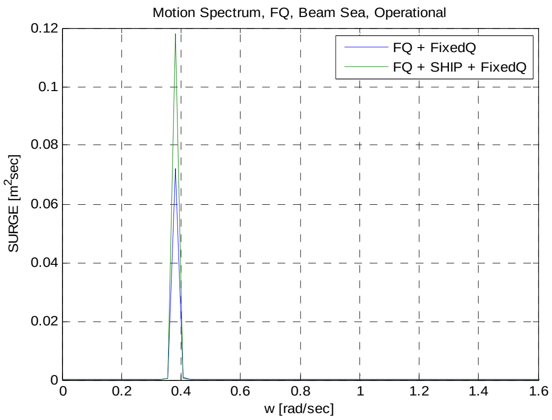

(a)

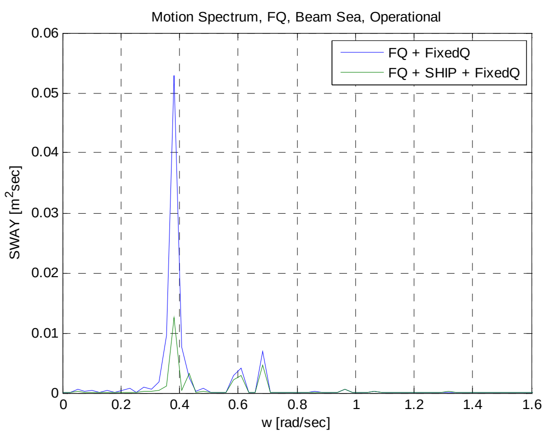

(b)

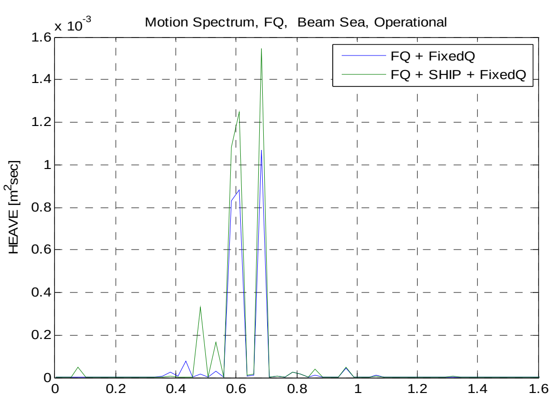

(c)

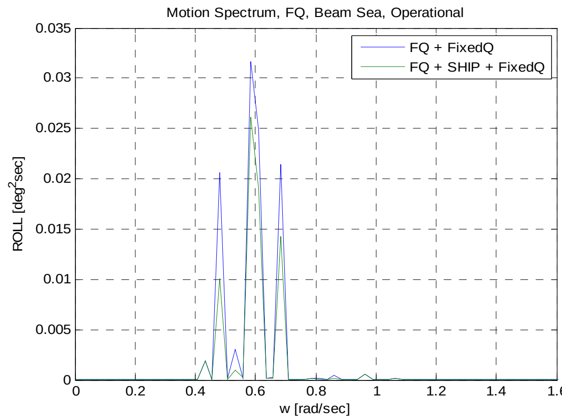

(d)

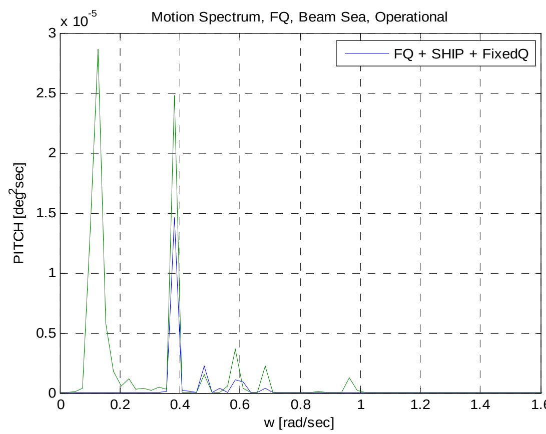

(e)

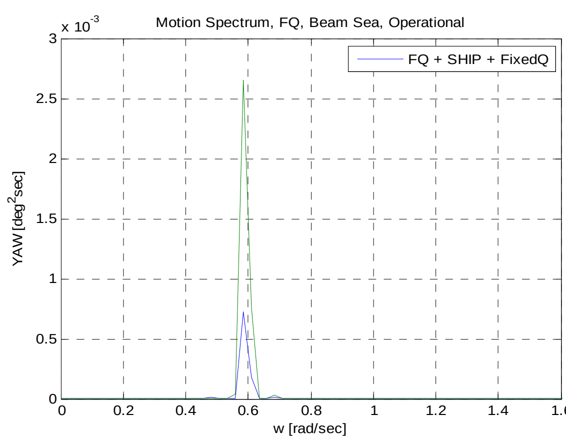

(f)

Fig. 3-46. Motion Response Spectrum, Beam Sea, Operational

Motion Response Spectrum of Container Ship, Quartering Sea, Operational

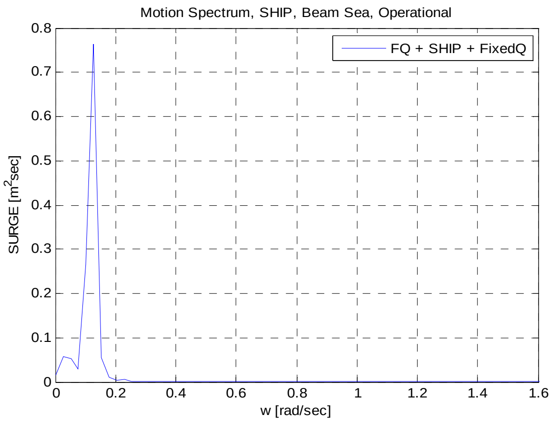

(g)

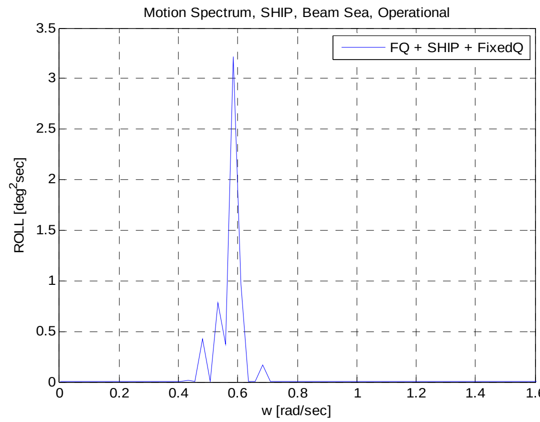

(j)

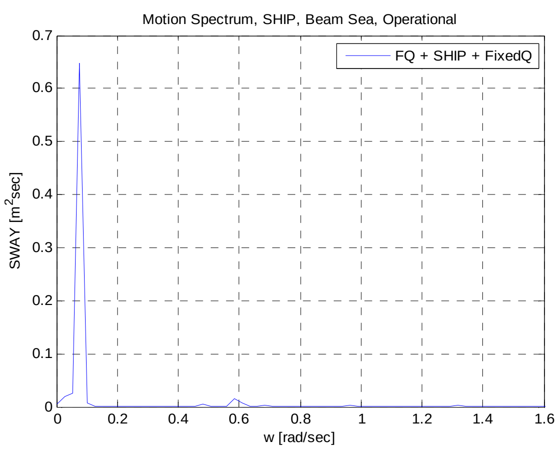

(h)

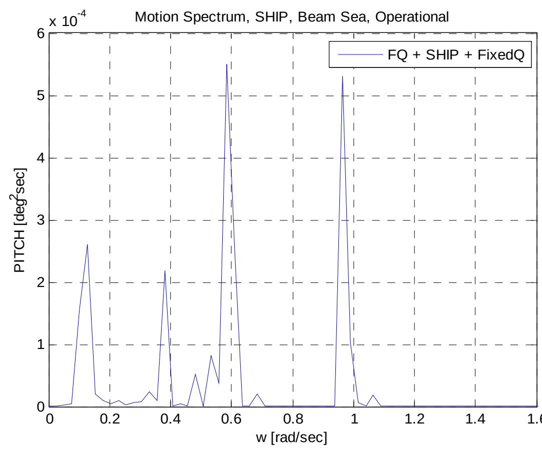

(k)

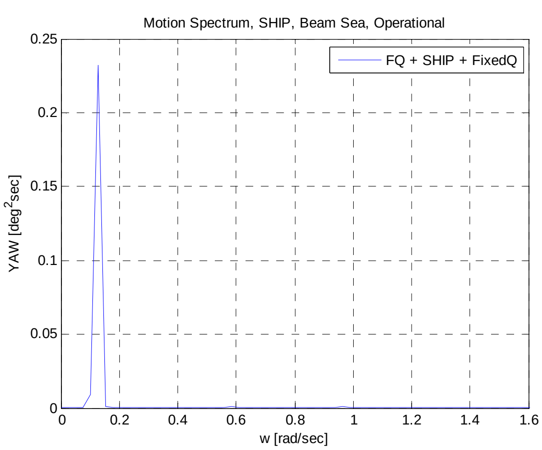

(i)

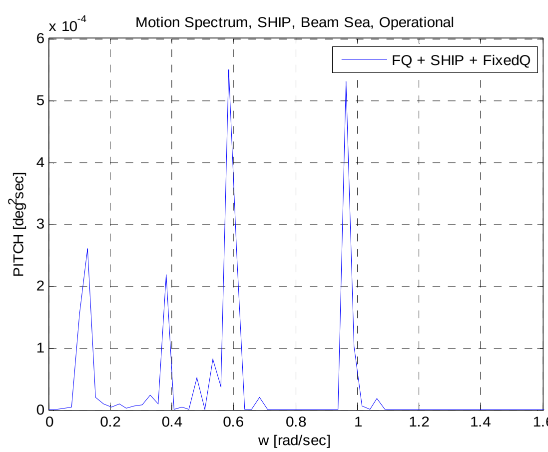

(l)

Fig. 3-46. Continued

Motion Time History of Floating Quay and Container Ship, Operational

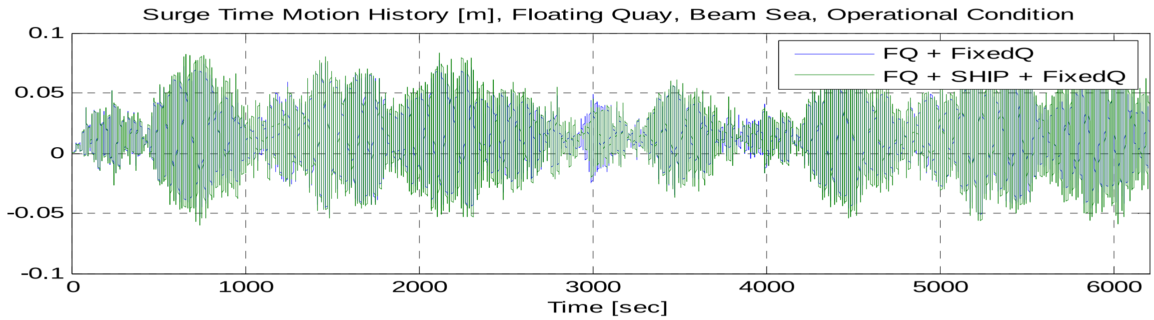

(a)

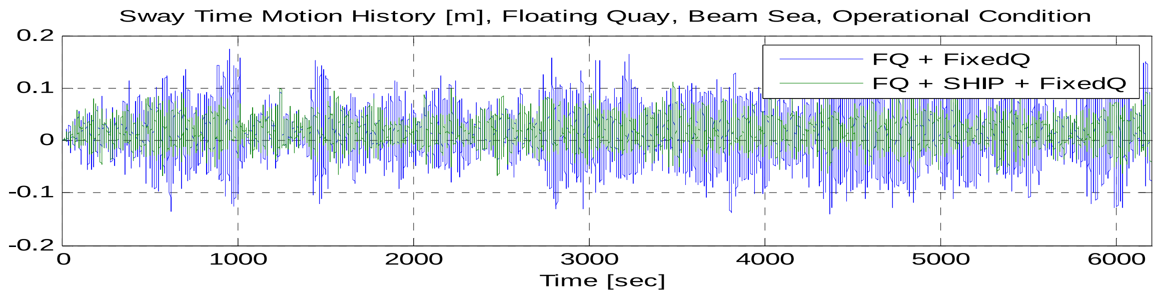

(b)

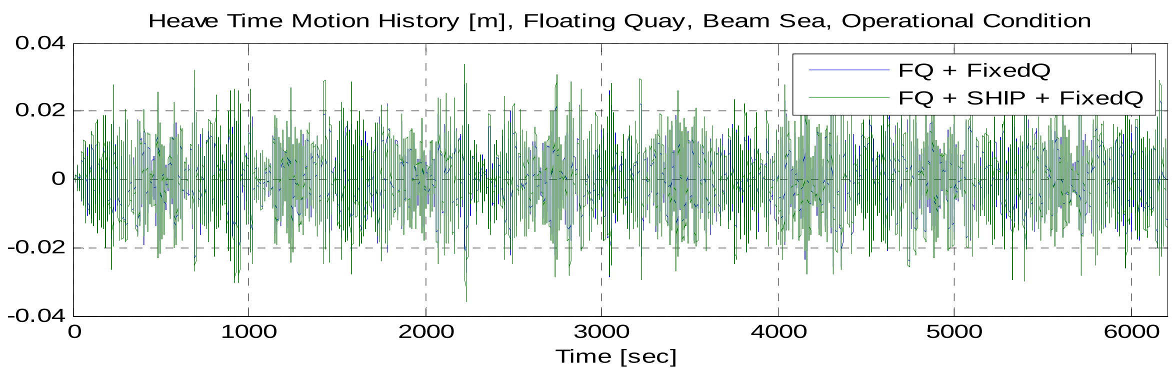

(c)

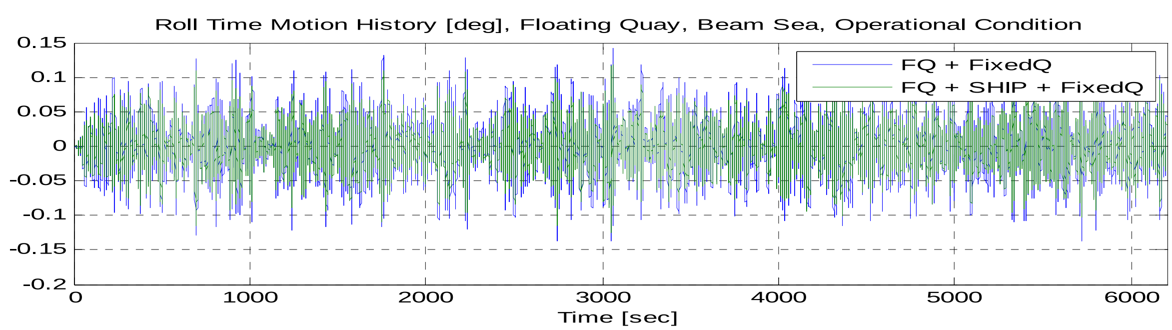

(d)

Fig. 3-47. Time Motion History, Beam Sea, Operational

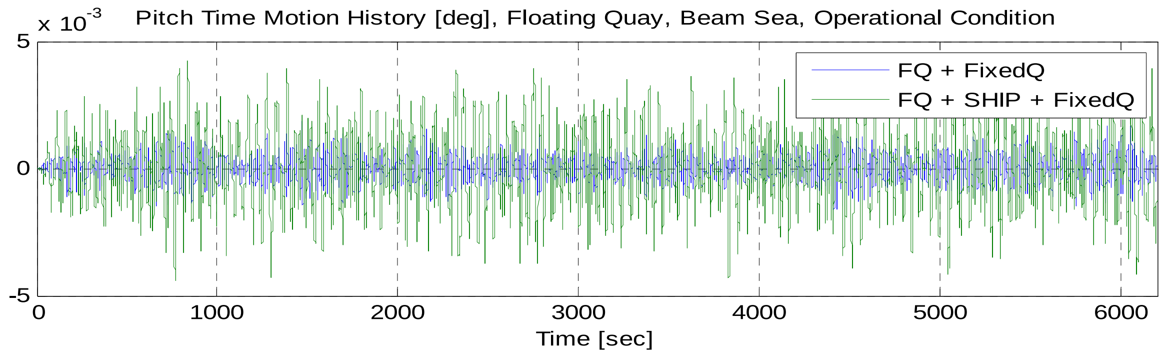

(e)

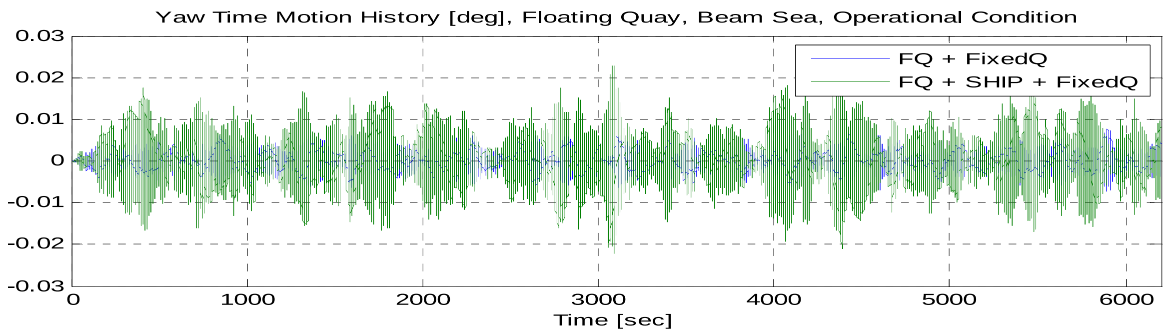

(f)

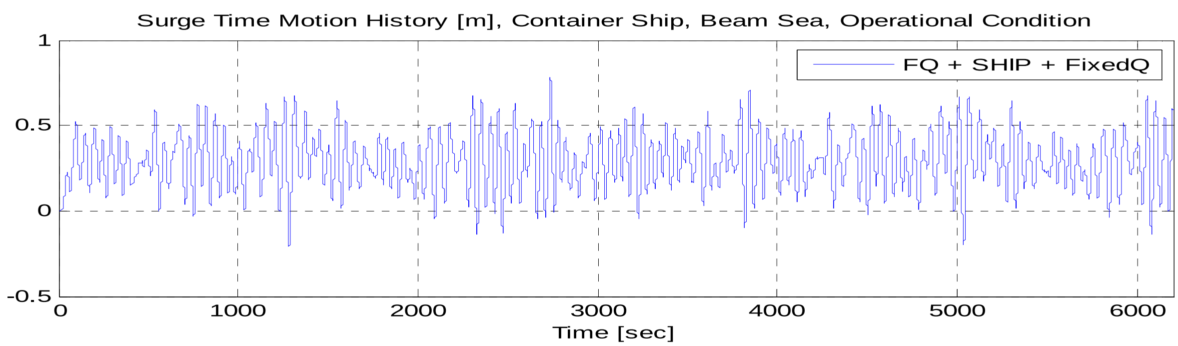

(g)

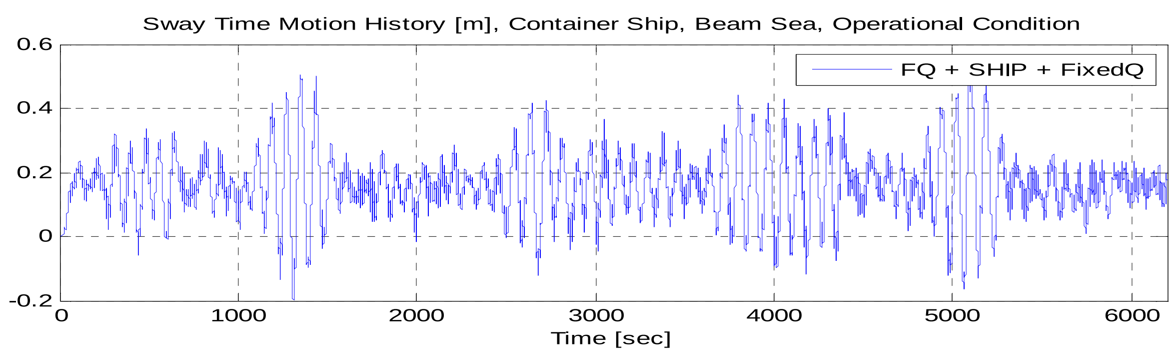

(h)

Fig. 3-47. Continued

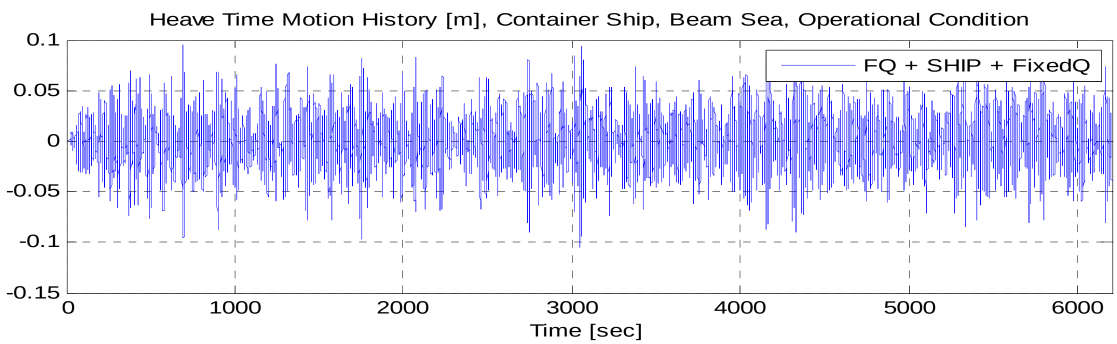

(i)

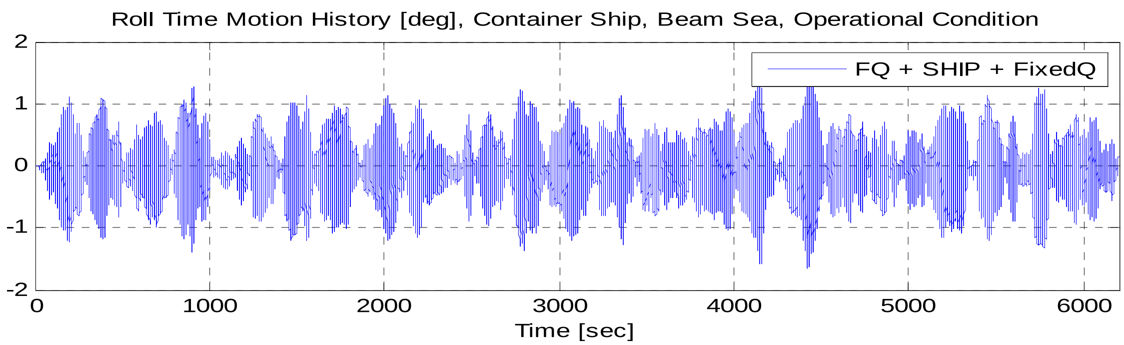

(j)

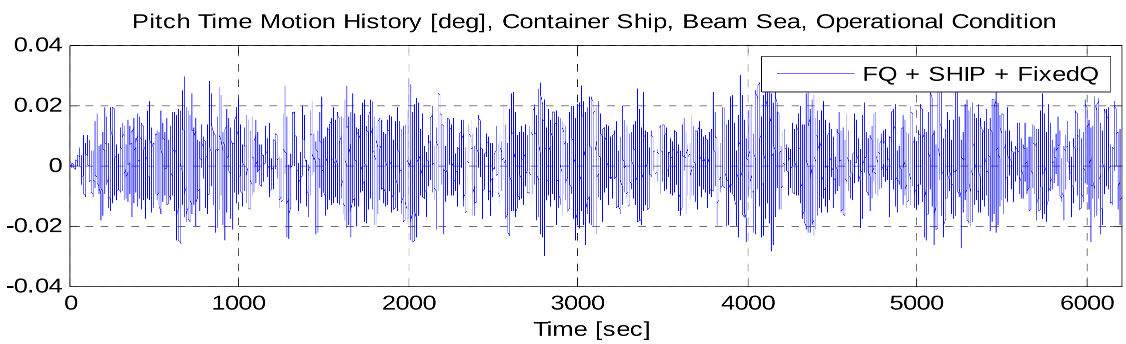

(k)

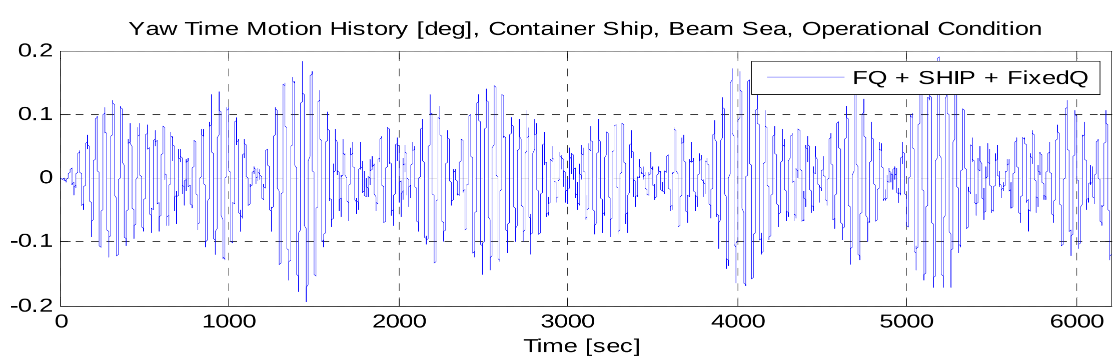

(l)

Fig. 3-47. Continued

Relative Motion Time History, Beam Sea, Operational Condition

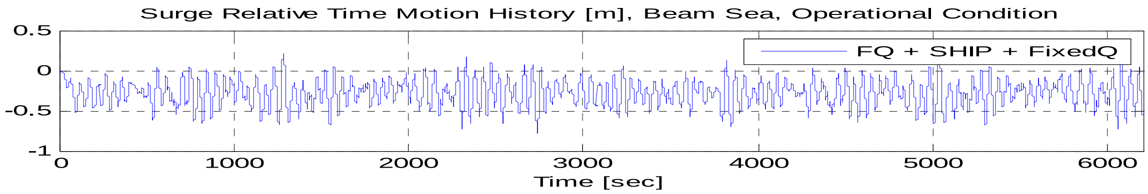

(a)

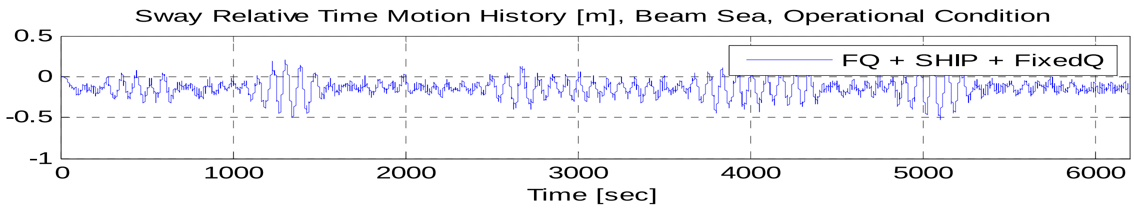

(b)

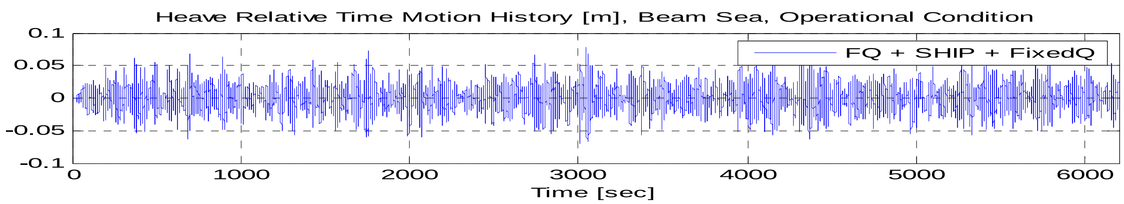

(c)

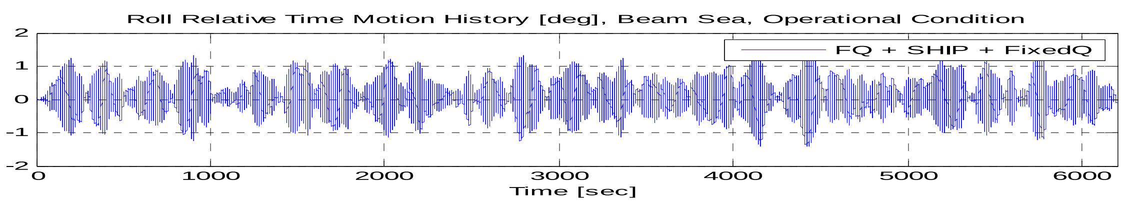

(d)

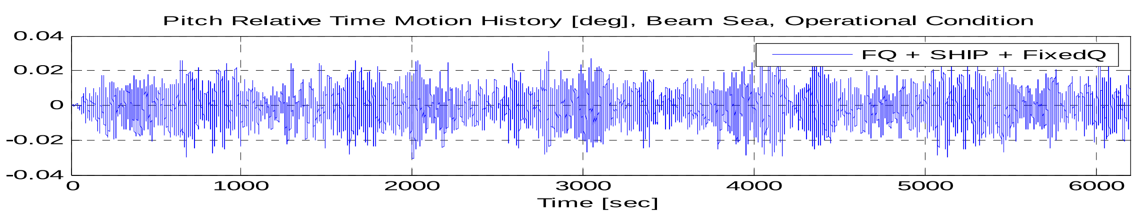

(e)

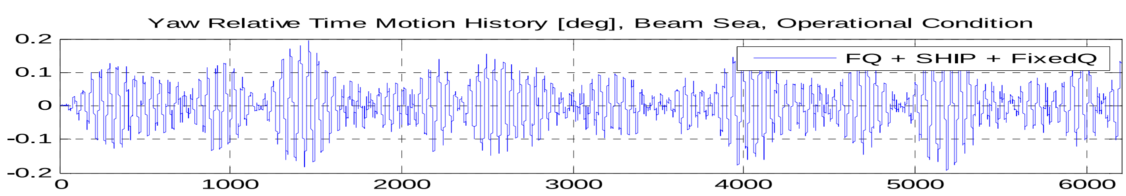

(f)

Fig. 3-48. Relative Motion Time History, Beam Sea, Operational

3.2.3.2 Beam Sea Case, Survival Condition

Motion Response Spectrum of Floating Quay, Beam Sea, Survival

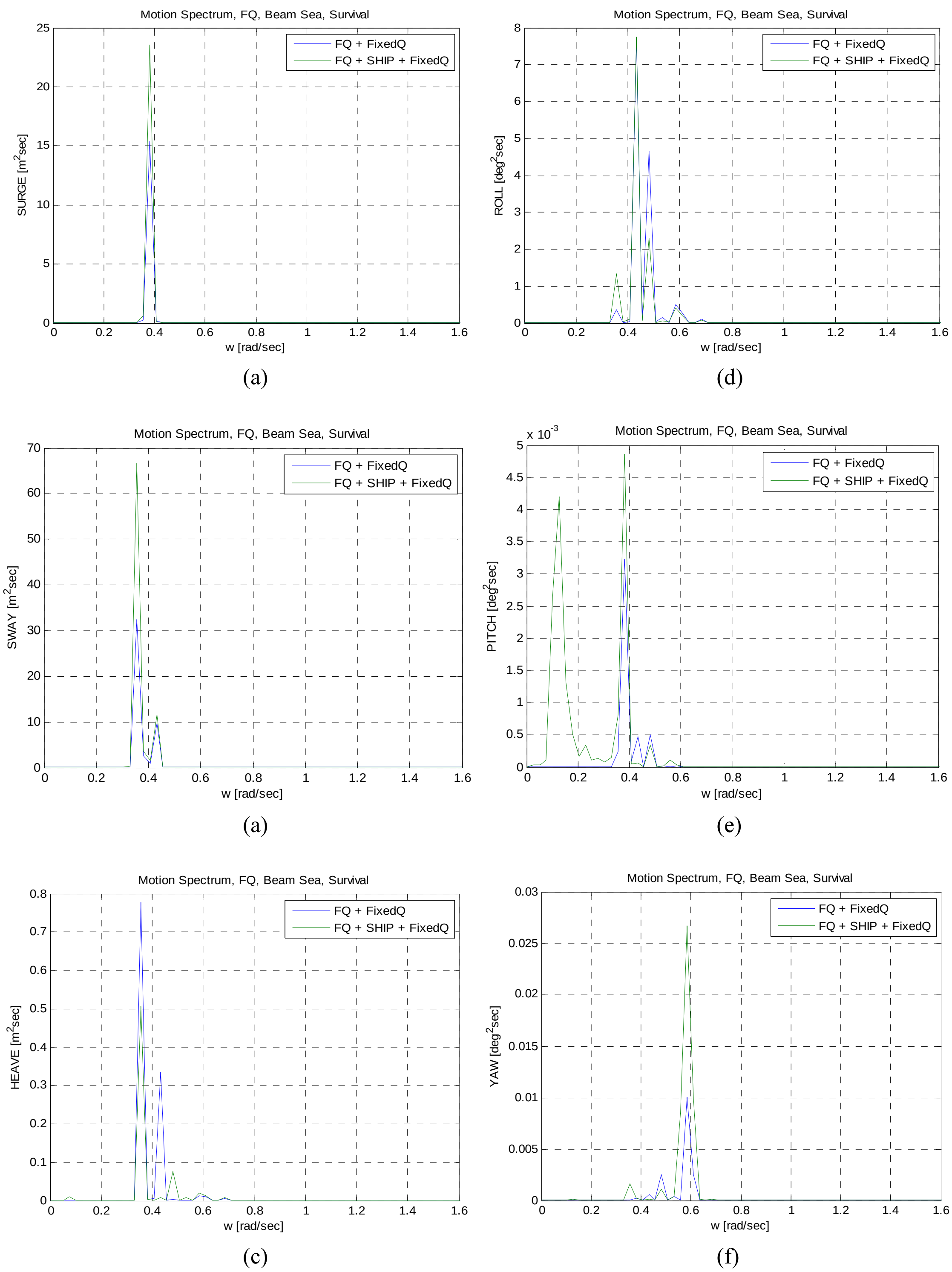

Fig. 3-49. Motion Response Spectrum, Beam Sea, Survival

Motion Response Spectrum of Container Ship, Beam Sea, Survival

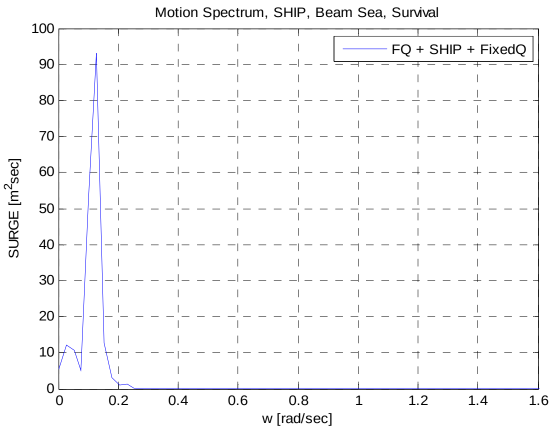

(g)

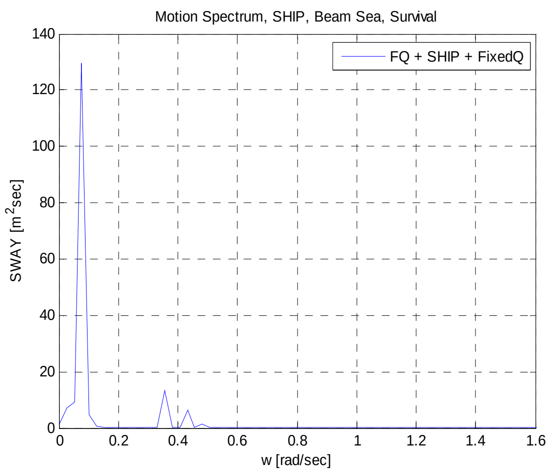

(h)

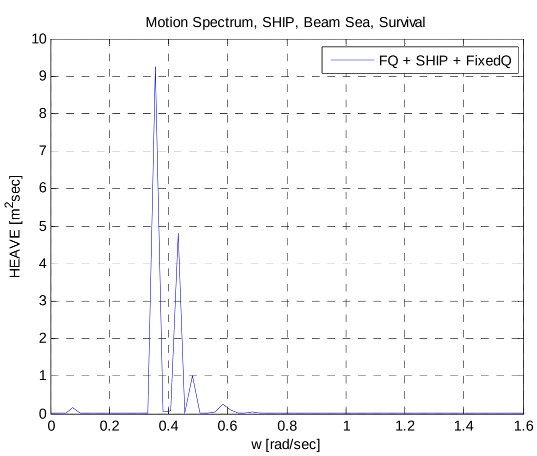

(i)

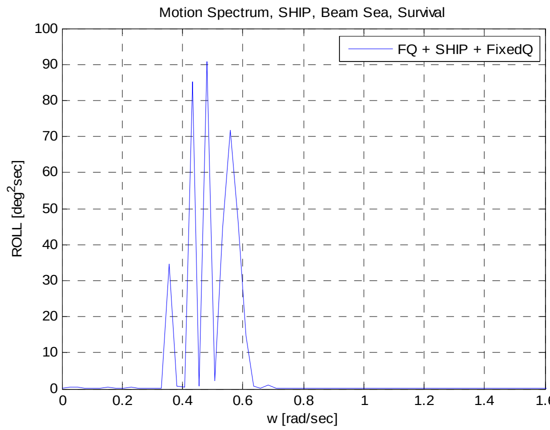

(j)

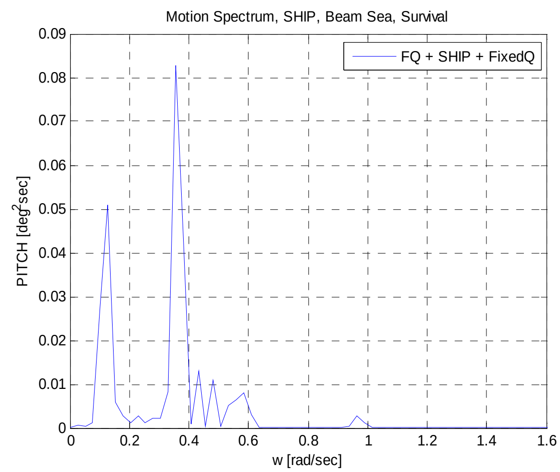

(k)

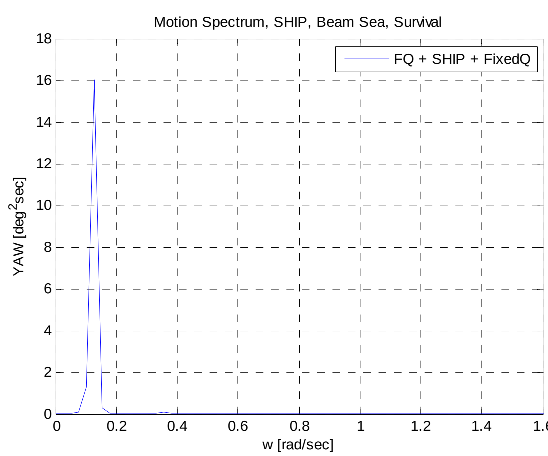

(l)

Fig. 3-49. Continued

Motion Time History of Floating Quay and Container Ship, Operational

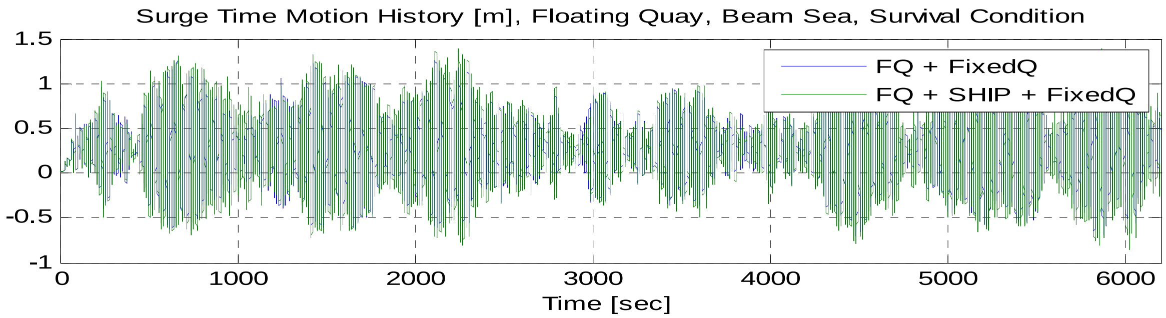

(a)

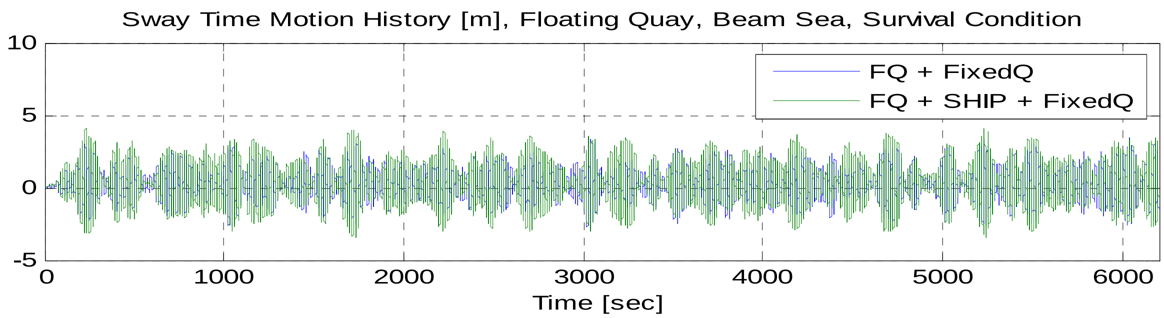

(b)

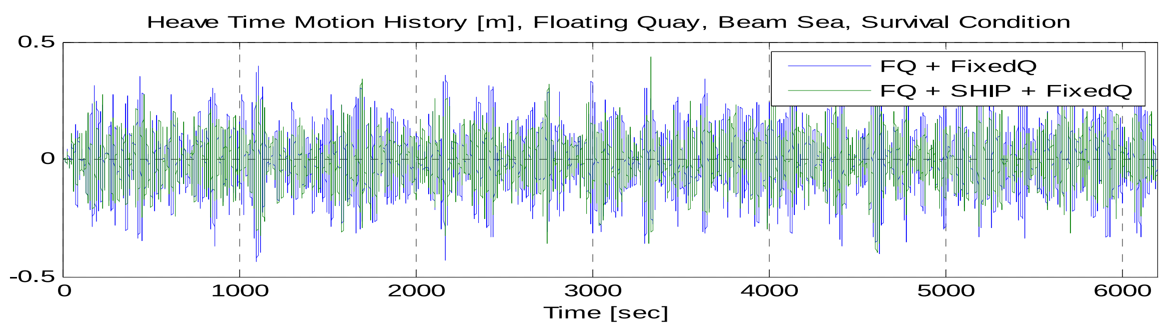

(c)

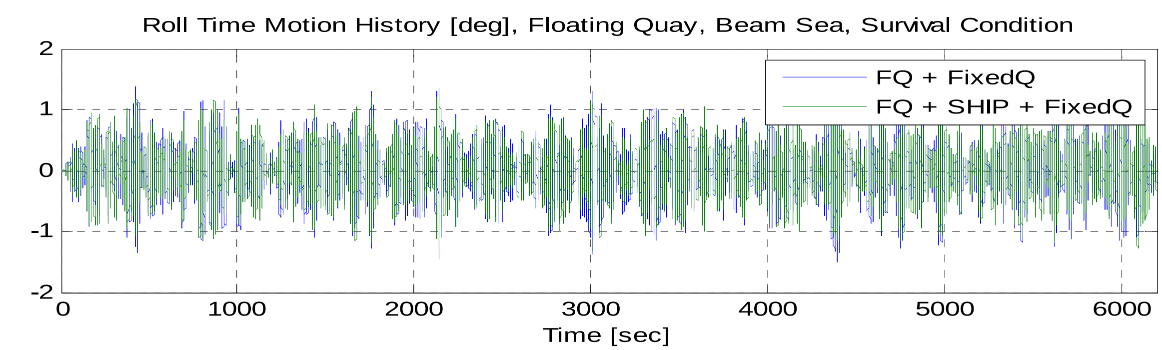

(d)

Fig. 3-50. Time Motion History, Beam Sea, Survival

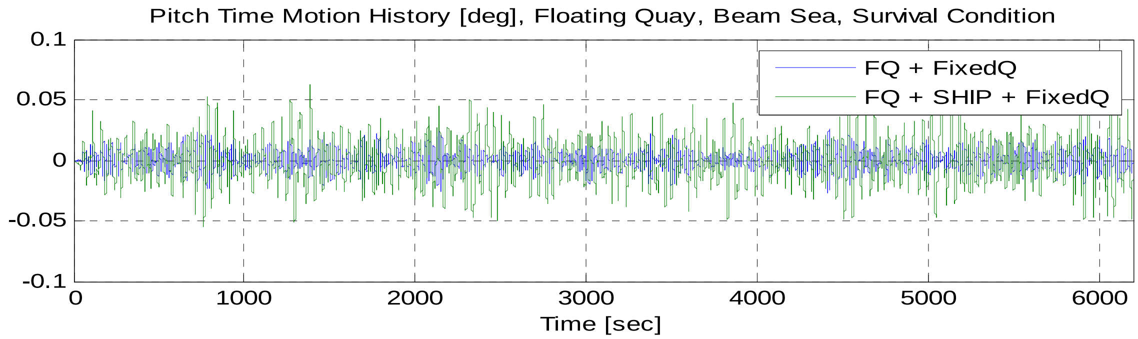

(e)

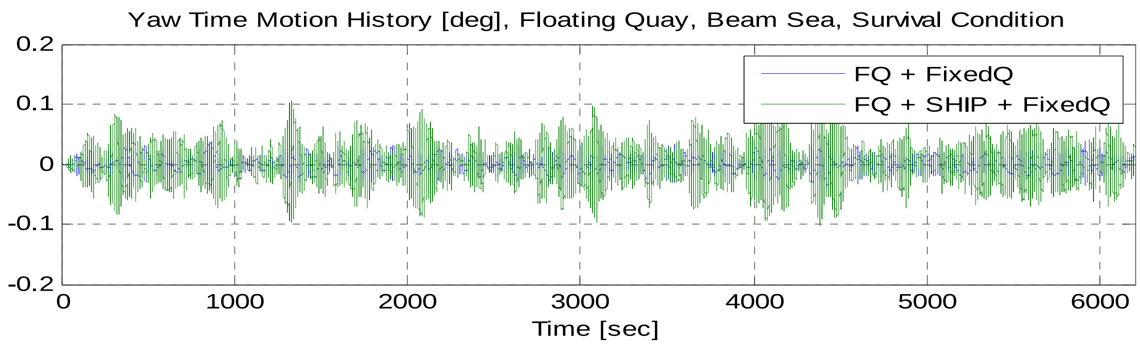

(f)

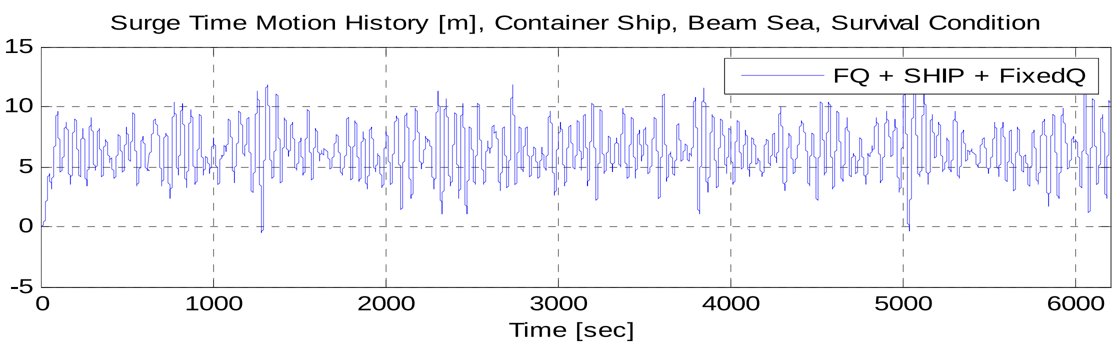

(g)

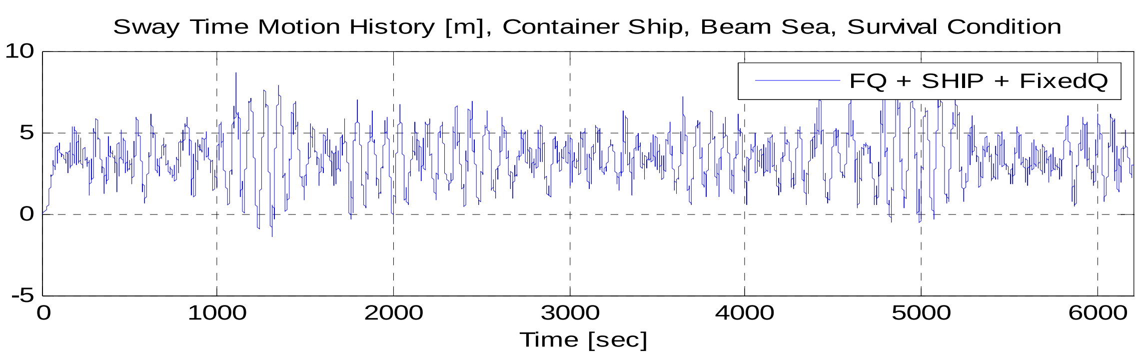

(h)

Fig. 3-50. Continued

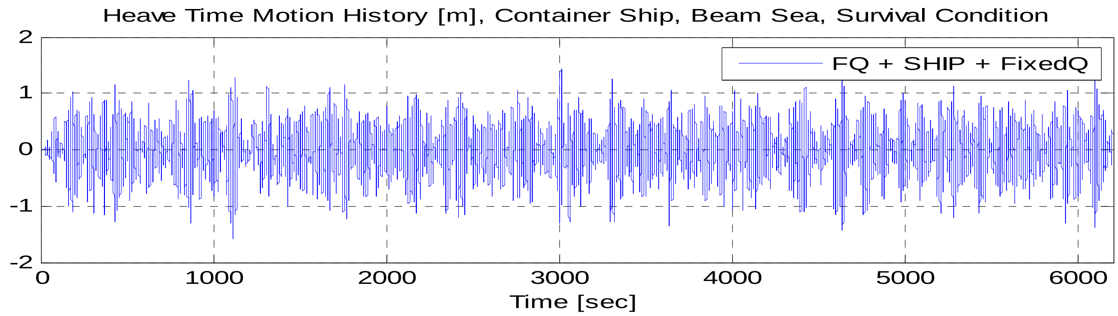

(i)

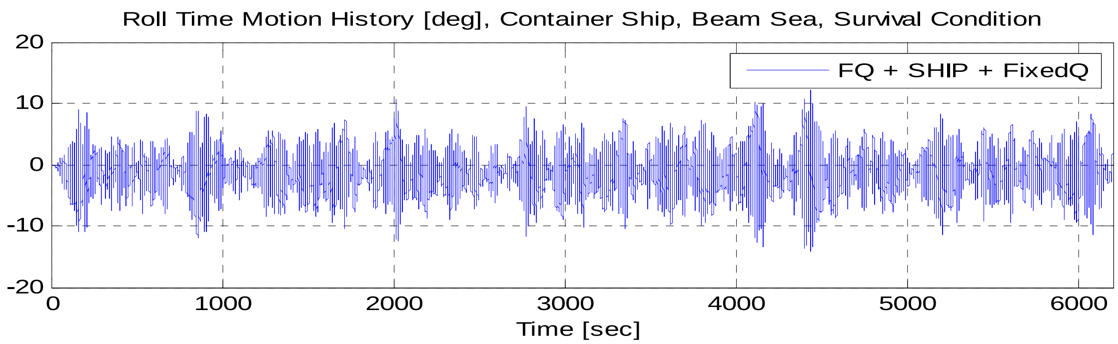

(j)

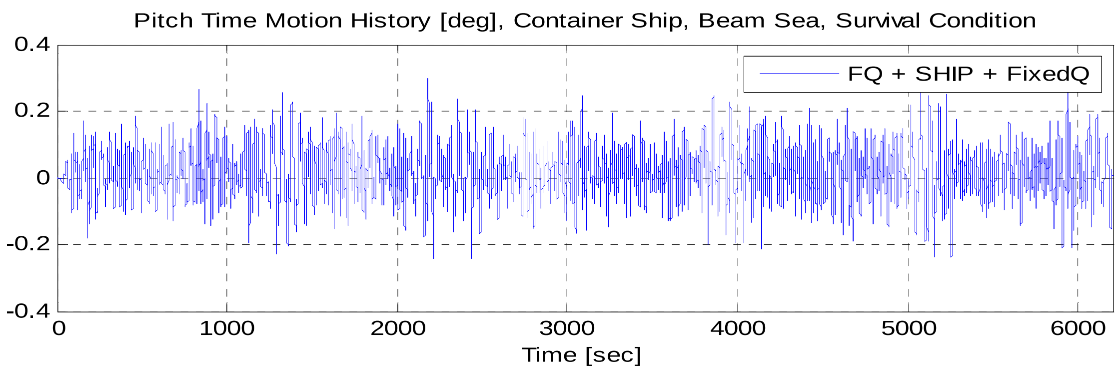

(k)

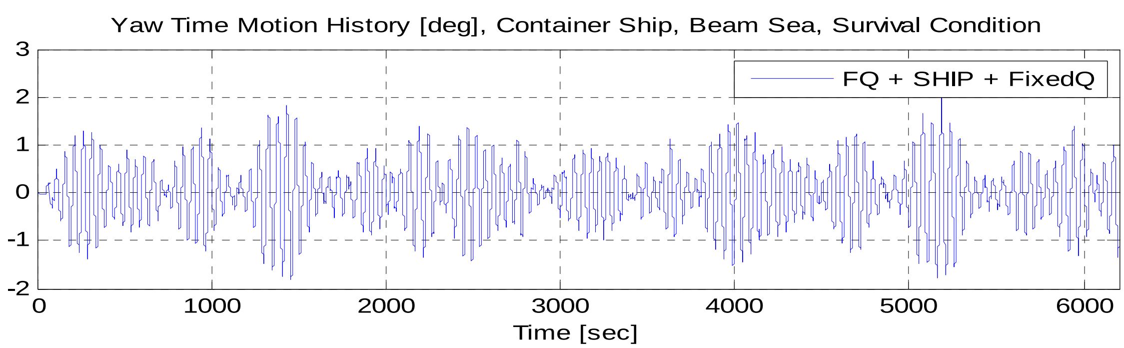

(l)

Fig. 3-50. Continued

Relative Motion Time History, Survival Condition, Beam Sea

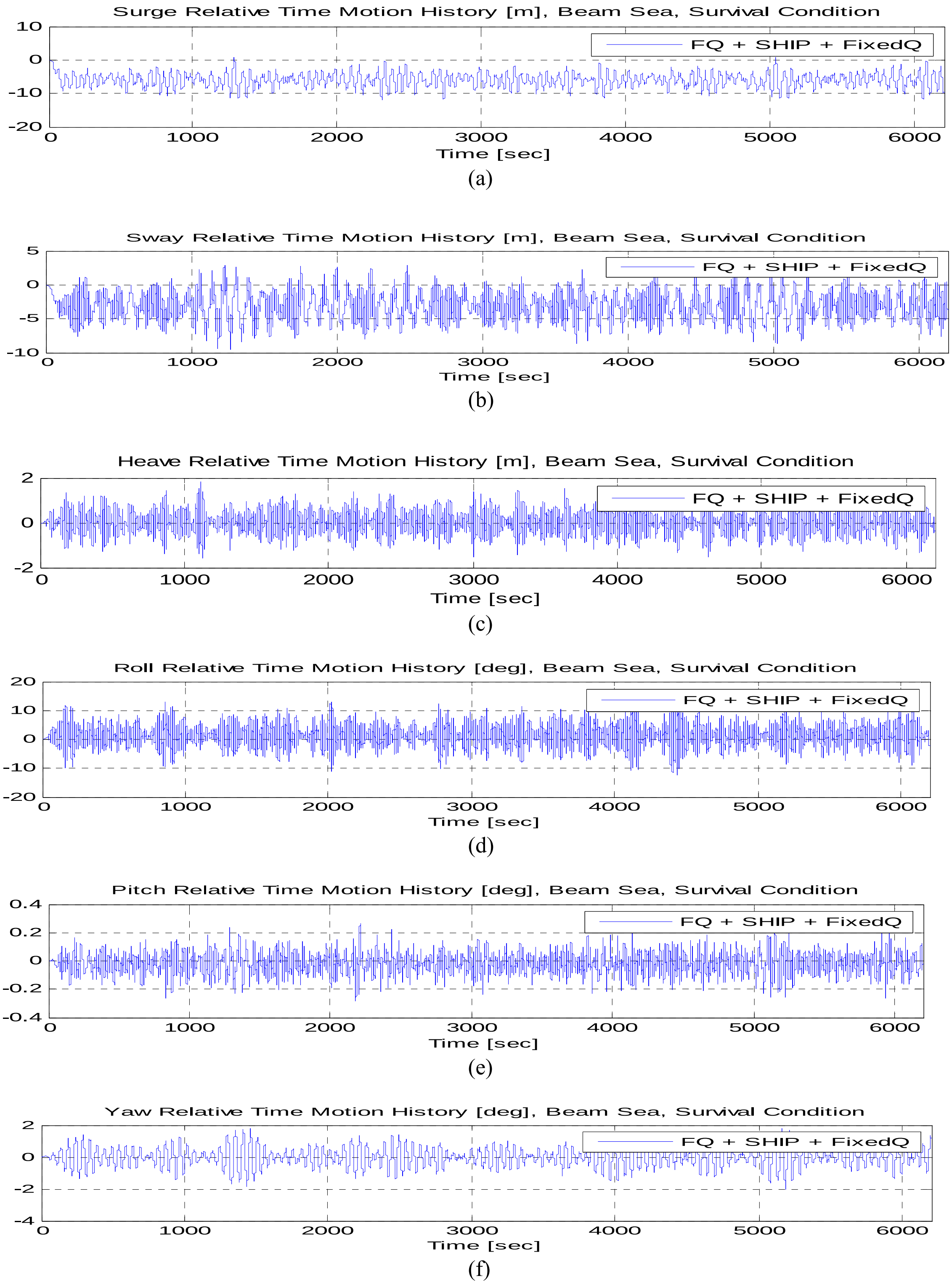

Fig. 3-51. Relative Motion Time History, Beam Sea, Survival

Table 3-10. Motion Statistics, Beam Sea

Motion	Floating Quay 3body Beam Sea Operational Con't	Container Ship 3body Beam Sea Operational Con't	Floating Quay 3body Beam Sea Survival Con't	Container Ship 3body Beam Sea Survival Con't	Floating Quay 2body (FQ + FixedQ) Beam Sea Survival Con't
SURGE [m]	Max = 0.0848 Min = -0.05939 Mean = 0.01296 Std. Dev. = 0.029	Max = 0.7857 Min = -0.2081 Mean = 0.2908 Std. Dev. = 0.1618	Max = 1.3867 Min = -0.8601 Mean = 0.2779 Std. Dev. = 0.4419	Max = 11.805 Min = -0.576 Mean = 6.261 Std. Dev. = 2.0503	Max = 1.334 Min = -0.7173 Mean = 0.2787 Std. Dev. = 0.3949
SWAY [m]	Max = 0.1122 Min = -0.067 Mean = 0.01735 Std. Dev. = 0.0266	Max = 0.5569 Min = -0.1984 Mean = 0.1606 Std. Dev. = 0.1053	Max = 4.146 Min = -3.4881 Mean =0.3083 Std. Dev. = 1.4183	Max = 8.674 Min = -1.437 Mean = 3.435 Std. Dev. = 1.5133	Max = 3.54159 Min = -3.01359 Mean = 0.2641 Std. Dev. = 1.1205
HEAVE [m]	Max = 0.03365 Min = -0.03585 Mean = -6.589E-05 Std. Dev. = 0.0098	Max = 0.0945 Min = -0.1048 Mean = -3.484E-04 Std. Dev. = 0.0274	Max = 0.4339 Min = -0.3996 Mean = -0.0064 Std. Dev. =0.1039	Max = 1.4303 Min = -1.5752 Mean = -0.0233 Std. Dev. = 0.4589	Max = 0.39864 Min = -0.4387 Mean = -0.006 Std. Dev. = 0.13084
ROLL [deg]	Max = 0.1187 Min = -0.1258 Mean = 3.28E-05 Std. Dev. = 0.0337	Max = 1.4829 Min = -1.648 Mean = -0.05949 Std. Dev. =0.4831	Max = 1.2133 Min = -1.3196 Mean = -0.00186 Std. Dev. = 0.4366	Max = 12.1964 Min = -14.1924 Mean = -1.3224 Std. Dev. = 3.5913	Max = 1.5422 Min = -1.51169 Mean = -0.00653 Std. Dev. = 0.4521
PITCH [deg]	Max = 0.0043 Min = -0.00432 Mean = 1.193E-05 Std. Dev. = 0.0014	Max = 0.03236 Min = -0.02981 Mean = 8.274E-04 Std. Dev. = 0.0093	Max = 0.0629 Min = -0.0544 Mean = -1.297E-04 Std. Dev. = 0.0178	Max = 0.2992 Min = -0.244 Mean = 0.018139 Std. Dev. = 0.0757	Max = 0.02623 Min = -0.02695 Mean = 8.341E-05 Std. Dev. = 0.00777
YAW [deg]	Max = 0.02278 Min = -0.022179 Mean = -1.003E-05 Std. Dev.= 0.00646	Max = 0.1899 Min = -0.1939 Mean = -4.318E-04 Std. Dev. =0.06313	Max = 0.10827 Min = -0.1037 Mean = -1.468E-04 Std. Dev. = 0.0318	Max = 2.027 Min = -1.80839 Mean = 3.103E-04 Std. Dev. = 0.6191	Max = 0.0425 Min = -0.0457 Mean = -1.4435E-04 Std. Dev.= 0.012

Table 3-11. Relative Motion Statistics, Beam Sea

Relative Motion	Beam Sea, 3body Operational Condition	Beam Sea, 3body Survival Condition
SURGE **[m]**	Max = 0.2205 Min = -0.79159 Mean = -0.2778 Std. Dev. = 0.164	Max = 0.8726 Min = -12.0301 Mean = -5.983 Std. Dev. = 2.095
SWAY **[m]**	Max = 0.2048 Min = -0.5284 Mean = -0.1432 Std. Dev. = 0.10639	Max = 2.951 Min = -9.543 Mean = -3.1267 Std. Dev.= 2.088
HEAVE **[m]**	Max = 0.07726 Min = -0.06994 Mean = 2.82E-04 Std. Dev. = 0.02053	Max = 1.8446 Min = -1.5953 Mean = 0.0169 Std. Dev. = 0.5158
ROLL **[deg]**	Max = 1.6109 Min = -1.41554 Mean = 0.0595 Std. Dev. = 0.47496	Max = 14.7223 Min = -12.548 Mean = 1.3206 Std. Dev. = 3.7858
PITCH **[deg]**	Max = 0.03139 Min = -0.0307 Mean = -8.1551E-04 Std. Dev. = 0.00918	Max = 0.26276 Min = -0.2857 Mean = -0.01826 Std. Dev. = 0.07328
YAW **[deg]**	Max = 0.1965 Min = -0.193 Mean = 4.217E-04 Std. Dev.= 0.0636	Max = 1.8149 Min = -2.04425 Mean = -4.571E-04 Std. Dev.= 0.6208

Table 3-12. Statistics of Force on Dolphin Moorings, Beam Sea

3body	Forward Dolphin Beam Sea Operational Condition	Afterward Dolphin Beam Sea Operational Condition	2body (FQ+ FixedQ)	Forward Dolphin Beam Sea Survival Condition	Afterward Dolphin Beam Sea Survival Condition
FORCE [N]	Max = 1.365E+06 Mean = 4.1857E+05 Std. Dev. = 2.23E+05	Max = 1.354E+06 Mean = 4.266E+05 Std. Dev. = 2.279E+05	FORCE [N]	Max = 3.44E+07 Mean = 1.0618E+07 Std. Dev. = 6.043E+06	Max = 3.52E+07 Mean = 1.065E+07 Std. Dev. = 6.0789E+06

CHAPTER IV

CONCLUSION AND SUMMARY

A feasibility study is conducted for the use of floating quay to allow offloading operation from both sides of a container ship. The relative motions between land wall, container ship, and the floating quay are assessed both in typical operational and survival condition of Busan New Port, Korea. The hydrodynamic interactions of the three bodies become complex when they move in close proximity to each other. The hydrodynamic coefficients and wave forces among multiple bodies in close proximity are significantly different from those of a single body, which is numerically assessed by using a three dimensional diffraction/radiation panel program including three bodies. The numerical results show that the motion responses of the interacting bodies can be significantly altered compared to the single body case primarily due to the reflected waves among neighboring bodies. The motion response of the interacting bodies in the case of multi body interaction doubles the motion response of the single body due to interaction effect and phasing but the responses are less when waves are shielded by the front body or waves have proper phasing that makes those cancel out each other.

The primary object of the present study is to find out whether the use of floating harbor may be beneficial or detrimental for the loading/unloading operation in typical operational and survival condition. Typical wind and current environments for both cases are also included to simulate more realistic conditions. It can be concluded from the simulation results that the presence of floating mobile container terminal does give rise to elevated motion responses due to interaction effects, but they are within acceptable limits. In particular, the offloading condition in the operational condition with the floating harbor is as good as that without it. The loading-offloading operation close to the survival condition is very challenging, as expected, and the relative motions can be reduced by using tighter hawser lines. It is recommended that container ships should be removed from the harbor in the survival condition. The interaction effects are particularly pronounced in the 90-degree (beam sea) wave incident angle compared to the other wave incident angles.

REFERENCES

Buchner, B., Dijk, A., Wilde, J., 2001. Numerical multi-body simulations of side-by-side mooring to an FPSO. Proc. 11th International Offshore and Polar Engineering Conf. Stavanger, Norway, 343-353.

Hong, S.Y., Kim, J.H., Cho, S.K., Choi, Y.R., Kim, Y.S., 2005. Numerical and experimental study on hydrodynamic interaction of side-by-side moored multiple vessels. Ocean Engineering 32, 783-801.

Kumar, B. 2005, Dynamic analysis of floating quay and container ship for container loading and offloading operation, M.S. Thesis, Texas A&M University, College Station, TX.

Lee, D. H. & Kim, M. H. , 2005. Two-body resonant interactions by fully coupled and partially coupled method. Civil Engineering in the Oceans VI, p 949.

Mercier, Richard, 2005. Dynamics of Offshore Structures, Lecture Notes, OCEN-676-600, Ocean Engineering Program, Civil Engineering Department, Texas A&M University, College Station, TX.

Ran, Z., 2000. Coupled dynamic analysis of floating structures in waves and current, Ph. D. Dissertation, Texas A&M University, College Station, TX.

Tahar, A. & Kim, M. H., 2003. Hull/mooring/riser coupled dynamic analysis and sensitivity study of a tanker-based FPSO. Applied Ocean Research, Volume 25, 367-382.

Supplemental Sources Consulted

Buchner, B., Gerrit B., Jaap W., 2004. The interaction effects of mooring in close proximity of other structures. Proc. 14th Conf. ISOPE, 297-306.

Chen, H. C., Huang, E. T., 2004. Time-domain simulation of floating pier/ship interactions and harbor resonance. Proc. 14th International Conf. Offshore and polar engineering, Volume 1, 772-774.

Choi, Y.R., Hong, S.Y., 2002. An analysis of hydrodynamic interaction of floating multi body using higher-order boundary element method, 12th International Conference on Offshore and Polar Engineering, ISOPE, 303-308.

Jain, R.K., 1980. A simple method of calculating the equivalent stiffness in mooring cables. Applied Ocean Research 2, 3, 139-142.

Kim, M. H., 1997. WINTCOL/WINPOST User's Manual. Ocean Engineering Program, Civil Engineering Department, Texas A&M University, College Station, TX.

Kodan, N., 1984. The motions of adjacent floating structures in oblique waves. Proc. 3rd International Conf. Offshore Mechanics & Arctic Engineering, 1, 206-213.

Lee, C. H., 1995. WAMIT Theory Manual. Department of Ocean Engineering, Massachusetts Institute of Technology, Cambridge, MA.

Lee, D. H., Choi, H. S., 1998. The motion behavior shuttle tanker connected to a turret-moored FPSO. Proc. 3rd International Conf. Hydrodynamics, Seoul, South Korea, 173-178.

Sannasiraj, S. A., Sundaravadivelu, R., Sundar, V. 2000. Diffraction-radiation of multiple floating structures in directional waves. Ocean Engineering, 28, 201-234.

APPENDIX

Force Time History on Dolphin Mooring, Head Sea, Operational Condition

The force time history on the forward and afterward dolphins of Floating Quay for 0 [deg] wave heading case is shown in Figure A. and Table 3-7. Dolphin moorings do not suppress vertical motion, so resultant force below is horizontal force, vector summation of surge direction force and sway direction force. The force time history on the dolphins is calculated by multiplying the dolphin stiffness with the motion time history at the location of the forward and afterward dolphin moorings.

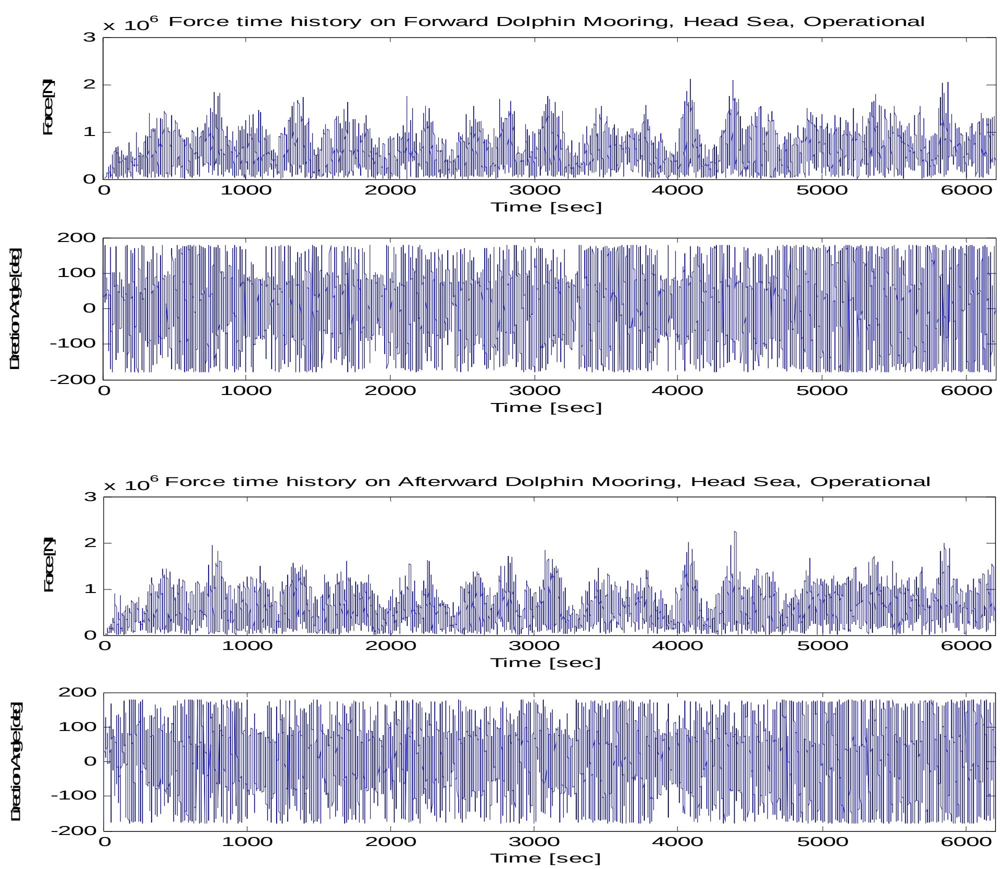

Fig. A. Force Time History on Dolphin Mooring, Head Sea, Operational

Force Time History on Dolphin Mooring, Head Sea, Survival Condition

Table 3-7 and Figure B illustrate force time history on Dolphin Moorings. Maximum force and mean force are minimum among Head Sea, Quartering Sea, and Beam Sea Operational conditions.

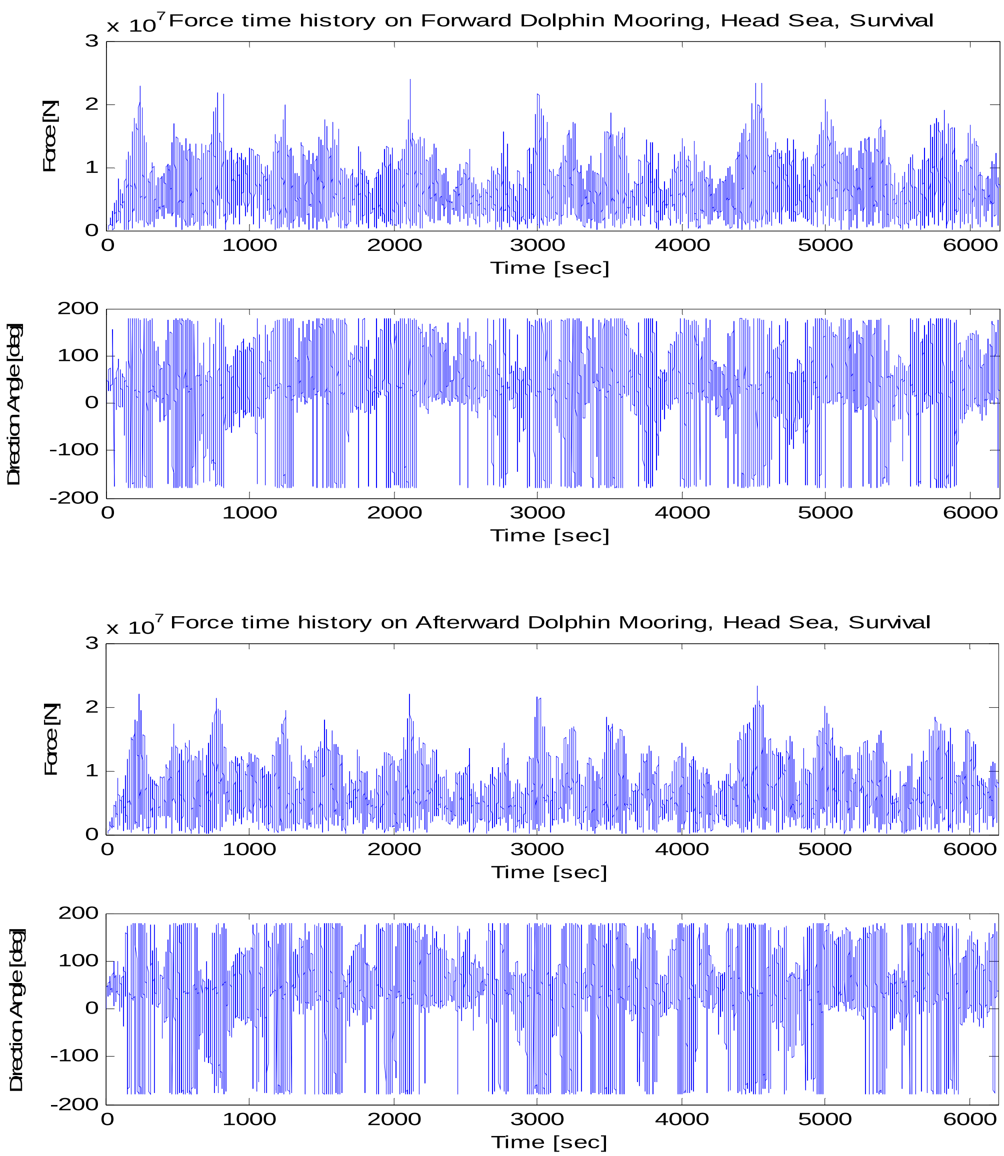

Fig. B. Force Time History on Dolphin Mooring, Head Sea, Survival

Force Time History on Dolphin Mooring, Quartering Sea, Operational Condition

As shown in Table 3-9 and Figure C, maximum value of force on Dolphin Moorings and average value of force on Dolphin are bigger than those in Head Sea and Beam Sea Operational conditions.

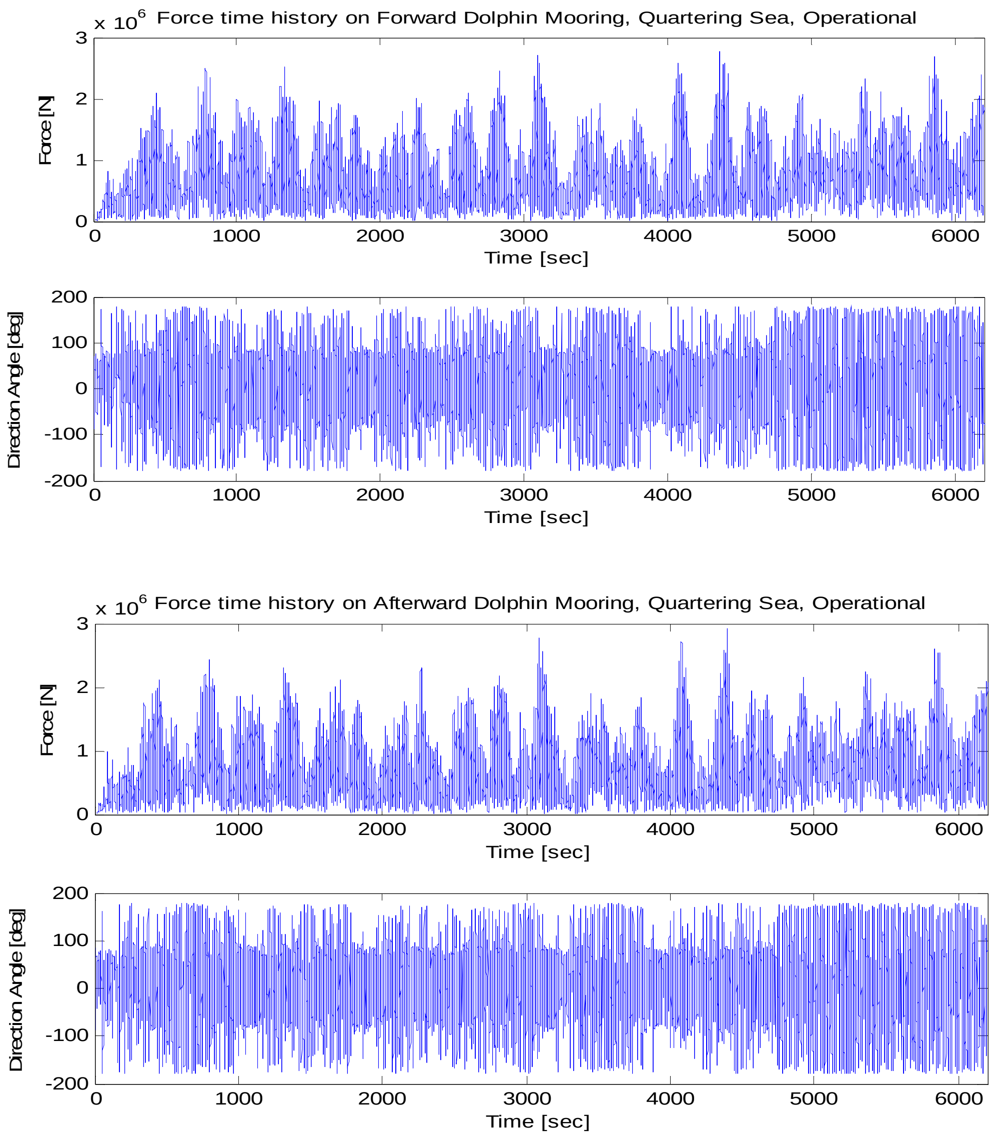

Fig. C. Force Time History on Dolphin Mooring, Quartering Sea, Operational

Force Time History on Dolphin Mooring, Quartering Sea, Survival Condition

Table 3-9 and Figure D show mean force and maximum force are similar with those in Head Sea survival condition. But force on Dolphin Moorings are a little higher than those in Head Sea Survival condition.

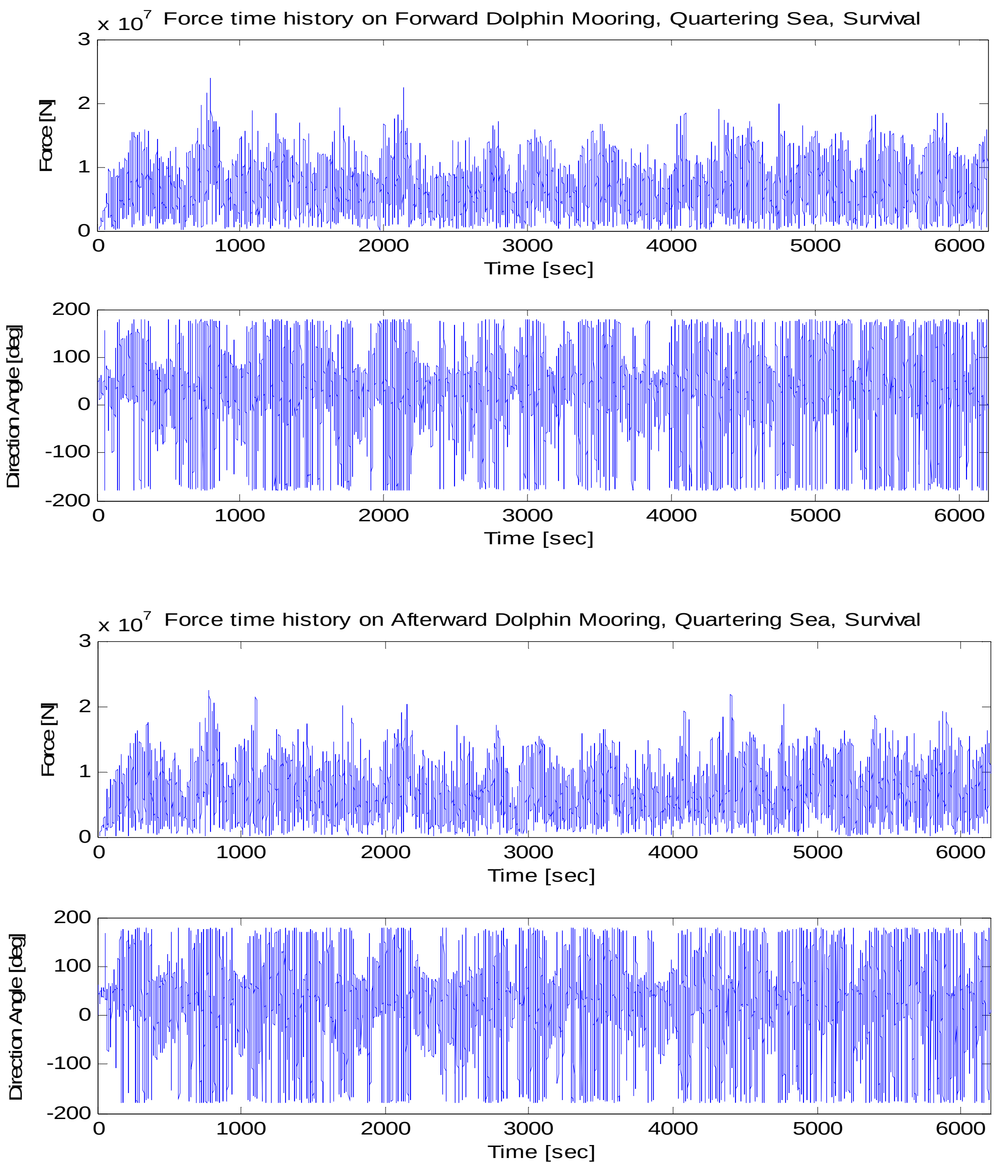

Fig. D. Force Time History on Dolphin Mooring, Quartering Sea, Survival

Force Time History on Dolphin Mooring, Beam Sea, Operational Condition

Table 3-12 and Figure E show the mean force and the maximum force on Dolphin Moorings in this case (Beam Sea Operational condition) are minimum among Head Sea, Quartering Sea, and Beam Sea Operational conditions.

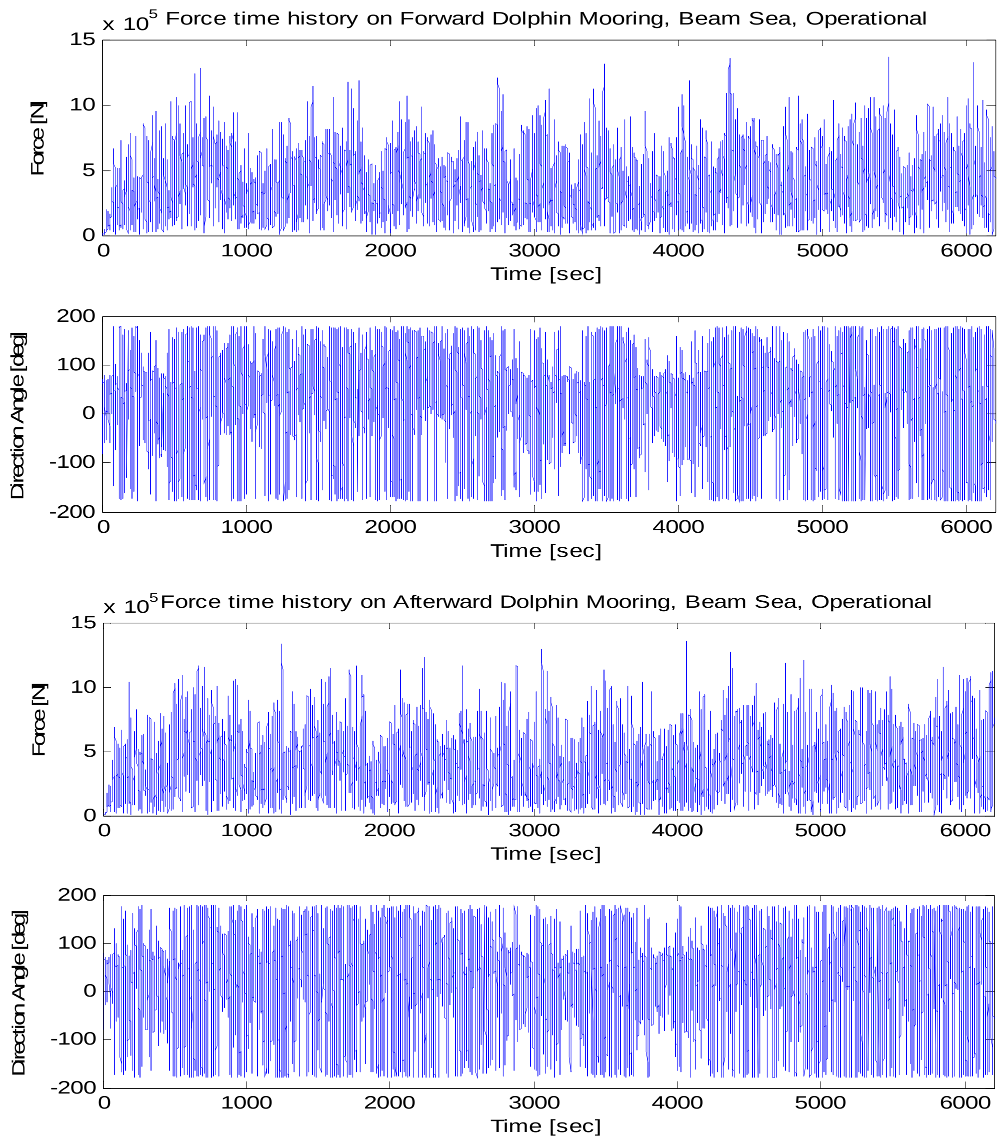

Fig. E. Force Time History on Dolphin Mooring, Beam Sea, Operational

Force Time History on Dolphin Mooring, Beam Sea Survival Condition

Table 3-12 and Fig. F show mean force and maximum force on Dolphin Moorings are biggest among Head Sea, Quartering Sea, and Beam Sea Survival conditions.

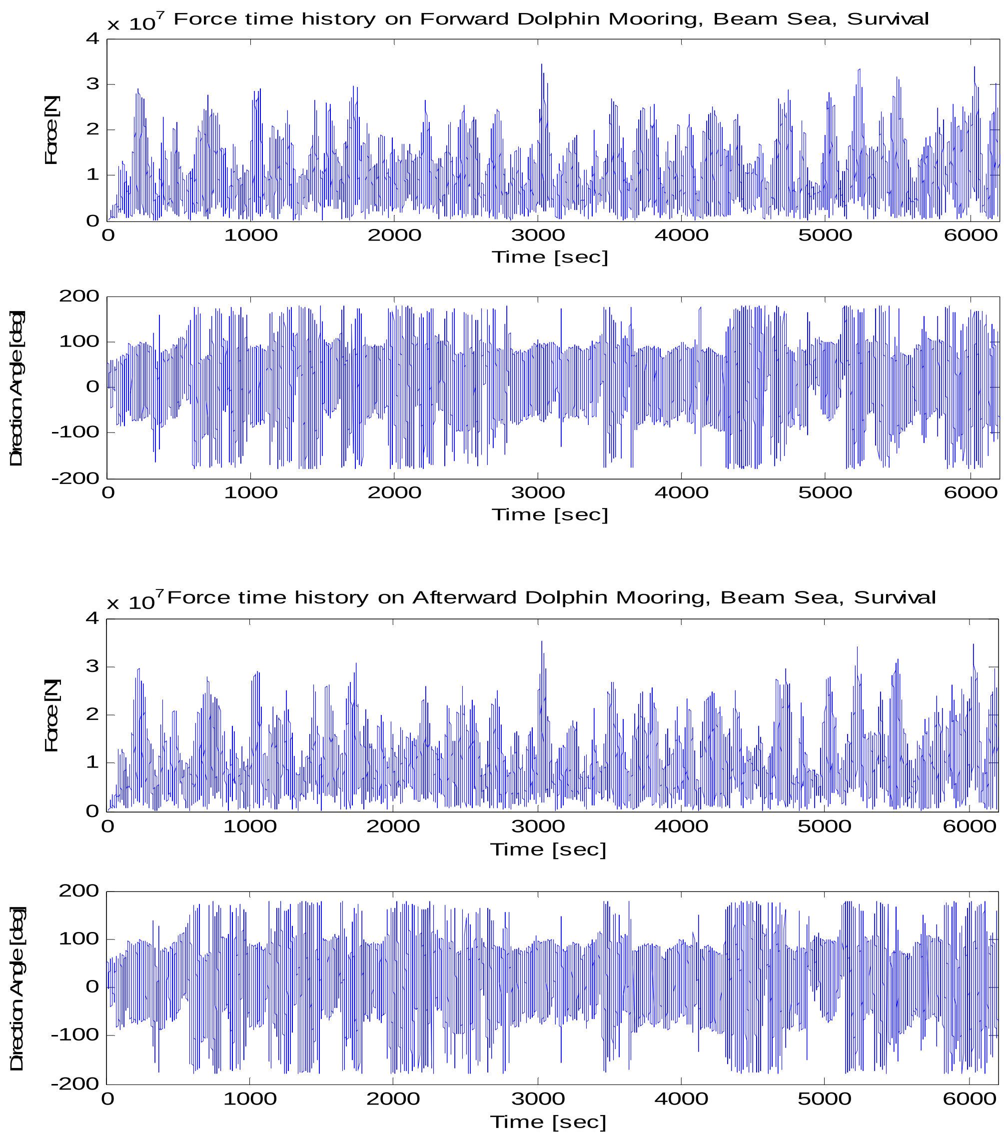

Fig. F. Force Time History on Dolphin Mooring, Beam Sea, Survival

VITA

Sung Ho Lim
Coastal and Ocean Engineering Division
Zachry Department of Civil Engineering
3136 Texas A&M University
College Station, TX 77843-3136
Phone: (979)845-4515
Fax:+1(979)862-8162
Email: denny0227@yahoo.com

EDUCATION

• Master of Science December 2007
  Major: Ocean Engineering
  Texas A&M University, College Station

• Bachelor of Engineering: February 2004
  Major: Naval Architecture
  Pusan National University, South Korea.

EXPERIENCE

• Worley Parsons Sea, Houston, Texas (June 2007 – Present)
• Texas A&M University, College Station, Texas (Sep. 2006 – Dec. 2007)
  Graduate Research Assistant, Civil Engineering Department
• Hyundai Heavy Industries, Co. LTD, Ulsan, South Korea (Nov. 2003 – Jan. 2004)
  Internship, Ship Outfitting Design Division